INSTITUTO POTOSINO DE INVESTIGACIÓN CIENTÍFICA Y TECNOLÓGICA, A.C.

POSGRADO EN CIENCIAS AMBIENTALES

Magnetic field stimulation of biological processes for the treatment of gaseous effluents

Tesis que presenta

Estheisy López Bello

Para obtener el grado de

Doctora en Ciencias Ambientales

Directores de la Tesis

Dra. Sonia Lorena Arriaga García

Dr. Aitor Aizpuru

San Luis Potosí, S.L.P., diciembre de 2025

Constancia de aprobación de la tesis

La tesis **"Magnetic field stimulation of biological processes for the treatment of gaseous effluents"** presentada para obtener el Grado de Doctora en Ciencias Ambientales fue elaborada por **(Estheisy López Bello)** y aprobada el **12 de diciembre de 2025** por los suscritos, designados por el Colegio de Profesores de la División de Ciencias Ambientales del Instituto Potosino de Investigación Científica y Tecnológica, A.C.

Dra. Sonia Lorena Arriaga García
Directora de tesis

Dr. Aitor Aizpuru
Codirector de tesis

Dra. Aura Virginia Ontiveros Valencia
Miembro del Comité Tutoral

Dr. J. Sergio Casas Flores
Miembro del Comité Tutoral

Dr. Armando Encinas Oropeza
Miembro del Comité Tutoral

Créditos Institucionales

Esta tesis fue elaborada en los Laboratorios de la División de Ciencias Ambientales del Instituto Potosino de Investigación Científica y Tecnológica, A.C., bajo la dirección de la Dra. Sonia Lorena Arriaga García y el Dr. Aitor Aizpuru.

Durante la realización del trabajo, el autor recibió una beca académica de la Secretaría de Ciencia, Humanidades, Tecnología e Innovación (Secihti) (No. CVU 909070).

Como parte de este trabajo se realizó una estancia de investigación nacional en Puerto Ángel, Oaxaca, bajo la dirección del Dr. Aitor Aizpuru. Parte de los resultados de dicha estancia se presentan en el capítulo II.

Se realizó también una estancia de investigación en el extranjero en el Instituto de Procesos Sostenibles en la Universidad de Valladolid, España, bajo la dirección del Dr. Raúl Muñoz. Los resultados de dicha estancia se presentan en el capítulo IV.

Página en blanco que se va a utilizar para colocar la copia del acta de examen

Dedicatoria

A mi esposo, por creer en mí incluso cuando yo dudaba, por su paciencia, su amor incondicional, su apoyo y por acompañarme en cada paso de este largo camino.

A mis padres, por enseñarme con su ejemplo el valor del esfuerzo, la honestidad y la perseverancia; todo lo que soy se lo debo a ustedes.

A mi hermana, por su apoyo constante, sus palabras de aliento y por recordarme que no estoy sola.

Agradecimientos

A la Secretaría de Ciencia, Humanidades, Tecnología e Innovación (SECIHTI) por la beca otorgada para la realización de mis estudios de posgrado.

Al Instituto Potosino de Investigación Científica y Tecnológica, A.C. (IPICYT) y a la División de Ciencias Ambientales por la infraestructura, el equipo y los materiales brindados para realizar mi doctorado.

Expreso mi más profundo agradecimiento a mis directores de tesis, la Dra. Sonia Lorena Arriaga y el Dr. Aitor Aizpuru, por permitirme trabajar bajo su dirección, por compartir su conocimiento y experiencia, así como por su apoyo, paciencia y guía a lo largo de todo este proceso.

A mi comité tutoral la Dra. Aura Ontiveros, el Dr. Sergio Casas y el Dr. Armando Encinas por sus valiosos aportes, sus críticas constructivas y el tiempo dedicado a este trabajo.

Al Dr. Raúl Muñoz, a la Dra. Laura Vargas y a la Mtra. Ingrid Hernández por el apoyo y las facilidades otorgadas durante mi estancia de investigación en el Instituto de Procesos Sostenibles, en la Universidad de Valladolid, España.

A los técnicos académicos, al M. en C. Guillermo Vidriales, al M. en C. Juan Pablo Rodas, a la Dra. Elizabeth Isaacs, a la M. en C. Ma. Carmen Rocha y al M. en C. Alberto Barrera por su apoyo técnico y administrativo durante la realización de este proyecto.

A las Dras. Mariana Candia y Mónica Cortés por su amistad y por compartir generosamente sus conocimientos conmigo. A mis amigos de IPICYT, Jesús Montoya y Paola Arjona, por su compañía, apoyo y amistad. Gracias por los consejos y las tardes de interminables pláticas.

A mi esposo, por creer en mí más que nadie, por su paciencia, cuidado y apoyo incondicional.

A mis padres y a mi hermana, por apoyar cada una de mis decisiones y ser mi mayor fuente de fortaleza y motivación.

Table of contents

Constancia de aprobación de la tesis ii
Créditos Institucionales iii
Dedicatoria v
Agradecimientos vi
List of tables x
List of figures xii
Abreviaturas xv
Resumen xvii
Abstract xviii
CHAPTER I. Introduction 1
1.1 Volatile Organic Compounds 1
1.1.1 Treatment of Volatile Organic Compounds 3
1.2 CO_2 as a Global Pollutant 6
1.2.1 CO_2 treatment 7
1.2.2 CO_2 Mitigation by Microalgae 9
1.3 Static Magnetic Field in Biological Process 11
1.3.1 Biological treatment of VOCs Stimulated by Static Magnetic Fields 13
1.3.2 Effect of Static Magnetic Field on CO_2 Mitigation by Microalgae 14
1.4 Justification of the Thesis Work 16
1.5 Hypothesis 17
1.3 References 19
CHAPTER II. Effects of static magnetic field exposure on the biodegradation of volatile organic compounds with different hydrophilicities 25
2.1 Abstract 26
2.2 Introduction 27
2.3 Material and Methods 32
2.3.1 Microorganism's acclimation and preparation in mineral medium 32
2.3.2 Microcosm set-up 33
2.3.3 Chemical analytical methods 34
2.3.4 Bacterial community analysis 35

2.3.5 Data analysis 36
2.3.6 Statistical analysis 39
2.4 Results and discussion 39
2.4.1 Characterization of the magnetic field 39
2.4.2 Determination of Henry's law coefficient 41
2.4.3 Kinetic consumption parameters for toluene, hexane and methanol 42
2.4.4 SMF effect on CO_2 production, mineralization, OD, and TOC 52
2.4.5 Bacterial diversity analysis 54
2.4.6 Shift in microbial community 56
2.5 Conclusions 58
2.6 References 59
2.7 Supplementary materials 65
CHAPTER III. Stimulation of toluene biofiltration under continuous and intermittent operation by a static magnetic field 69
Highlights 69
3.1 Abstract 70
3.2 Introduction 71
3.3 Methodology 75
3.3.1 Experimental setup 75
3.3.2 Analytical methods 76
3.3.3 Cell viability 77
3.3.4 Treatment of data 77
3.3.5 Carbon balance 78
3.3.6 Statistical analysis 78
3.4 Results and Discussion 79
3.4.1 SMF characterization 79
3.4.2 Effect of the magnetic field on the toluene removal performance 80
3.4.3 Effect of the SMF on biomass, CO_2 production and TOC content 84
3.4.4 Carbon fate 91
3.4.5 Effect of SMF exposure on EPS content and composition 92
3.5 Conclusions 98

3.6 References 99
3.7 Supplementary materials 104
CHAPTER IV. Stimulation of microalgae growth and high-value compounds production by magnetic field exposure 105
Highlights 105
4.1 Abstract 106
4.2 Introduction 107
4.3 Material and methods 109
4.3.1 Microalgae strains and culture conditions 109
4.3.2 Magnetic field exposure 109
4.3.3 Experimental set-up 109
4.3.4 Analytical procedures 111
4.3.5 Statistical analysis 113
4.4 Results and discussion 113
4.4.1 Influence of MF intensity and exposure time on microalgae growth 113
4.4.2 Influence of MF intensity and exposure time on biomolecules accumulation 122
4.4.3 Influence of MF intensity and exposure time on pigment production 126
4.5 Conclusions 130
4.6 References 131
4.7 Supplementary materials 137
CHAPTER V. General discussion and conclusions 142
5.1 General discussion 142
5.2 Conclusions 150
5.3 Perspectives 151
5.4 References 152
CHAPTER VI. Products derived from this thesis 154

List of tables

Table 1.1 Common VOCs emitted and health effects 2

Table 1.2 Technologies involved in VOC emissions treatment 4

Table 1.3 Carbon capture and storage and utilization strategies 7

Table 1.4 Effects of Static Magnetic Fields on Microbial Processes 12

Table 1.5 Effect of Static Magnetic Fields on VOCs biodegradation 13

Table 1.6 Effects of Static Magnetic Field Exposure on Microalgae 15

Table 2.1 Average Magnetic field intensities inside all three systems 41

Table 2.2 SMF effect on CO_2 production, mineralization, OD, TOC and pH on toluene, hexane, and methanol at the end of the kinetics 53

Table 2.3 The diversity indices of different experiments in the final kinetic evaluated..... 55

Table S2.1 Average of kinetic parameters of the Gompertz model for the biodegradation of toluene, hexane, and methanol with and without magnetic field..... 67

Table 3.1 Carbon recovery for the biofiltration of toluene with/without magnetic field during the continuous load stage 92

Table S3.1 Carbon recovery for the biofiltration of toluene with/without magnetic field during the first 24 days and at the end of the continuous load stage 104

Table 4.1. Effects of magnetic field (MF) intensity (30, 60, 120 mT) and exposure time (1, 2, 4 h d^{-1}) on biomass productivity (Px) and specific growth rate (μ) after 8 days of cultivation for *C. vulgaris* and *Coelastrella* sp., and after 9 days of cultivation for *A. platensis* 116

Table S4.1 Average Magnetic Field intensities inside all three systems 137

Table S4.2 Evolution of pH and QY in the kinetic assays of the last cultivation of *C. vulgaris* 139

Table S4.3 Evolution of pH and QY in the kinetic assays of the last cultivation of *Coelastrella* sp. 140

Table S4.4 Evolution of pH and QY in the kinetic assays of the last cultivation of *A. platensis* …….. 141

List of figures

Fig. 1.1 Carbon concentration mechanism in microalgae *Chlamydomonas reinhardtii* (A) showing: (i) Bicarbonate/Ci pumps for Ci transportation; (ii) passive diffusion of CO2 through membrane pores; (iii) pyrenoid packed with Rubisco. (B) Magnified view of chloroplast where photosynthetic CO_2 reduction takes place through Calvin–Benson cycle 9

Fig. 1.2 Magnetic field lines generated by a bar magnet (a), between unlike poles (b), between like poles (c). *Taken and modified from: OpenStax College (2016)*..... 11

Fig. 2.1 Results of the different SMF exposure on Henry´s law for hexane, toluene and methanol 42

Fig. 2.2 Example of a replica of the Gompertz fitting taken in the last day of the kinetic study for a) toluene (day 17) under a SMF of 0 and 70 mT, b) hexane (day 20) under a SMF of 20 and 70 mT, and c) methanol (day 17) under a SMF of 0 and 40 mT 43

Fig. 2.3 Beta parameter (β) for a) toluene, b) hexane and c) methanol and consumption rate (K, h^{-1}) for d) toluene, e) hexane and f) methanol at the beginning, intermediate and final days of sequential batch experiments, under different magnetic field intensities (0, 20, 40 and 70 mT). Different letters indicate statistically significant differences under different SMF intensities, for a given day and a given VOC, at a 95 % confidence interval 45

Fig. 2.4 Maximum consumption rates of a) toluene, b) hexane and c) methanol consumption at the beginning, intermediate and final days of sequential batch experiments, under different magnetic field intensities (0, 20, 40 and 70 mT). Different letters indicate statistically significant differences under different SMF intensities, for a given day and a given VOC, at a 95 % confidence interval..... 49

Fig. 2.5 Heatmaps displaying the changes in the relative abundance of the most prevalent microbial taxa in the batch systems with and without the application of magnetic field. Panels a, b, and c, display the most abundant microbial taxa in the experiments fed with toluene, methanol, and hexane respectively 56

Fig. S2.1 Microcosm, case with two stacked neodymium magnetic blocks (a) Location of static magnetic field measurements inside the flasks. Magnets were placed at angles of 0 and 180º (b) 65

Fig. S2.2 Distribution of magnetic field inside the flask 20 mT (1 magnet on each side), 40 mT (2 magnets on each side), 70 mT (3 magnets on each side) 66

Fig. 3.1 Schematic diagram of the biofilter set-up with neodymium magnets 76

Fig. 3.2 SMF intensity inside the biofilter (mT). Horizontal cross sections at heights of a) 6 and 16 cm, b) 8 and 14 cm, and c) 10 and 12 cm 79

Fig. 3.3 Evolution of toluene removal efficiency (RE) (a) along biofilters' operation and after shutdown periods (SD) of (b) 60 and (c) 16 h; and (d) evolution of inlet load (IL) and elimination capacity (EC) along biofilters' operation with and without the SMF..... 81
Fig. 3.4 Evolution of (a) biomass content, (b) cell viability, (c) P_{CO2}, and (d) TOC during the biofiltration of toluene with and without the SMF. Error bars represent the standard deviation between triplicates 86
Fig. 3.5 EPS (a) content and (b) composition during the biofiltration of toluene with and without SMF. Error bars represent the standard deviation between triplicates……..... 94
Fig. 4.1 Magnetic field intensity and time of exposure tested in *Chlorella vulgaris*, *Coelastrella* sp., and *Arthrospira platensis* cultures 111

Fig. 4.2 Time course of the influence of the exposure time of *C. vulgaris* to 30, 60 and 120 mT on CO_2 consumption (a, b, c), O_2 production (d, e, f), and biomass concentration (g, h, i) 114
Fig. 4.3 Time course of the influence of the exposure time of *Coelastrella* sp. to 30, 60 and 120 mT on CO_2 consumption (a, b, c), O_2 production (d, e, f), and biomass concentration (g, h, i) 118

Fig. 4.4 Time course of the influence of the exposure time of *A. platensis* to 30, 60 and 120 mT on CO_2 consumption (a, b, c), O_2 production (d, e, f), and biomass concentration (g, h, i) 120

Fig. 4.5 Influence of MF intensity and exposure time on the final concentrations of carbohydrates (a, b, c), lipids (d, e, f) and proteins (g, h and i) of *C. vulgaris, Coelastrella* sp., *A. platensis*. *Significant difference compared to the control with $p \leq 0.05$ 123

Fig. 4.6 Influence of MF intensity and exposure time on the chlorophyll content of *C. vulgaris* (a), carotenoid content of *Coelastrella* sp. (b) and phycocyanin content of *A. platensis* (c). * Significant difference compared with control $p \leq 0.05$ 127

Fig. S4.1 Time course of CO_2 consumption (main axis) and O_2 production (secondary axis) by *C. vulgaris* cultures exposed to 30 mT, a) first cultivation; b) second cultivation; c) third cultivation; to 60 mT, d) first cultivation; e) second cultivation; f) third cultivation; and to 120 mT, g) first cultivation; h) second cultivation; i) third cultivation 137

Fig. S4.2 Time course of CO_2 consumption (main axis) and O_2 production (secondary axis) by *Coelastrella* sp. cultures exposed to 30 mT, a) first cultivation; exposed to 60 mT, b) first cultivation; and exposed to 120 mT, c) first cultivation..... 138

Fig. S4.3 Time course of CO_2 consumption (main axis) and O_2 production (secondary axis) by *A. platensis* cultures exposed to 30 mT, a) first cultivation, b) second cultivation; 60 mT, c) first cultivation, d) second cultivation; and to 120 mT, e) first cultivation, f) second cultivation 138

Fig. 5.1 Effects observed on the biodegradation of (a) toluene, (b) hexane, and (c) methanol, under different SMF intensities 142

Fig. 5.2 Effect of SMF exposure on toluene biofiltration 145

Fig. 5.3 Principal effects of 60 mT SMF exposure for 2 and 4 h^{-1} per day on *C. vulgaris* 147

Fig. 5.4 Effects of SMF exposure on *Coelastrella* sp. under 60-120 mT exposure for 1, 2, and 4 h^{-1} per day 148

Fig. 5.5 Effects of SMF on *Arthospira platensis* under 30-120 mT exposure for 1, 2, and 4 h^{-1} per day 149

Abreviaturas

VOCs	Volatile Organic Compounds
NOx	Nitrogen Oxides
SMF	Static Magnetic Field
WWT	Waste water treatment
TCE	Trichloroethylene
EPS	Extracellular Polymeric Substances
COD	Chemical Oxygen Demand
MF	Magnetic Field
DMFs	Dynamic Magnetic Fields
DC	Direct Current
DNA	Deoxyribonucleic Acid
AC	Alternating Currents
mT	Militeslas
TOC	Total Organic Carbon
CO_2	Carbon Dioxide
O_2	Oxygen
RA	Relative Abundance
MM	Mineral Medium
GC-FID	Gas Chromatograph with a Flame Ionization Detector
GC-TCD	Gas Chromatograph Thermal Conductivity Detector
SD	Standard Deviation
GHG	Greenhouse Gases
DACC	Direct Air Carbon Capture
CCS	Carbon Capture and Storage
CCM	Carbon Concentration Mechanism
CB	Chlorobenzene

PBRs	Photobioreactors
RE	Removal Efficiency
EC	Elimination Capacity

Resumen

Esta investigación doctoral exploró el potencial de la estimulación del campo magnético estático de baja intensidad (SMF, por sus siglas en inglés) como una estrategia innovadora para mejorar los procesos biológicos involucrados en el tratamiento de efluentes gaseosos. El objetivo principal fue estudiar los efectos del SMF de baja intensidad (20-120 mT) en sistemas microbianos y microalgales para la degradación de compuestos orgánicos volátiles (COVs) y la fijación de dióxido de carbono(CO_2).

En la primera etapa experimental, consorcios mixtos fueron expuestos a SMF (20-70 mT) durante la biodegradación de tolueno, hexano y metanol en reactores de lote alimentado. Los resultados mostraron que la exposición magnética incrementó significativamente las tasas de eliminación de los COV menos hidrofóbicos (tolueno y metanol), con un efecto óptimo en intensidades intermedias (40 mT), mientras que la biodegradación de hexano no presentó mejoras.

Al trasladar esta aproximación a un sistema de biofiltración para el tratamiento de vapores de tolueno (segunda etapa experimental), un SMF de 50 mT mejoró la eficiencia de eliminación tanto bajo operación continua como intermitente. Esta mejora se asoció con una mayor actividad microbiana, evidenciada por un incremento en la producción de CO_2, sugiriendo que la exposición magnética podría favorecer procesos celulares relacionados con el transporte de electrones y la actividad enzimática.

En la tercer etapa experimental, se evaluó el efecto del SMF sobre la fijación de CO_2 en *Chlorella vulgaris*, *Coelastrella* sp. y *Arthrospira platensis*. Los cultivos en lote revelaron que la exposición magnética moduló el crecimiento, la síntesis de pigmentos y la composición bioquímica de manera dependiente de la cepa, la intensidad del campo magnético y el tiempo de exposición. En conjunto, los parámetros evaluados indican que el SMF puede influir en la homeostasis redox mediante la modulación de vías de señalización y del transporte electrónico asociado a especies de oxígeno reactivas (ROS, por sus siglas en inglés), contribuyendo así a una mayor fijación de CO_2.

Los hallazgos integrados en las diferentes etapas experimentales demuestran que los SMF de baja intensidad pueden mejorar tanto la biodegradación de COV como la biofijación de CO_2, posicionándose como una herramienta energética y operativamente eficiente, especialmente mediante el uso de imanes en lugar de bobinas, para optimizar tecnologías de biofiltración y mitigación de emisiones.

Abstract

This doctoral research explored the potential of static magnetic field (SMF) stimulation as an innovative strategy to enhance biological processes involved in gaseous effluent treatment. The main objective was to study the effects of low-intensity SMF (20–120 mT) on microbial and microalgal systems for the degradation of volatile organic compounds (VOCs) and the biofixation of carbon dioxide (CO_2).

In the first experimental stage, mixed consortia were exposed to SMF (20-70 mT) during the biodegradation of toluene, hexane, and methanol in fed-batch reactors. The results showed that magnetic exposure increased elimination rates of less hydrophobic VOCs (toluene and methanol), with an optimal effect at intermediate intensities (40 mT), while hexane biodegradation did not improve.

By transferring this approach to a biofiltration system for treatment of toluene vapors (second experimental stage), a SMF of 50 mT improved the removal efficiency under both continuous and intermittent operation. This improvement was associated with increased microbial activity, evidenced by an increase in CO_2 production, suggesting that magnetic exposure could favor cellular processes related to electron transport and enzyme activity.

In the third experimental stage, the effect of SMF on CO_2 fixation in *Chlorella vulgaris*, *Coelastrella* sp., and *Arthrospira platensis* was evaluated. Batch cultures revealed that magnetic exposure modulated growth, pigment synthesis, and biochemical composition in a strain-dependent manner, magnetic field strength, and exposure time. Overall, the parameters evaluated indicate that SMF can influence redox homeostasis by modulating signaling pathways and electronic transport associated with reactive oxygen species (ROS), thus contributing to increased CO_2 fixation.

Findings integrated into the different experimental stages demonstrate that low-intensity SMFs can improve both VOC biodegradation and CO_2 biofixation, positioning themselves as an energy- and operationally efficient tool, particularly by using magnets instead of coils, to optimize biofiltration and emission mitigation technologies.

CHAPTER I. Introduction

Industrial and urban activities release significant quantities of gaseous pollutants, particularly volatile organic compounds (VOCs) and carbon dioxide (CO_2). VOCs are denominated as hazardous pollutants, contribute to air pollution, atmospheric photochemical reactions, and pose significant health risks, while CO_2 is the primary anthropogenic greenhouse gas driving global climate change. Addressing these emissions is essential for environmental protection and sustainable development.

Biological treatments have emerged as environmentally friendly and cost-effective options for both VOC biodegradation and CO_2 biofixation. However, despite their advantages, biological systems often face mass-transfer limitations, microbial inhibition, and unstable performance under variable environmental conditions. These operational bottlenecks highlight the need for process intensification strategies to enhance biological efficiency. In this context, the application of static magnetic fields (SMFs) has gained attention as a low-energy and non-invasive stimulus capable of modulating cellular processes in microorganisms and microalgae. This thesis explores how SMFs can improve both VOC biodegradation and CO_2 biofixation.

1.1 Volatile Organic Compounds

Volatile Organic Compounds (VOCs) are a class of airborne pollutants that pose serious threats to both human health and the environment, due to their toxicity, volatility, and photochemical reactivity. VOCs are a group of chemicals that have high vapor pressures at room temperature, allowing them to evaporate easily into the air [1]. They are commonly found in various industrial and household products, including paints, solvents, glues, cleaning agents, and fuels [2]. VOCs have numerous adverse effects on both the environment and human health:

- Environmental Impact:

- Air Quality: VOCs contribute to air pollution by forming ground-level ozone and secondary particulate matter through reactions with nitrogen oxides (NOx) in the presence of sunlight. This leads to smog formation, which can damage crops and ecosystems [3].
- Water Pollution: VOCs can contaminate water reservoirs, affecting water quality and aquatic life [1].

- Human Health Impact:
  - Respiratory problems: Exposure to VOCs can cause throat irritation, headaches, loss of coordination, nausea, and vomiting [4].
  - Organ Damage: Long-term exposure can lead to liver and kidney damage, and harm the central nervous system [5].
  - Carcinogenic Effects: Some VOCs, benzene, formaldehyde, and acetaldehyde, are known to be carcinogenic, increasing the risk of cancer [5], [6].
  - Other Health Problems: VOCs can cause asthma, allergies, intoxication, and even depression [6], [7]. They can also disrupt glucose metabolism, leading to diabetes and its complications [8], [9].

Table 1.1 Common VOCs emitted and health effects

VOC	Common Sources	Health Effects	References
Benzene	Industrial emissions, tobacco smoke	Carcinogenic, neurologic symptoms, respiratory issues	
Toluene	Paints, solvents, fuel combustion	Neurological effects, cardiotoxicity, hepatotoxicity, and nephrotoxicity	
Formaldehyde	Building materials, household products	Irritation of the eyes and upper respiratory system, as well as	[5], [6]

		nasopharyngeal carcinoma and leukemia	
Xylene	Paints, varnishes, vehicle emissions	Respiratory issues, neurological effects	
Acetaldehyde	Combustion processes, industrial emissions	Carcinogenic, respiratory issues	
1,3-Butadiene	Vehicle emissions, industrial processes	Carcinogenic, respiratory issues	
Styrene	Plastics manufacturing, vehicle emissions	Cancers of the esophagus, lung, cervix, and other female reproductive organs were shown to have a higher fatality rate	
Methanol	Industrial processes (chemical and wood industries)	Liver damage, vision disturbance, and central nervous system depression.	[10], [11]
Hexane	Industrial processes (manufacturing, leather products, furniture, cleaning agents)	Potential carcinogenic, neurotoxic effects, and reproductive health	[12]–[14]

VOCs are prevalent in both indoor and outdoor environments and pose significant risks to human health and the environment. Effective measures to monitor and control VOC emissions are crucial to mitigate their harmful effects.

1.1.1 Treatment of Volatile Organic Compounds

Over the years, several technologies have been developed to mitigate VOC emissions. Each of these approaches exhibits distinct advantages and limitations, as summarized in Table 1.2.

Table 1.2 Technologies involved in VOC emissions treatment

Category	Technology	Description & Advantages	Limitations / Challenges	References
Biological Treatment	Biofiltration	Cost-effective and environmentally friendly; removes VOCs via biodegradation, adsorption, and aeration.	Limited efficiency with recalcitrant and toxic metabolites. Treats low concentrations at high fluxes	[15], [16]
	Bio-scrubber / Bio-filter / Bio-trickling Filter	Utilizes specific bacteria to treat high VOC concentrations, especially hard-to-degrade compounds; simple and low-cost operation.	Performance depends on VOC type and microbial community resilience.	
Adsorption	Biomass Adsorbents	Naturally porous, inexpensive materials; enhanced through pyrolysis, activation, or doping.	May require chemical modification to improve performance by selectivity.	[17]
	Carbonaceous Adsorbents	Includes activated carbon, biochar, and carbon nanotubes; large surface area and high capacity; widely used in VOC recovery.	Cost and regeneration/disposal of adsorbents.	[18]
Advanced Oxidation Processes	Catalytic Oxidation	Effective for a broad range of VOCs (e.g., chlorinated, sulfur-containing); long-established method.	Needs further improvement for diverse mixtures and high concentrations of VOCs	[19]

	Photocatalytic Oxidation (PCO)	TiO_2-based, good for indoor air purification; enhanced by doping and surface modifications to work under visible light.	Requires light source; performance may vary with VOC type.	[20]
Emerging Technologies	Plasma Catalysis	Combines plasma and catalysts; enables simultaneous VOC removal and in situ catalyst regeneration.	Still under development, energy efficiency and scalability are under study.	[21]
	Hybrid Methods	Synergistic combinations, improve VOC removal efficiency and reduce energy use.	Complexity in design and optimization.	

Among these, biological treatments stand out for their low operational cost and environmental compatibility [18], [22]. Biological processes rely on the metabolic activity of microorganisms to degrade VOCs into CO_2, H_2O, and biomass. However, their performance can be limited by factors such as low compound solubility, high inlet concentrations, or short gas residence times. The efficiency of these systems also depends on the characteristics of the inoculum and the physicochemical properties of the packing material, which influence the mass transfer of pollutants from the gas to the aqueous phase, where biodegradation occurs [23].

In order to optimize the limitations of conventional bio-based systems, coupling biological treatment with physical stimuli, such as the use of static magnetic field (SMF), has emerged as an innovative strategy. SMFs have been shown to improve wastewater treatment (WWT) and waste gases treatments processes by enhancing microbial activity, biofilm formation, and enzymatic performance (see Section 1.3). However, the application of SMFs in VOC treatment remains relatively underexplored.

1.2 CO_2 as a Global Pollutant

CO_2 is a naturally occurring gas, under standard conditions of temperature and pressure, and constitutes a key component of the Earth's atmosphere [24]. However, the combustion of fossil fuels, such as coal, oil, and natural gas, is the primary source of anthropogenic CO_2 emissions. Other major contributors include transportation, manufacturing, and industrial activities [25].

CO_2 is the most significant anthropogenic greenhouse gas, contributing extensively to global warming, climate change, glacial retreat, sea-level rise, and extreme weather patterns [26], [27]. Moreover, elevated CO_2 concentrations are linked to air pollution, exacerbating public health risks and negatively impacting ecosystems. Beyond environmental effects, rising CO_2 levels also result in economic consequences, including job losses, reduced industrial productivity, and decreased foreign investment, driven by climate-related damage and public health burdens [28].

1.2.1 CO_2 treatment

To mitigate these effects, a range of CO_2 control strategies has been developed. These include physicochemical and biological approaches, which can be used independently or in combination to enhance overall carbon capture performance. Table 1.3 summarizes the most relevant CO_2 capture, storage, and utilization technologies.

Table 1.3 Carbon capture and storage and utilization strategies

Strategy	Description	Key Benefits	References
Carbon Capture and Storage (CCS)	Captures CO_2 emissions from sources (e.g., power plants) and stores them in geological or marine reservoirs.	Long-term CO_2 removal from the atmosphere.	[29]
Carbon Capture and Utilization (CCU)	Converts captured CO_2 into value-added products such as methanol, dimethyl carbonate, and polymers.	Environmental and economic value through product generation.	[30]
Bioelectrochemical Systems (BES)	Combine electrochemical processes with microbes to convert CO_2 into fuels like methanol, acetic acid, and ethanol.	Produces valuable chemicals and reduces CO_2.	[31]
Biological Sequestration	Utilizes photosynthetic or chemoautotrophic organisms (bacteria, cyanobacteria, algae) to fix CO_2 via metabolic cycles such as the Calvin cycle	Cost-effective, produces biofuels and bioplastics.	[32], [33]

Duckweed Ponds (DWP)	Treat municipal wastewater while simultaneously capturing atmospheric CO_2. Efficient nutrient uptake and carbon fixation.	Dual function: wastewater treatment and CO_2 mitigation.	[34]
Microalgae Cultivation	Uses CO_2 from coal flue gas to promote algal biomass growth, which can be converted into biofuels and other bioproducts.	Reduces GHGs and pollutants; produces valuable biomass.	[35], [36]

Despite the promising potential of these technologies, many remain economically and technically challenging at large scales. Direct air carbon capture (DACC) is limited by the low ambient concentration of CO_2 and high energy requirements. Current cost estimates range between $246 and $557 per ton of CO_2, depending on the energy source and region [37]. Similarly, traditional Carbon Capture and Storage (CCS) technologies are projected to increase the cost of electricity, making them economically unfeasible without significant cost reductions [38].

Microalgae-based CO_2 mitigation techniques have high production costs, including initial capital investment and ongoing operational costs for microalgae cultivation, which are significant. This includes photobioreactors, land, and infrastructure systems, low photosynthetic efficiency, high water and nutrient requirements [39], [40]. Microalgae represent a promising strategy for CO_2 mitigation, as they utilize CO_2 during photosynthesis and convert it into biomass and oxygen. However, their large-scale application requires overcoming key challenges related to operational costs, water demand, CO_2 supply variability, energy consumption, and nutrient availability. Continued research and technological advancements are needed to optimize microalgae-based systems for large-scale CO_2 capture and sustainable biomass production.

1.2.2 CO_2 Mitigation by Microalgae

Microalgae, as efficient photosynthetic microorganisms, are widely recognized for their ability to fix CO_2 and convert it into valuable biomass and bioproducts. They utilize photosynthesis to convert CO_2 into organic compounds, effectively reducing atmospheric CO_2 levels [41]. Microalgae absorb and utilize CO_2 through several physiological and biochemical mechanisms, primarily driven by photosynthesis and the carbon concentration mechanism (CCM). The CCM is a specialized system in microalgae that enhances the efficiency of CO_2 fixation. The algae fix CO_2 through the Calvin-Benson cycle, where the enzyme Rubisco converts CO_2 into organic compounds [42], [43]. Fig. 1.1 illustrates the pathway of photoautotrophic metabolism.

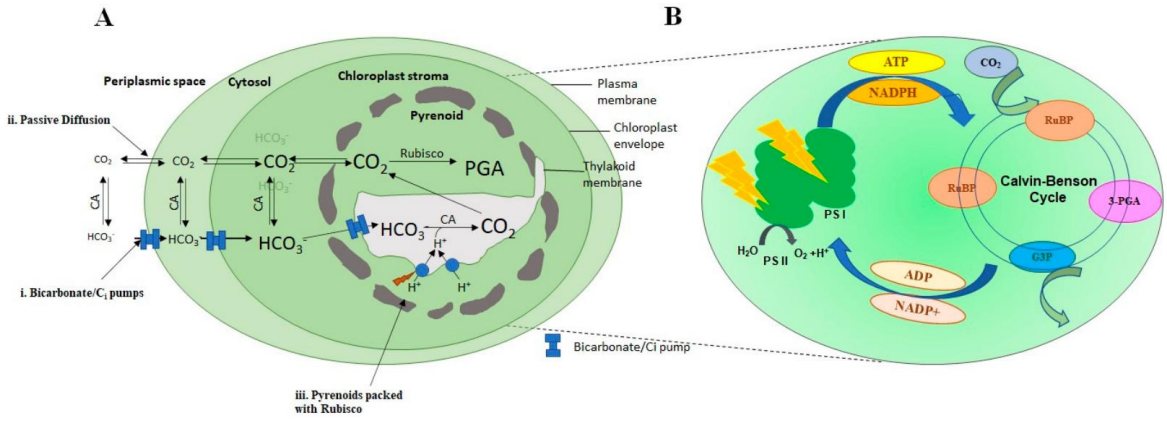

Fig. 1.1 Carbon concentration mechanism in microalgae *Chlamydomonas reinhardtii* (A) showing: (i) Bicarbonate/Ci pumps for Ci transportation; (ii) passive diffusion of CO2 through membrane pores; (iii) pyrenoid packed with Rubisco. (B) Magnified view of chloroplast where photosynthetic CO_2 reduction takes place through Calvin–Benson cycle. *Taken and modified from:* [43]

In microalgae, photosynthesis can be divided into two main stages: the light-dependent reactions and the light-independent (dark) reactions. During the light-dependent stage, solar energy drives the conversion of $NADP^+$ and ADP into the

energy-rich molecules NADPH and ATP. The subsequent light-independent stage, also known as the Calvin–Benson cycle, utilizes these energy carriers to fix and assimilate CO_2 into organic compounds such as glucose. A key enzyme in this process is ribulose-1,5-bisphosphate carboxylase/oxygenase (Rubisco), which catalyzes the incorporation of CO_2 into 3-phosphoglycerate. However, due to its dual carboxylase and oxygenase activities, Rubisco exhibits a relatively low affinity for CO_2, which limits its overall efficiency as a CO_2-fixing enzyme [43].

To mitigate CO_2 emissions using microalgae, several technologies and strategies have been explored and developed. Some of the most studied are photobioreactors (PBRs) and open ponds. PBRs are closed systems, such as flat panels, vertical tubes, and horizontal tubes, that offer higher growth rates, productivity, and protection against contamination compared to open systems. However, they are expensive to install and operate [44]. Open ponds, such as simple ponds, circular ponds, and raceway ponds, are most widely studied systems for microalgae cultivation due to their simplicity, low construction cost, and scalability. These systems—typically designed as raceway ponds or circular basins—enable direct contact between the culture and atmospheric or industrial CO_2 sources. Despite their economic advantages, open ponds often face challenges such as limited control of environmental parameters, water evaporation, and contamination, which can affect productivity and carbon capture efficiency. Nevertheless, they remain a practical option for large-scale CO_2 biofixation and biomass production [44], [45].

Microalgae offer a multifaceted strategy for CO_2 mitigation, coupling environmental sustainability with the generation of valuable bioproducts. However, to fully harness their potential in large-scale applications, further research and technological innovation are required to enhance the efficiency and stability of cultivation systems. In this context, the application of SMF has emerged as a promising approach to stimulate microalgal metabolism and improve their CO_2 fixation capacity, representing a novel avenue for process optimization.

1.3 Static Magnetic Field in Biological Process

Magnetic fields (MFs) are regions in space where a moving electric charge creates a magnetic force. They arise from the movements of electrical charges, such as those found in permanent magnets or electric currents, and are typically quantified by their magnetic flux density, expressed in milliteslas (mT) (Fig. 1.2) [46], [47].

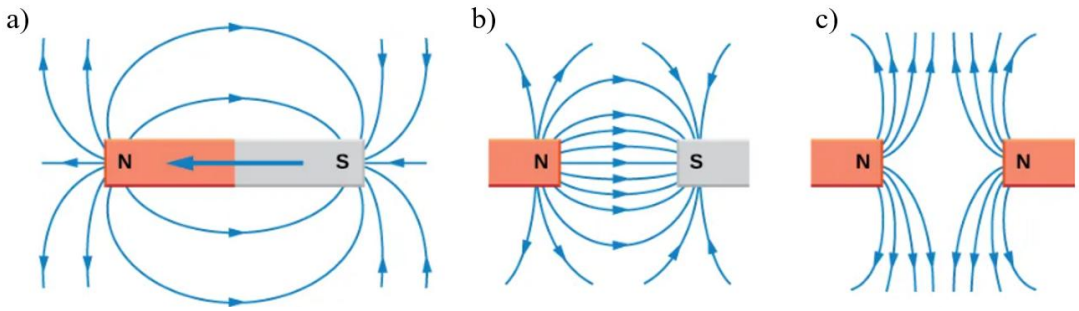

Fig. 1.2 Magnetic field lines generated by a bar magnet (a), between unlike poles (b), between like poles (c). *Taken and modified from: OpenStax College (2016).*

Magnetic Field can be characterized based on several criteria, including their temporal behavior (static vs. dynamic), spatial distribution (homogeneous vs. inhomogeneous), and intensity (weak, moderate, high, and ultra-high) [46], [49], [50]–[52].

SMFs are time-invariant and typically generated by stationary sources such as permanent magnets or direct current (DC) electromagnets [47]. SMFs have been shown to influence biological processes such as oxidative stress, cell growth, and DNA integrity, with both beneficial and adverse effects depending on the intensity and exposure time [53], [54].

In recent years, considerable progress has been made in understanding the interactions between SMFs and biological systems, particularly in the context of microbiology and biotechnology applications. SMFs can influence a wide range of microbial processes, affecting physiological, biochemical, and molecular responses.

As is shown in Table 1.4, microorganisms exposed to SMFs may present changes in enzymatic activity, membrane permeability, and oxidative balance. These effects

can be either stimulatory or inhibitory, depending on the field intensity, exposure duration, frequency, and the type of organism.

Table 1.4 Effects of Static Magnetic Fields on Microbial Processes

Aspect	Effect	Reference
Enzyme Activity	Altered enzyme activity and protein stability	[55], [56]
Cell Membrane Permeability	Increased nutrient transport and ion exchange	[57]
Oxidative Stress	Induced oxidative stress affecting metabolism	[55], [58]
Growth Stimulation/Inhibition	Varied effects based on intensity, frequency, and duration	[59]
Environmental Remediation	Enhanced microbial processes in wastewater and soil treatment	[56]
Food Industry	Optimized microbial metabolism in fermentation processes	[55]
Species-Specific Effects	Varied responses among different microbial species and strains	[59]
Gut Microbiota	Significant changes in composition and structure	[60]
Cellular and Molecular Changes	Structural damage and DNA alterations	[53]
Biochemical Pathways	Impact on electron transfer during respiration and photosynthesis	[56]

These findings underscore the potential of SMFs on microbial systems. While some responses suggest potential for enhancing microbial functions, others indicate possible risks, such as oxidative damage. Consequently, a deeper understanding of the mechanisms underlying its effects is essential to harness SMFs effectively and safely in applied microbiology.

1.3.1 Biological treatment of VOCs Stimulated by Static Magnetic Fields

Recent research has explored the use of SMF as a non-invasive method to stimulate microbial processes and enhance biodegradation efficiency. SMF exposure can influence enzymatic activity, cell membrane permeability, and electron transport, potentially improving microbial growth and pollutant degradation. When applied to biofiltration systems, magnetic fields may strengthen biofilm development, increase oxygen transfer, and enhance the removal of poorly soluble VOCs [12], [61], [62]. Thus, understanding the mechanisms and operational conditions under which SMF stimulation improves biological VOC treatment could lead to more robust and efficient bioreactor designs for air pollution control. Table 1.5 summarizes the effect of SMF exposure on the treatment of several VOCs.

Table 1.5 Effect of Static Magnetic Fields on VOCs biodegradation

VOC Target	Experimental set-up	SMF intensity	Effects	References
Formaldehyde	Bioreactor	7 mT	Improved degradation by 30% and COD reduction by 26% and microbial activity	[63]
Phenol	Fed-batch	370 mT	Increased phenol oxidation by ~34% and respiration activity by ~10%; promoted biomass growth by ~28%	[64]
Trichloroethylene (TCE)	Biotrickling filter	30-130 mT	Increase TCE removal by 11% and change the microbial activity	[62]
Hexane	Biofilter	10-30 mT	Increase hexane removal by 40% and EPS	[12]

Chlorobenzene (CB)	Two-phase partitioning biotrickling filter	1-3 mT	Improvement in CB removal by 37.2% and in EPS secretion by 26.8%	[65]
n-hexane	Two-phase partitioning bioreactor	20 mT	Increase n-hexane elimination by 11% and by 10.3% the electron transport chain activity	[13]

SMF has a positive effect on the biodegradation of VOCs by enhancing microbial activity, increasing removal rates, and optimizing conditions for microbial growth and enzyme activity. These findings open new avenues for improving bioremediation processes and waste gases treatment efficiency. Nevertheless, further research and optimization of SMF parameters are necessary to fully realize their potential in environmental remediation.

1.3.2 Effect of Static Magnetic Field on CO_2 Mitigation by Microalgae

Magnetic fields have recently gained attention as a non-invasive and energy-efficient strategy to stimulate biological activity, offering novel possibilities for enhancing carbon capture and utilization processes. In particular, microalgae, highly efficient photosynthetic microorganisms, play a crucial role in CO_2 sequestration, converting inorganic carbon into biomass and a wide range of valuable bioproducts (such as pigments). Despite this potential, large-scale implementation of microalgae-based systems remains limited by intrinsic biological constraints, such as relatively slow growth rates, suboptimal light utilization, and environmental variability [66]. Emerging evidence indicates that SMF can influence microalgal physiology by modulating cellular metabolism, photosynthetic performance, and pigment biosynthesis, ultimately leading to improved biomass productivity and CO_2 fixation rates. However, the impact of SMF is species-specific and closely linked to the field intensity, exposure duration, and magnetic sensitivity of each strain. While moderate magnetic intensities tend to enhance growth and photosynthetic efficiency, excessively strong fields may elicit oxidative stress or metabolic inhibition. A

synthesis of key findings from recent studies is presented in Table 1.6 to highlight these contrasting responses and their potential mechanistic explanations.

Table 1.6 Effects of Static Magnetic Field Exposure on Microalgae

Parameter	Effect	Reference
CO_2 capture	96% increase with 4h/day exposure to 45 mT Increased 50% under 60 mT for1h/day	[61] [67]
Chlorophyll content	Increased from 6.8 mg/L to 18.4 mg/L under 4h of exposure to 45 mT	[61]
Oxygen production	24.6% increase in the algal-bacterial system	[68]
Biomass Yield	9.8% increase in Tribonema sp. 34% increase in Chlorella fusca.	[69] [67]
Photosynthetic activity	Increased by a factor of 2.1 at 10 mT	[70]
Economic Benefits	Low-cost, non-toxic, energy-efficient, supports the circular economy	[61], [71]

CO_2 mitigation remains a critical global challenge, and while many technologies offer partial solutions, their integration and optimization are essential for a scalable, sustainable impact. SMF enhanced biological systems—particularly those involving microalgae—represent a promising frontier in carbon capture technology, with potential to significantly improve the efficiency, feasibility, and multifunctionality of CO_2 treatment systems.

1.4 Justification of the Thesis Work

Industrial and urban emissions release a wide variety of gaseous pollutants into the atmosphere, including VOCs and greenhouse gases, such as CO_2. These emissions are primary contributors to air pollution, acid rain, photochemical smog, and climate change, posing significant risks to environmental and public health.

VOCs are known to affect human health and the environment adversely; thus, several treatment technologies have been developed to mitigate VOC emissions. Among these, biological treatments offer a cost-effective and environmentally friendly alternative. However, the efficiency of these processes is often limited by several factors, including the presence of recalcitrant compounds and high inlet pollutant loads, which can lead to excessive biomass accumulation. To overcome this limitation, physical stimuli, such as the SMFs, have been explored to enhance biodegradation performance. SMFs have demonstrated promising results in wastewater treatment, including improvements in denitrification process rates and controlled biomass proliferation. More recently, SMF exposure has also been associated with enhanced removal efficiency of various gas-phase pollutants, including VOCs and CO_2.

According to the U.S. Environmental Protection Agency [72], methanol, hexane, and toluene ranked among the most emitted VOCs in the United States, occupying the 1st, the 2nd, and the 6th positions, respectively, with point-source air emissions of 26 781, 10 891, and 3 938 tons. Additionally, CO_2 emissions reached 36,300 million tons per year, surpassing the Earth's natural CO_2 absorption capacity of 21,000 million tons. These values highlight the environmental relevance of selecting these compounds as model gas waste effluents for experimental analysis.

In this context, the present study investigates the influence of SMF exposure on the biological treatment of selected VOCs with differing physicochemical properties, particularly solubility, and CO_2 biofixation using different pure strains of microalgae to determine whether SMF application can improve treatment performance.

1.5 Hypothesis

The application of low-intensity static magnetic fields, ranging from 20 to 120 mT, to biological systems involved in the treatment of pollutant emissions will stimulate physicochemical and microbial processes, which will improve the biological treatment of waste gaseous streams.

1.1 Objectives

1.1.1 General objective

Study the effect of low-intensity SMF (20-120 mT) on the biological treatment of gaseous pollutants, such as VOCs and CO_2.

1.1.2 Specific objectives

- To evaluate the effect of exposure to low-intensity magnetic fields (20-70 mT) on the biodegradation performance, microbial viability, biomass growth and the diversity of the microbial community during the treatment of volatile organic compounds with different solubilities (toluene, hexane and methanol) in fed-batch systems.
- Assess the impact of a 50 mT magnetic field on the biological treatment of toluene in a biofilter operated under two different experimental periods (continuous for 45 days and intermittent for 20 days).
- Investigate the influence of different magnetic field intensities (30-120 mT) and exposure times (1-4 h d^{-1}) on CO_2 fixation and O_2 production in batch cultures of three pure microalgae strains.

1.2 Overview of Experimental Studies

Chapter II aimed to evaluate the influence of the exposure to different SMF intensities (20, 40, and 70 mT) on the biodegradation of a hydrophobic (hexane), moderately hydrophilic (toluene), and hydrophilic (methanol) VOCs in fed-batch bioreactors. The effect was evaluated in terms of physicochemical modifications, such as partition coefficients, and in biological responses of the microbial community in terms of biodegradation efficiency, biomass production, cell viability, and microbial diversity shifts.

In Chapter III, the effect of exposure to SMF was evaluated on the biological removal of toluene vapors in biofiltration systems. The research focused on determining whether the presence of 50 mT could enhance toluene removal efficiency and improve the robustness of biofilters subjected to both continuous and intermittent pollutant loads. The study also aimed to identify the underlying mechanisms associated with improved performance, focusing on biomass accumulation, extracellular polymeric substances composition, and cell viability. By comparing the performance of identical biofilters operated with and without magnetic stimulations, this work intends to provide new insights into the potential applications of SMF.

Chapter IV aimed to evaluate the influence of SMF exposure to 30, 60, and 120 mT for 1, 2, or 4 hours per day on the growth, CO_2 biofixation, and biomolecule synthesis of three model microalgae: *Chlorella vulgaris*, *Coelastrella* sp., and *Arthrospira platensis*. The research also aimed to identify potential “magnetic windows” that enhance cellular metabolism and improve the efficiency of microalgae-based CO_2 capture systems. Batch cultures of each species were grown under a “dragging process” to maintain a period of exposure of 8-9 days. This design enabled the identification of MF intensity and exposure-time combinations that enhanced CO_2 biofixation and pigment synthesis, demonstrating the presence of an optimal magnetic stimulation range for improved microalgal productivity.

1.3 References

[1] A. Mangotra and S. K. Singh, “Volatile organic compounds: A threat to the environment and health hazards to living organisms – A review,” *J. Biotechnol.*, vol. 382, no. August 2023, pp. 51–69, 2024, doi: 10.1016/j.jbiotec.2023.12.013.

[2] H. Haug, L. Klein, T. Sauerwald, B. Poelke, J. Beauchamp, and A. Roloff, “Sampling Volatile Organic Compound Emissions from Consumer Products: A Review,” *Crit. Rev. Anal. Chem.*, vol. 54, no. 7, pp. 1895–1916, 2024, doi: 10.1080/10408347.2022.2136484.

[3] S. Liang, S. Gao, S. Wang, W. Chai, W. Chen, and G. Tang, “Characteristics, sources of volatile organic compounds, and their contributions to secondary air pollution during different periods in Beijing, China,” *Sci. Total Environ.*, vol. 858, no. November 2022, p. 159831, 2023, doi: 10.1016/j.scitotenv.2022.159831.

[4] C. Sonne, C. Xia, P. Dadvand, A. C. Targino, and S. S. Lam, “Indoor volatile and semi-volatile organic toxic compounds: Need for global action,” *J. Build. Eng.*, vol. 62, no. June, p. 105344, 2022, doi: 10.1016/j.jobe.2022.105344.

[5] M. S. Hussain *et al.*, “Unlocking the secrets: Volatile Organic Compounds (VOCs) and their devastating effects on lung cancer,” *Pathol. Res. Pract.*, vol. 255, no. December 2023, p. 155157, 2024, doi: 10.1016/j.prp.2024.155157.

[6] Y. Xiong, K. Du, and Y. Huang, “One-third of global population at cancer risk due to elevated volatile organic compounds levels,” *npj Clim. Atmos. Sci.*, vol. 7, no. 1, pp. 1–11, 2024, doi: 10.1038/s41612-024-00598-1.

[7] L. Tang, M. Liu, and J. Tian, “Volatile organic compounds exposure associated with depression among U.S. adults: Results from NHANES 2011–2020,” *Chemosphere*, vol. 349, no. June 2023, p. 140690, 2024, doi: 10.1016/j.chemosphere.2023.140690.

[8] C. Li *et al.*, “Volatile organic compounds exposure in relation to glucose homeostasis and type 2 diabetes in older adults from the NHANES,” *Sci. Rep.*, vol. 14, no. 1, pp. 1–10, 2024, doi: 10.1038/s41598-024-81255-8.

[9] S. Chen *et al.*, “Urinary metabolites of multiple volatile organic compounds, oxidative stress biomarkers, and gestational diabetes mellitus: Association analyses,” *Sci. Total Environ.*, vol. 875, no. January, p. 162370, 2023, doi: 10.1016/j.scitotenv.2023.162370.

[10] X. W. P, G. A. Akowuah, and J. H. Chin, “Evaluation of the sub-acute oral toxic effect of methanol extract of Clinacanthus nutans leaves in rats,” *J. Acute Dis.*, vol. 2, no. 1, pp. 29–32, 2013, doi: 10.1016/S2221-6189(13)60090-6.

[11] B. Cruz-García, A. S. Geronimo-Meza, C. Martínez-Lievana, S. Arriaga, Y. Huante-González, and A. Aizpuru, “Biofiltration of high concentrations of methanol vapors: removal performance, carbon balance and microbial and fly populations,” *J. Chem. Technol. Biotechnol.*, vol. 94, no. 6, pp. 1925–1936, 2019, doi: 10.1002/jctb.5974.

[12] M. Cortés-Castillo, A. Encinas, A. Aizpuru, and S. Arriaga, “Effect of applying a magnetic field on the biofiltration of hexane over long-term operation period,” *Environ. Sci. Pollut. Res.*, no. 0123456789, 2024, doi: 10.1007/s11356-024-34671-2.

[13] Q. Li *et al.*, “Static magnetic field enhances the purification of gaseous n-hexane in airlift two-phase partitioning bioreactor,” *Process Biochem.*, vol. 156, no. June, pp.

209–216, 2025, doi: 10.1016/j.procbio.2025.06.003.

[14] L. Ruiz-García *et al.*, “Possible role of n-hexane as an endocrine disruptor in occupationally exposed women at reproductive age,” *Toxicol. Lett.*, vol. 330, no. April, pp. 73–79, 2020, doi: 10.1016/j.toxlet.2020.04.022.

[15] R. Pachaiappan, L. Cornejo-Ponce, R. Rajendran, K. Manavalan, V. Femilaa Rajan, and F. Awad, “A review on biofiltration techniques: recent advancements in the removal of volatile organic compounds and heavy metals in the treatment of polluted water,” *Bioengineered*, vol. 13, no. 4, pp. 8432–8477, 2022, doi: 10.1080/21655979.2022.2050538.

[16] K. Vikrant *et al.*, “Bio-filters for the treatment of VOCs and odors - a review,” *Asian J. Atmos. Environ.*, vol. 11, no. 3, pp. 139–152, 2017, doi: 10.5572/ajae.2017.11.3.139.

[17] G. Zheng *et al.*, “A new attempt to control volatile organic compounds (VOCs) pollution - Modification technology of biomass for adsorption of VOCs gas,” *Environ. Pollut.*, vol. 336, no. August, p. 122451, 2023, doi: 10.1016/j.envpol.2023.122451.

[18] X. Zhang, B. Gao, A. E. Creamer, C. Cao, and Y. Li, “Adsorption of VOCs onto engineered carbon materials: A review,” *J. Hazard. Mater.*, vol. 338, pp. 102–123, 2017, doi: 10.1016/j.jhazmat.2017.05.013.

[19] S. Ojala *et al.*, “Utilization of volatile organic compounds as an alternative for destructive abatement,” *Catalysts*, vol. 5, no. 3, pp. 1092–1151, 2015, doi: 10.3390/catal5031092.

[20] Z. Shayegan, F. Haghighat, and C. S. Lee, “Anatase/brookite biphasic surface fluorinated Fe–TiO2 photocatalysts to enhance photocatalytic removal of VOCs under visible and UV light,” *J. Clean. Prod.*, vol. 287, p. 125462, 2021, doi: 10.1016/j.jclepro.2020.125462.

[21] R. El Khawaja *et al.*, “Boosting VOCs elimination by coupling different techniques,” *Chem. Synth.*, vol. 2, no. 2, 2022, doi: 10.20517/cs.2022.10.

[22] Y. Cheng *et al.*, “Challenges and solutions for biofiltration of hydrophobic volatile organic compounds,” *Biotechnol. Adv.*, vol. 34, no. 6, pp. 1091–1102, 2016, doi: 10.1016/j.biotechadv.2016.06.007.

[23] S. Keramati, M. Ferdowsi, and S. M. Zamir, “Compounds interactions during simultaneous biodegradation of hydrophobic n-hexane and hydrophilic methanol vapors in one- and two-liquid phase conditions,” *Process Saf. Environ. Prot.*, vol. 147, pp. 283–291, 2021, doi: 10.1016/j.psep.2020.09.040.

[24] D. H. Jeon, S. T. Bae, and S. J. Park, “Preparation and characterization of chemically activated carbon materials for CO2 capture,” *Carbon Lett.*, vol. 17, no. 1, pp. 85–89, 2016, doi: 10.5714/CL.2016.17.1.085.

[25] M. Crippa *et al.*, “Carbon dioxide emissions of all world countries,” 2022. doi: 10.2760/07904.

[26] A. Shakoor, F. Ashraf, S. Shakoor, A. Mustafa, A. Rehman, and M. M. Altaf, “Biogeochemical transformation of greenhouse gas emissions from terrestrial to atmospheric environment and potential feedback to climate forcing,” *Environ. Sci. Pollut. Res.*, vol. 27, no. 31, pp. 38513–38536, 2020, doi: 10.1007/s11356-020-10151-1.

[27] D. J. Soeder, “Greenhouse Gas and Climate Change,” in *Energy Futures*, 2025, pp. 97–141.

[28] S. Yüksel and A. Mikhaylov, “The Effect of the Carbon Tax to Minimize Emission,” in *Clean Energy Investments for Zero Emissions Projects*, 2022, pp. 1–11.

[29] E. Hanson, C. Nwakile, and V. O. Hammed, “Carbon capture, utilization, and storage (CCUS) technologies: Evaluating the effectiveness of advanced CCUS solutions for reducing CO2 emissions,” *Results in Surfaces and Interfaces*, vol. 18, no. December 2024, p. 100381, 2025, doi: 10.1016/j.rsurfi.2024.100381.

[30] X. Gu *et al.*, “Technical-environmental assessment of CO2 conversion process to dimethyl carbonate/ethylene glycol,” *J. Clean. Prod.*, vol. 288, p. 125598, 2021, doi: 10.1016/j.jclepro.2020.125598.

[31] G. Chen, R. Wang, M. Sun, J. Chen, E. Iyobosa, and J. Zhao, “Carbon dioxide reduction to high–value chemicals in microbial electrosynthesis system: Biological conversion and regulation strategies,” *Chemosphere*, vol. 344, no. September, p. 140251, 2023, doi: 10.1016/j.chemosphere.2023.140251.

[32] S. Karishma, R. Kamalesh, A. Saravanan, V. C. Deivayanai, P. R. Yaashikaa, and A. S. Vickram, “A review on recent advancements in biochemical fixation and transformation of CO2 into constructive products,” *Biochem. Eng. J.*, vol. 208, no. April, p. 109366, 2024, doi: 10.1016/j.bej.2024.109366.

[33] H. Onyeaka and O. C. Ekwebelem, “A review of recent advances in engineering bacteria for enhanced CO2 capture and utilization,” *Int. J. Environ. Sci. Technol.*, vol. 20, no. 4, pp. 4635–4648, 2023, doi: 10.1007/s13762-022-04303-8.

[34] R. A. Mohedano, G. Tonon, R. H. R. Costa, C. Pelissari, and P. Belli Filho, “Does duckweed ponds used for wastewater treatment emit or sequester greenhouse gases?,” *Sci. Total Environ.*, vol. 691, pp. 1043–1050, 2019, doi: 10.1016/j.scitotenv.2019.07.169.

[35] A. Aslam *et al.*, “Heavy metal bioremediation of coal-fired flue gas using microalgae under different CO2 concentrations,” *J. Environ. Manage.*, vol. 241, no. March, pp. 243–250, 2019, doi: 10.1016/j.jenvman.2019.03.118.

[36] A. Jacob, A. Xia, and J. D. Murphy, “A perspective on gaseous biofuel production from micro-algae generated from CO2 from a coal-fired power plant,” *Appl. Energy*, vol. 148, pp. 396–402, 2015, doi: 10.1016/j.apenergy.2015.03.077.

[37] M. Sendi, M. Bui, N. Mac Dowell, and P. Fennell, “Geospatial techno-economic and environmental assessment of different energy options for solid sorbent direct air capture,” *Cell Reports Sustain.*, vol. 1, no. 8, p. 100151, 2024, doi: 10.1016/j.crsus.2024.100151.

[38] S. Budinis, S. Krevor, N. Mac Dowell, N. Brandon, and A. Hawkes, “An assessment of CCS costs, barriers and potential,” *Energy Strateg. Rev.*, vol. 22, no. January, pp. 61–81, 2018, doi: 10.1016/j.esr.2018.08.003.

[39] P. Xu *et al.*, “Scale-up of microalgal systems for decarbonization and bioproducts: Challenges and opportunities,” *Bioresour. Technol.*, vol. 398, no. January, p. 130528, 2024, doi: 10.1016/j.biortech.2024.130528.

[40] A. P. Abreu, R. C. Morais, J. A. Teixeira, and J. Nunes, “A comparison between

microalgal autotrophic growth and metabolite accumulation with heterotrophic, mixotrophic and photoheterotrophic cultivation modes," *Renew. Sustain. Energy Rev.*, vol. 159, no. September 2021, 2022, doi: 10.1016/j.rser.2022.112247.

[41] X.-G. Zhu, S. P. Long, and D. R. Ort, "What is the maximum efficiency with which photosynthesis can convert solar energy into biomass?," *Curr. Opin. Biotechnol.*, vol. 19, no. 2, pp. 153–159, 2008, doi: 10.1016/j.copbio.2008.02.004.

[42] S. K. Singh, S. Sundaram, S. Sinha, M. A. Rahman, and S. Kapur, "Recent advances in CO2 uptake and fixation mechanism of cyanobacteria and microalgae," *Crit. Rev. Environ. Sci. Technol.*, vol. 46, no. 16, pp. 1297–1323, 2016, doi: 10.1080/10643389.2016.1217911.

[43] R. Prasad *et al.*, "Role of microalgae in global co2 sequestration: Physiological mechanism, recent development, challenges, and future prospective," *Sustain.*, vol. 13, no. 23, 2021, doi: 10.3390/su132313061.

[44] A. Al-Dailami, I. Koji, I. Ahmad, and M. Goto, "Potential of Photobioreactors (PBRs) in Cultivation of Microalgae," *J. Adv. Res. Appl. Sci. Eng. Technol.*, vol. 27, no. 1, pp. 32–44, 2022, doi: 10.37934/araset.27.1.3244.

[45] G. Yadav, B. K. Dubey, and R. Sen, "A comparative life cycle assessment of microalgae production by CO2 sequestration from flue gas in outdoor raceway ponds under batch and semi-continuous regime," *J. Clean. Prod.*, vol. 258, p. 120703, 2020, doi: 10.1016/j.jclepro.2020.120703.

[46] W. Li, H. Ma, R. He, X. Ren, and C. Zhou, "Prospects and application of ultrasound and magnetic fields in the fermentation of rare edible fungi," *Ultrason. Sonochem.*, vol. 76, no. May, p. 105613, 2021, doi: 10.1016/j.ultsonch.2021.105613.

[47] A. Perrin, "MRI and static electric and magnetic fields," in *Electromagnetic Fields, Environment and Health*, 2012, pp. 11–24.

[48] OpenStax College, "Magnetic Forces and Files," in *University Physics Volume 2*, 2016.

[49] X. Zhang, K. Yarema, and A. Xu, *Biological Efects of Static Magnetic Fields*. 2017.

[50] T. Yoshino, Y. Maeda, and T. Matsunag, "Bioengineering of bacterial magnetic particles and their applications in biotechnology," *Recent Pat. Biotechnol.*, vol. 4, no. 3, pp. 214–225, 2010, doi: 10.2174/187220810793611455.

[51] C. T. Yavuz, A. Prakash, J. T. Mayo, and V. L. Colvin, "Magnetic separations: From steel plants to biotechnology," *Chem. Eng. Sci.*, vol. 64, no. 10, pp. 2510–2521, 2009, doi: 10.1016/j.ces.2008.11.018.

[52] S. Ueno and M. Sekino, "Biomagnetics and bioimaging for medical applications," *J. Magn. Magn. Mater.*, vol. 304, no. 1, pp. 122–127, 2006, doi: 10.1016/j.jmmm.2006.01.252.

[53] J. Miyakoshi, "Effects of static magnetic fields at the cellular level," *Prog. Biophys. Mol. Biol.*, vol. 87, no. 2-3 SPEC. ISS., pp. 213–223, 2005, doi: 10.1016/j.pbiomolbio.2004.08.008.

[54] S. Romeo, A. Sannino, M. R. Scarfì, R. Massa, R. Dangelo, and O. Zeni, "Lack of effects on key cellular parameters of MRC-5 human lung fibroblasts exposed to 370

mT static magnetic field," *Sci. Rep.*, vol. 6, no. December 2015, pp. 1–10, 2016, doi: 10.1038/srep19398.

[55] T. M. Guzmán-Armenteros, J. Ruales, and L. Ramos-Guerrero, "A Review of Electromagnetic Fields in Cellular Interactions and Cacao Bean Fermentation Tania," *Foods*, vol. 13, no. 3058, pp. 1–17, 2024, [Online]. Available: https://doi.org/10.3390/foods13193058.

[56] S. Chen, Y. Jin, N. Yang, L. Wei, D. Xu, and X. Xu, "Improving microbial production of value-added products through the intervention of magnetic fields," *Bioresour. Technol.*, vol. 393, no. August 2023, p. 130087, 2024, doi: 10.1016/j.biortech.2023.130087.

[57] V. Savchenko, O. Synyavskiy, A. Dudnyk, A. Nesvidomin, V. Ramsh, and V. Bunko, "The Impact of a Direct Magnetic Field on the Cells," *2020 IEEE KhPI Week Adv. Technol. (KhPIWeek), Kharkiv, Ukr.*, pp. 193–198, 2020, [Online]. Available: 10.1109/KhPIWeek51551.2020.9250104.

[58] A. Kthiri, S. Hidouri, T. Wiem, R. Jeridi, D. Sheehan, and A. Landouls, "Biochemical and biomolecular effects induced by a static magnetic field in Saccharomyces cerevisiae: Evidence for oxidative stress," *PLoS One*, vol. 14, no. 1, pp. 1–12, 2019, doi: 10.1371/journal.pone.0209843.

[59] M. Woroszyło *et al.*, "The impact of intraspecies variability on growth rate and cellular metabolic activity of bacteria exposed to rotating magnetic field," *Pathogens*, vol. 10, no. 11, pp. 1–24, 2021, doi: 10.3390/pathogens10111427.

[60] C. Guo-Fu *et al.*, "Static magnetic field exposure modulates gut microbiota and host metabolism to alleviate high-fat diet-induced metabolic dysfunction-associated fatty liver disease," *Zool. Res.*, vol. 46, no. 0, pp. 1–12, 2025, doi: 10.24272/j.issn.2095-8137.2024.462.

[61] L. Torres, J. O. Saucedo-Lucero, A. Aizpuru, and S. Arriaga, "Post-Treatment of CO_2 Emissions With Microalgae: Magnetic Field-Induced Improvements in an AirLift Photoreactor," *Biotechnol. Bioeng.*, 2025, doi: 10.1002/bit.29032.

[62] Y. Quan, H. Wu, Z. Yin, Y. Fang, and C. Yin, "Effect of static magnetic field on trichloroethylene removal in a biotrickling filter," *Bioresour. Technol.*, vol. 239, pp. 7–16, 2017, doi: 10.1016/j.biortech.2017.04.121.

[63] M. Łebkowska, A. Rutkowska-Narozniak, E. Pajor, and Z. Pochanke, "Effect of a static magnetic field on formaldehyde biodegradation in wastewater by activated sludge," *Bioresour. Technol.*, vol. 102, no. 19, pp. 8777–8782, 2011, doi: 10.1016/j.biortech.2011.07.040.

[64] L. Křiklavová, M. Truhlář, P. Škodová, T. Lederer, and V. Jirků, "Effects of a static magnetic field on phenol degradation effectiveness and Rhodococcus erythropolis growth and respiration in a fed-batch reactor," *Bioresour. Technol.*, vol. 167, pp. 510–513, 2014, doi: 10.1016/j.biortech.2014.06.060.

[65] D. Chen *et al.*, "Enhanced gaseous chlorobenzene removal and its microbial mechanism through innovative modified packings coupled with magnetic field in a biotrickling filter," *Front. Environ. Sci. Eng.*, vol. 19, no. 11, 2025, doi: 10.1007/s11783-025-2072-x.

[66] Y. Gao, O. Bernard, A. Fanesi, P. Perré, and F. Lopes, “The effect of light intensity on microalgae biofilm structures and physiology under continuous illumination,” *Sci. Rep.*, vol. 14, no. 1, pp. 1–11, 2024, doi: 10.1038/s41598-023-50432-6.

[67] K. M. Deamici, L. O. Santos, and J. A. V. Costa, “Use of static magnetic fields to increase CO2 biofixation by the microalga Chlorella fusca,” *Bioresour. Technol.*, vol. 276, no. December 2018, pp. 103–109, 2019, doi: 10.1016/j.biortech.2018.12.080.

[68] R. Tu, W. Jin, T. Xi, Q. Yang, S. F. Han, and A. E. F. Abomohra, “Effect of static magnetic field on the oxygen production of Scenedesmus obliquus cultivated in municipal wastewater,” *Water Res.*, vol. 86, pp. 132–138, 2015, doi: 10.1016/j.watres.2015.07.039.

[69] F. Zhu *et al.*, “Weak magnetic field intervention on outdoor production of oil-rich filamentous microalgae: Influence of seasonal changes,” *Bioresour. Technol.*, vol. 348, no. January, p. 126707, 2022, doi: 10.1016/j.biortech.2022.126707.

[70] D. P. Small, N. P. Hüner, and W. Wan, “Effect of static magnetic fields on the growth, photosynthesis and ultrastructure of Chlorella kessleri microalgae,” *Bioelectromagnetics*, vol. 33, no. 4, pp. 298–308, 2012, [Online]. Available: https://doi.org/10.1002/bem.20706.

[71] L. O. Santos, K. M. Deamici, B. C. Menestrino, J. Garda-Buffon, and J. A. V. Costa, “Magnetic treatment of microalgae for enhanced product formation,” *World J. Microbiol. Biotechnol.*, vol. 33, no. 9, pp. 1–6, 2017, doi: 10.1007/s11274-017-2332-4.

[72] EPA, (2025). United States Environmental Protection Agency. 2022. “TRI Explorer (2023 National Analysis Dataset (updated July 2025, released July 2025)) [Internet database]. Retrieved from https://enviro.epa.gov/triexplorer/, (September23, 2025).

CHAPTER II. Effects of static magnetic field exposure on the biodegradation of volatile organic compounds with different hydrophilicities

The present chapter is a modified version of the article under preparation: López-Bello E, Valenzuela Edgardo I., Arriaga S, Aizpuru A, 2025. Effects of static magnetic field exposure on the biodegradation of volatile organic compounds with different hydrophilicities.

2.1 Abstract

Biodegradation of three Volatile Organic Compounds (VOCs) was carried out in fed batch bioreactors, in absence or in presence of static magnetic fields (SMFs) of different intensities (20, 40, and 70 mT). The VOCs were selected to represent highly hydrophobic, moderately hydrophilic and hydrophilic pollutants commonly encountered in gaseous industrial emissions (hexane, toluene, and methanol, respectively). The biodegradation rate in toluene consumption increased up to 30%. The performance follows the order SMF 70mT (11.5 gm-3h-1) > SMF 40 mT (10.9 gm-3h-1) > SMF 20 mT (10.4 gm-3h-1) > SMF 0mT (8.8 gm-3h-1). The fed batch with methanol shows a positive effect under SMF 40 mT (2.1 gm-3h-1) > SMF 70 mT (1.9 gm-3h-1) > SMF 20 mT (1.67 gm-3h-1) > 0 mT (1.42 gm-3h-1). For hexane, 20 mT decreased its consumption by 29%, with no effects at 40 and 70 mT. SMF exposure also induces changes in the microbial community. The fed batch with toluene increases the relative abundance (RA) of Pseudomonas and *Luteimonas*. Experiments with hexane increase the RA of *Rhodoccoccus* and Flavobacterium, and the methanol-degrading batch test presented an increase in *Luteimonas* and *Hyphomicrobium*. These results confirmed that a proper SMF could improve the biodegradation of different VOCs.

2.2 Introduction

Volatile organic compounds (VOCs), a major group of atmospheric pollutants, have a recognized impact on environment and human health [1], [2]. Methanol, hexane, and toluene currently stand out among the most typical emitted VOCs, being the first, the second, and the sixth most released VOCs in the United States, with point source air emissions, for the year 2023, of around 24, 13, and 3 kilotons, respectively. Of such emissions, the paper industry generates most methanol releases (76%), while the food industry is the main responsible of hexane emissions (75%). On the contrary, toluene vapors are more equitably emitted, with major contributions by the chemical, paper and petroleum industry (around 23.2, 13.5, and 12.7%, respectively) (EPA, 2025). All three compounds produce eye irritations, headaches, and affect the respiratory and central nervous systems. These three VOCs are particularly interesting as model compounds, as they are members of different structural groups (oxygenated, aliphatic, and aromatic VOCs), with different polarities. Particularly, methanol, hexane, and toluene have a wide difference in hydrophilicity, being considered hydrophilic (dimensionless Henry´s law constant (H)<0.1; H≈0.0016), hydrophobic (H>1; H≈70), and moderately hydrophilic (0.1<H<1; H≈0.272), respectively [4], [5].

Several physicochemical and biological treatments are available for the mitigation of VOCs emissions. However, in many cases, biofiltration, a typical biological VOC treatment technology, is the most cost-effective and environmentally friendly option [4], [6]. In a biofilter, the contaminated airstream passes through a porous packing material colonized by a biofilm. A thin layer of water covers such biofilm, and a mineral solution occasionally sprays the packing material to maintain adequate moisture content and to provide nutrients for microorganisms [2], [4]. The treatment of VOCs consists of two sequential steps, with a first transfer of the pollutants from the gas to the water phase, and a subsequent biological conversion of VOCs to CO_2, H_2O, and biomass [2]. Thus, biofiltration removal capacity can be limited by one of these two steps [5], [6]. Particularly, the low water solubility and high resistance to mass transfer of hydrophobic VOCs hinders their elimination capacities [2], [4], [7]. This is the case for the highly hydrophobic hexane, which poor transfer to the water

phase and consequently lower availability for microorganisms restricts biofilter efficiency [5]. Contrastingly, for highly hydrophilic VOCs, particularly at elevated gaseous concentrations, the fast mass transfer to the water phase can generate high amounts of VOCs in the biofilm, which may exceed microorganisms assimilation rates [4]. Such accumulation of hydrophilic VOC in the biofilm can be toxic to the cells or lead to the inhibition of the substrate consumption [4]–[6]. In the case of the highly hydrophilic methanol, the inhibition of biofilter efficiency at high concentrations due to methanol toxicity has already been noted [6]. Particularly, under the same inlet load, high methanol concentrations of around 14 g m^{-3} have been related to a 15 % reduction of biofilter elimination capacity compared to the operation at concentrations no higher than 10.5 g m^{-3} [8].

In this context, many studies have focused on overcoming biofiltration limitations, in order to improve specific VOCs removal efficiencies. However, systematic evaluation of biofilters under numerous working settings is prohibitively expensive and time-consuming. In practice, an alternative reactor configuration, usually referred to as a “microcosm”, historically provides valuable information regarding biofiltration potential under specific conditions. Microcosms, designed to mimic the biofiltration environment, consist in a biphasic gas-tight sealed batch reactor. They contain microorganisms inoculated in a packing material or in a mineral medium, above which a gaseous headspace holds a given initial amount of VOC vapor [9]. Such microcosms have allowed the comparison of the kinetics of VOC consumption under different configurations. As such, they have been used to select the most suitable microorganisms for treating specific gaseous components, or to assess the potential VOC degradation capabilities of particular microbial consortiums [10] [11]. Microcosms have also been used to establish advantageous biofiltration operating conditions, by assessing the impact of temperature, pH, and MM composition, or by addressing the potential inhibitions when treating mixtures of VOCs, as well as the pollutant transfer alterations by adding different fractions of silicon oil [12][11] [6]. Similarly, microcosms have indicated an improvement of chlorobenzene vapors degradation with magnetic bioaugmentation. In the first 10 hours of operation, the chlorobenzene removal rate achieved 14.7 instead of 10.0 mg L^{-1} h^{-1}, when

incorporating magnetized powder in the microbial packing material, providing an internal magnetic field intensity range between 0.5-4 mT. Such was a result of both a higher chlorobenzene gas-liquid mass transfer and a higher enzymatic activity in presence of the internal magnetic field [13].

The presence of an external magnetic field of constant intensity (Static Magnetic Field (SMF)), provided by magnets or electromagnetic coils, can also have a significant impact on microorganisms and their activity. Particularly, within a specific intensity window, SMFs can strongly improve the efficiency of biological pollutant removal. As such, many studies have already confirmed that magnetic fields could boost the capacities of biological wastewater treatments [14], e.g. by allowing a further reduction of the chemical oxygen demand or of the nitrogen content [15]–[17]. Similarly, SMFs have allowed for an improvement of bioenergy production, either during fermentation of glucose for the production of hydrogen [18], or during anaerobic digestion for the production of methane [19]. However, the studies dealing with the effect of SMFs during the biological treatment of VOC vapors remain scarce. To date, only four studies have addressed the impact of SMFs in biofilters treating VOCs. The first two studies treated a recalcitrant chlorinated VOC, trichloroethylene (TCE) [20], [21]. In the case of the removal of TCE in a bacterial consortium biofilter, the SMF intensity was a key parameter, as such intensity determined the positive or negative outcome compared to the non-exposed biofilter. Indeed, for inlet loads of about 4.3 g m^{-3} h^{-1}, the presence of a 60 or 130 mT SMF stimulated (+30%) or inhibited (-14 %) the TCE maximum elimination capacity (EC_{max}) compared to the non-exposed biofilter (1.97 g m^{-3} h^{-1}), respectively [20]. In the case of a fungal biofilter, for an inlet load of about 9 g m^{-3} h^{-1}, in presence of a SMF of 20, 60 and 80 mT, the EC_{max} reached 35, 16 and 11 % higher values than the non-exposed biofilter (3.6 g m^{-3} h^{-1}), respectively [21]. Very recently, a study evaluated the biofiltration of hexane in presence of SMFs. After a period of 93 days without a clear difference in removal efficiency between biofilters, hexane removal efficiency (RE) finally achieved a significant improvement with SMFs, reaching similar average values of 35% under 10 and 30 mT, while achieving a RE of only 25% without SMF. Two recent studies combined SMFs with the presence of silicon oil as a non-aqueous phase to

facilitate hydrophobic VOC transfer from the gas to the liquid phase [22], [23]. One of the studies treated chlorobenzene (CB) in biofilters operated with a modified packing material, which incorporated silicon oil with and without magnetic powders delivering a 1-3 mT SMF range [22]. The SMF complemented the RE improvement due to the addition of silicon oil, particularly at high inlet concentrations (500 mg m^{-3}), where the RE surpassed that of the non-magnetic packing material by 10%. The other study, which treated vapors of hexane, did not operate a typical biofilter, but a biphasic airlift bioreactor [23]. In all operational periods, the performance was always higher in presence of an external 20 mT SMF, achieving average REs of 93 and 82%, in presence or in absence of the SMF, respectively.

Although the exact mode of action of SMF within biological processes remains not well understood, several mechanisms have been proposed [24]. However, the desired effects generally occur within a specific SMF intensity “window”, above a minimum triggering threshold, and below a lethal or inhibitory level. Within such appropriate intensity range, which depends on the microorganisms involved, SMF can boost metabolic activity, and thus pollutant consumption [19]. Enhancement of metabolic activity may be linked with structural modifications of polarized or charged components, molecules, or particles induced by SMFs. Particularly, under SMFs, changes in the polarization and arrangement of the phospholipid membrane may allow for its higher fluidity and permeability, which can favor the transfer of nutrients and substrates [14], [25]. Similarly, SMFs can strengthen many crucial enzymatic activities by affecting electron spin states, electron transport activity and the interactions between metallic ions (Mg^{2+}, Ca^{2+}, Zn^{2+}) and intracellular enzymes [14], [24], [26]. Such enhancement of enzymatic activity has been many times observed during wastewater treatment [14]. For example, average hydroxylamine oxidoreductase activity has significantly increased in presence of a 10 mT SMF (14.917 vs. 14.676 U mg VSS^{-1}) during the denitrification of wastewater [26]. Similarly, in the case of air treatment, during the biodegradation of chlorobenzene vapors in microcosms, the dehydrogenase activity was promoted from 0.207 to 0.810 □mol L^{-1} h^{-1}, when strengthening the internal SMF intensity from 0 to 9 mT, by increasing the proportion of magnetized material in the microbial packing [13]. Such

faster transfer of substrate across the membrane, and/or higher enzymatic activity can also explain the higher microbial growth sometimes observed in presence of SMFs [13], [20], [21], [24], [25]. Thus, by stimulating biomass growth and enzymatic activities, SMFs can potentially dampen the biodegradation kinetic limitations present in biofilters treating hydrophilic compounds.

Additionally, several studies indicate that SMFs can also influence the quantity and composition of extracellular polymeric substances (EPS) secreted by microorganisms, particularly in studies dealing with wastewater treatment [14], [19], but also in some dealings with the treatment of VOCs vapors [22], [25]. In a biofilter treating chlorobenzene vapors in presence of an additional non-aqueous phase, the presence of a 1-3 mT SMF induced a higher amount of tightly bounded EPS, with a higher content of proteins. A higher secretion of proteins, which are part of the hydrophobic components of EPS, can elevate cell surface hydrophobicity (CSH), and in turn, make hydrophobic carbon sources more readily available, favoring their transfer to the cells [22]. In a microcosm study treating the same VOC, the CSH gradually increased from 50.6 to 72.6% when rising the internal SMF intensity from 0 to 9 mT, by increasing the proportion of magnetized material in the microbial packing. Again, the higher CSH (derived from a higher protein secretion) could explain the higher removal of the pollutant under a SMF, by the enhancement of the gas-liquid transfer of the hydrophobic substrate [13]. Thus, by modifying EPS production and composition, and the CSH, SMF can also dampen the gas-liquid mass transfer limitations of hydrophobic compounds during biofiltration treatments.

Finally, it should highlighted that the effects of SMFs are different between microbial species, as each microorganisms have their own intrinsic magnetic susceptibility. As such, the alteration of growth and metabolic activity under SMFs depends on the exposed microorganisms [19]. As a result, SMFs exert a specific pressure on microbial populations. As such, in many studies, the presence of a SMF induced a reduction of microbial diversity, depicted by a lowering of the Shannon index. For example, during the anaerobic digestion of wastewater, a 20 mT SMF reduced the Shannon index from 7.28 to 6.38 [19]. Similarly, during the treatment of TCE,

Shannon indexes dropped from 6.00 to 5.67, and from 3.80 to 2.33, when SMFs of 60 and 20 mT were applied in bacterial and fungal biofilters, respectively [20], [21]. In several studies, such reduction of microbial diversity was associated to an increase in microbial specialization, with a higher abundance of the species specifically implicated in the process [18], [20], [26]. However, such modification of microbial population could also be detrimental to the process, as in the case of a study dealing with the nitrogen removal of wastewater, where the application of a 3.5 mT SMF altered microbial populations, destroying the synergy of functional bacteria [27].

Despite these promising insights, studies examining the application of SMFs to the biodegradation of VOC vapors remain limited. Moreover, until now, no study has reported the impact of the same SMFs for the treatment of VOCs with contrasting physicochemical characteristics. It should be particularly interesting to assess if SMFs can dampen the specific removal limitations proper to hydrophobic VOCs and to high inhibiting concentrations of hydrophilic VOCs. Therefore, this study aims to investigate the physicochemical and biological effects of different intensities of SMFs on the biodegradation of three model VOCs (hexane, toluene, and methanol). By using microcosms as model bioreactors, this work seeks to elucidate the potential of SMF exposure to improve the biodegradation efficiency for VOC emissions. Special attention is put on the impact of SMFs on removal performance, and on the evolution of microbial populations.

2.3 Material and Methods

2.3.1 Microorganism's acclimation and preparation in mineral medium

The wastewater treatment plant of the Universidad del Mar (Oaxaca, Mexico) served as the source of the original microbial inoculum. Three 200 mL samples of wastewater were diluted in 300 mL of mineral medium (MM), and placed in 1 L glass bottles, providing a gaseous headspace of 500 mL. Microorganisms were separately acclimated to toluene, hexane, and methanol under agitation of 120 rpm and at 25ºC. Each culture received a 10 µL dose of the respective VOC three times per week over a two-month acclimation period. Before each VOC addition, headspace was

renewed by opening the microcosm under a laminar hood for 20 min. The mineral medium (MM) was prepared as previously described [28], and adjusted to pH 7. The resulting acclimated microbial consortia were used as inoculum for the microcosm experiments. Fed-batch kinetic assays were initiated with the inoculum properly diluted in MM, in order to provide an initial optical density (OD_{600}) of 0.1, measured using a UV/Vis spectrophotometer (Thermo Scientific, model Genesys 10uv).

2.3.2 Microcosm set-up

Experiments were carried out separately for each VOC, and by triplicate for each SMF (0 (control), 20, 40, and 70 mT), in an orbital incubator under 120 rpm agitation, at 25ºC. Thus, a set of 12 fed-batch biodegradation kinetics was evaluated for each VOC.

Microcosm bioreactors consisted of cylindrical glass serum bottles (120 mL) with an inner diameter of 4.4 cm, sealed with Teflon Mininert valves (Supelco, Bellefonte, PA). They contained 30 mL of inoculated MM (covering a height of 2 cm from the bottom of the flask). The first three kinetics started with the injection of 1, 3 and 5 □L of hexane, toluene and methanol in the 90 mL microcosm headspace, corresponding to theoretical initial vapor concentrations of 7.3, 28.9, and 44 g m^{-3}, respectively. After the first kinetic of VOC consumption, bioreactors were fed with 2, 3 and 5 µL, corresponding to an amount of 1.31, 2.60, and 3.96 mg of hexane, toluene and methanol, respectively, with previous headspace renewal by opening the microcosm under a laminar hood for 20 min, between each fed-batch cycle. Kinetic experiments had a total duration of 20, 17 and 20 days, for hexane, toluene and methanol, respectively. The SMFs were generated by fixing neodymium magnet blocks (50 x 10 x 4 mm) in the stainless steel clamps holding the bottles, in two positions facing each other. The SMF intensity was adjusted by stacking one, two, or three magnet blocks on each position. SMF intensity present in the cylindrical flasks was measured with a Tesla-Meter (HT20, Hengtong, Shanghai, China), at heights of 0, 1, and 2 cm from the flask bottom. Horizontal positions of the SMF intensity measurements were set by dividing the circle into 7 radius consecutively separated with an angle of 45 degrees, and taking measurements at a distance of 0, 0.5, 1, 1.5, 2 and 2.2 cm from the center of the bottle (Figure S2.1 a and b).

2.3.3 Chemical analytical methods

The content of VOC was measured in the liquid or gas phase. For the last kinetic, the production of CO_2 in the gas phase was measured, as well as the dissolved carbon and biomass content, and pH in the MM.

2.3.3.1 Analysis of VOC and of CO_2 by gas chromatography

Evolution of VOC content in the microcosms was evaluated all along each VOC degradation kinetic by gas chromatography, after taking gaseous or liquid samples. For hydrophobic VOCs, as toluene and hexane, 0.1 mL gaseous samples were regularly taken from the bioreactor headspace. For the hydrophilic VOC, methanol, 0.1 µL of the mineral medium was regularly sampled from the liquid phase. Gas or liquid samples were injected in the gas chromatograph equipped with a flame ionization 6890N Network GC System (equipped with an Agilent Technologies capillary column DB-624). The operation conditions were 140 ºC for the oven, and 250 ºC for the injector and detector. CO_2 concentration was measured with a thermal conductivity detector (GC-TCD) in a gas chromatograph (Agilent Technology GC, model 6850N Network GC System, fitted with an Agilent Technologies column HP Plot Q). The gas carrier was N_2, the oven temperature was 60 ºC and the detector and injector temperature were 200º C, respectively.

2.3.3.2 Analysis of the mineral medium at the end of the fed-batch kinetics

For each triplicate, and for each tested VOC, the mineral medium was analyzed at the end of the microcosm operation, after 20, 17, and 20 days of operation, for hexane, toluene and methanol, respectively. Total Organic Carbon (TOC) was measured with a TOC-V_{CSN} SHIDMADZU ASI-V apparatus according with the methodology previously reported [29]. The biomass content was also estimated at the end of batch experiments by measuring the OD_{600} with a UV/Vis spectrophotometer (Thermo Scientific, model Genesys 10uv). The values of pH were obtained with a pH-meter (OAKTON, pH/CON700).

2.3.4 Bacterial community analysis

2.3.4.1 Cell viability

The cell viability of the biomass was determined at the end of the last kinetic by epifluorescence microscopy as previously described [29]. Samples were examined under a 40X magnification in an epifluorescence microscope (EM) (Axon, Imager M2. Zeiss, Inc.). Cell counting was performed in stained samples. The microorganisms were stained with propidium iodide (red), which indicates dead cells and stained with thiazole orange, which indicates living cells (green). A digital camera was used to capture fluorescent micrographs, and ZEN 2012 acquisition software was used to process and analyze the images. Approximately 10 images per sample were processed and analyzed in duplicate. Cell viability was calculated according to previously reported methodology [29].

2.3.4.2 DNA extraction, qPCR and sequencing analysis

Samples from the non-exposed microcosms and the microcosms exposed to 70 mT SMF were taken for each VOC at the beginning and at the end of the experiment. The total genomic DNA of sludge samples were extracted according to the instructions of ZYMO Research kit. The concentration and quality of DNA were measured using a Nanodrop Thermo Scientific ND-100 equipment. DNA samples were stored at -20 ºC until DNA sequencing by NOVOGENE company. The DNA was used to amplify the V34 16S rDNA by using the primers 341F CCTAYGGGRBGCASCAG and 806R GGACTACNNGGGTATCTAAT. For taxonomic microbial community analysis, the retrieved 16S sequences were processed using the divisive amplicon denoising algorithm (DADA2) in the R environment version 4.4.1 via RStudio [30], [31]. For this purpose, high-quality (Q score ≥30) forward and reverse sequences were obtained by truncating their length to 225 bp. Sequences with more than two expected errors or undefined bases (N), as well as chimeric sequences, were discarded. The obtained consensus paired sequences for the amplicon sequence variants (ASVs) were then classified with the classify-sklearn classifier trained against the SILVA 16S rRNA gene reference set (release 138.1) [32]. The sequences, assigned to phylotype clusters, were analyzed using the Shannon, Simpson, and Pielou index (all sequences were taken for the analysis).

2.3.5 Data analysis

2.3.5.1 Percentage of mineralization

To facilitate analysis of the results regarding CO_2 concentrations, the amount of carbon recovered as CO_2 was converted to a percentage of mineralization. The theoretical complete mineralization reactions of toluene (Eq. 1), hexane (Eq. 2), and methanol (Eq. 3) were considered at the end of each VOC degradation kinetic:

$$C_7H_8 + 9\ O_2 \rightarrow 7\ CO_2 + 4\ H_2O \qquad \text{Eq. 1}$$

$$2\ C_6H_{14} + 19\ O_2 \rightarrow 12\ CO_2 + 14\ H_2O \qquad \text{Eq. 2}$$

$$2\ CH_4O + 3\ O_2 \rightarrow 2\ CO_2 + 4\ H_2O \qquad \text{Eq. 3}$$

Based on these stoichiometric relationships, complete mineralization corresponds to the production of 3.34, 3.06, and 1.37 g of CO_2 per g of toluene, hexane, or methanol degraded, respectively. The degree of mineralization was estimated as the ratio between the measured CO_2 and the theoretical maximum CO_2 expected from complete oxidation of all the introduced VOC, at the end of the microcosm kinetic [33].

2.3.5.2 Determination of the Henry's law partition coefficient in presence and in absence of a SMF

Several studies derive the concentration of VOC in the gaseous or liquid phase from the concentration measured from the liquid or gaseous phase, respectively, by using the Henry's law constant (H) available in the literature [34] (equation 4):

$$H = \frac{C_g}{C_l} \qquad \text{Eq. 4}$$

Where C_g and C_l are the gaseous and liquid VOC concentrations, respectively.

However, literature H values are available for infinite dilution in water, in absence of any mineral salt. For the specific configuration of the studied system, H values can be more precisely determined experimentally. Determination of H was carried out in three microcosm with identical configuration as previously described, but without

inoculation of the MM. Different amounts of each VOC were introduced into each microcosm headspace, till VOC equilibrium was established between the gaseous and liquid phase (>30 min), at 25^0C. Then, the previously described gas chromatography analysis allowed for the determination of the VOC concentration in the liquid or gaseous phase.

For the highly hydrophobic hexane, a very low concentration was present in the liquid phase. For accurate determination of H_{Hexane}, the liquid concentration needed to be precisely determined. Thus, hexane concentration was determined in the liquid phase by sampling the mineral medium after equilibrium. Volumes of 2 to 20 µL of hexane were introduced at 4 µL intervals.

The total amount of VOC introduced (g_{total}) is equal to the amount present at equilibrium in the liquid and in gaseous phase (equation 5).

$$g_{total} = C_l * V_l + C_g * V_g \qquad \text{Eq. 5}$$

Where V_l and V_g are the liquid and gaseous volume in the microcosm (30 and 90 mL), respectively.

From equation 4:

$C_g = H * C_l$

Combining equation 5 with the above equation, and reorganizing, H_{Hexane} is calculated as (Equation 6):

$$(H * C_l) * V_g + C_l * V_l = g_{total}$$

$$C_l(H * V_g + V_l) = g_{total}$$

$$\boldsymbol{H} = \frac{\left(\frac{\boldsymbol{g_{total}}}{\boldsymbol{C_l}}\right) - \boldsymbol{V_l}}{\boldsymbol{V_g}} \qquad \text{Eq. 6}$$

For the less hydrophobic VOCs (methanol and toluene), H was determined by measuring the gaseous concentration at equilibrium. For toluene, incremental injections ranging from 0.5 to 1.7 µL were introduced into the microcosm. For methanol, which is highly hydrophilic, in order to be able to determine gaseous concentrations at equilibrium, larger volumes ranging from 500 to 1800 µL in 200 µL increments were injected in the microcosm.

Henry´s law constants were obtained from VOC gaseous concentration at equilibrium. From equation 4:

$$C_l = \frac{C_g}{H}$$

Combining equation 2 with the above equation, and reorganizing, $H_{Toluene}$ and $H_{Methanol}$ were calculated as (Equation 7):

$$C_g * V_g + \frac{C_g}{H} * V_l = g_{total}$$

$$C_g \left(V_g + \frac{V_l}{H} \right) = g_{total}$$

$$\boldsymbol{H = \frac{V_g}{\left(\frac{g_{total}}{C_g}\right) - V_g}} \qquad \text{Eq. 7}$$

The H values for each VOC were estimated in absence of a SMF, and in presence of the three tested SMFs.

2.3.5.3 Data adjustment to the Gompertz model

For toluene and methanol, at all measured times along the kinetic study, the liquid concentration (methanol and toluene), or the gaseous concentrations obtained (hexane) was estimated according to the previously determined H constant.

The total amount of VOC present in the microcosm at a given time (g_{total}, g) was obtained by adding the quantity of VOC in liquid and gaseous phases (Eq. 2). To obtain the total amount of substrate consumed (S_c, g), the total amount of VOC

present at a given time was subtracted to the initial amount of VOC introduced ($g_{introduced}$, g) (Equation 8):

$$S_c = g_{introduced} - g_{total} \qquad \text{Eq.8}$$

Such consumption (Sc) was adjusted to the Gompertz model, to analyze the VOC consumption kinetics, as expressed in equation 9 (Acuña et al., 1999):

$$\boldsymbol{S_c = \alpha \exp\left(-\beta e^{-kt}\right)} \qquad \text{Eq. 9}$$

Where α (g) is the initial amount of VOC introduced; β is a parameter that can be related to the duration of the lag phase before the consumption of VOC starts (dimensionless); and k (h^{-1}) is the consumption rate of the VOC.

Additionally, the maximum rate of substrate consumed (V_{max}) was calculated as follows [28]: V_{max} =0.368 □ k.

2.3.6 Statistical analysis

The experimental results are shown as average ± standard deviation of the mean (SD). The data from the fed batch reactors with and without SMFs were compared with the control using One-way ANOVA with a post-hoc Fisher adjustment with a significant level of $p \leq 0.05$. The data were analyzed using Minitab Project 21.1.0. The data obtained from the kinetic were adjusted by the Gompertz model with sigmoidal growth using OriginPro 2021 [28].

2.4 Results and discussion

2.4.1 Characterization of the magnetic field

SMFs generated with magnets are known to be less homogeneous than those generated with electromagnetic coils [18], [25], [35]. Thus, the SMFs produced with permanent magnets have different intensities according to the specific coordinates

between the magnets. Figure S2 displays the contour map distribution of the SMF intensities inside the microcoms, for the three configurations, considering the two sets of one, two stacked, and three stacked magnets facing each other. Comparing the three configurations, the stacking of magnetic blocks increased the SMF intensity for a given position in the MM. Regarding the intensity vertical distribution, for a given horizontal cross section and configuration, the lowest values were observed at the bottom and at the top level of the MM (with comparable values at heights of 0, and 2 cm, respectively). Contrarily, the SMF intensity was always significantly higher at the core of the MM (height of 1 cm). Regarding the intensity horizontal distribution, the borders of the flask opposite to the magnets always received the lowest SMF intensities (points located at the angles of 90 and 270^0). Contrarily, the points located at the proximity of the magnets (angles of 0 and 180^0) received the highest SMF intensities. The SMF intensity quickly declined when getting far from the magnet and closer to the center of the microcosm. Excepting the small region located at the borders of the flask at 90 and 270^0, a large diagonal cross shape region covering the area of the microcosm center received the lowest SMF intensities. When using one single magnet, this diagonal cross shape region around the center of the microcosm received SMF intensities between 15-20 mT. In the small region close to the magnets, the SMF achieved values higher than 50 mT (at a height of 1 cm) (Fig S2-a). When using two stacked magnets, the low-intensity SMF in this diagonal cross shape region remained between 25-30, 25-35 and 30-35 mT for heights of 0, 1 and 2 cm, respectively. In close proximity to the magnets, the SMF achieved values higher than 100 mT (at a height of 1 cm) (Fig S2-b). Finally, for three stacked magnets, the lower intensity diagonal cross shape region received a SMF of 45-65 mT, with the higher values reaching as much as 200 mT in a tiny region close to the magnets at a height of 1 cm (Fig S2-c). The weighted average at different cross section heights considering the intensity contour map as well as the overall average of SMF intensity are presented in Table 2.1. On average, the SMF intensity was around 20, 40 and 70 mT in the microcosms equipped with 1, 2 and 3 magnets on each side.

Table 2.1 Average Magnetic field intensities inside all three systems

Magnets on each side	Height 0 cm	Height 1 cm	Height 2 cm	SMF average
1	17.9 mT	23.9 mT	18.5 mT	20.1 mT
2	34.5 mT	46.0 mT	37.5 mT	40.0 mT
3	62.7 mT	86.6 mT	65.7 mT	70.7 mT

2.4.2 Determination of Henry's law coefficient

Figure 2.1 shows the dimensionless Henry's law constants (H) for hexane, toluene, and methanol under all SMF conditions (0, 20, 40, and 70 mT). As expected, hexane exhibited the highest Henry's constant (H ≈ 10–20), reflecting its extremely low solubility in water and strong preference for the gas phase [36], [37]. Notably, SMF exposure did not alter hexane's Henry's constant, with values remaining statistically indistinguishable across all intensities. Toluene showed intermediate values of H (≈ 0.3–0.5), consistent with its moderate solubility and partial partitioning into the aqueous phase [37]. Similar to hexane, no significant variation in Henry's constant was observed among SMF treatments, indicating that magnetic exposure does not affect the intrinsic gas–liquid partitioning of toluene.

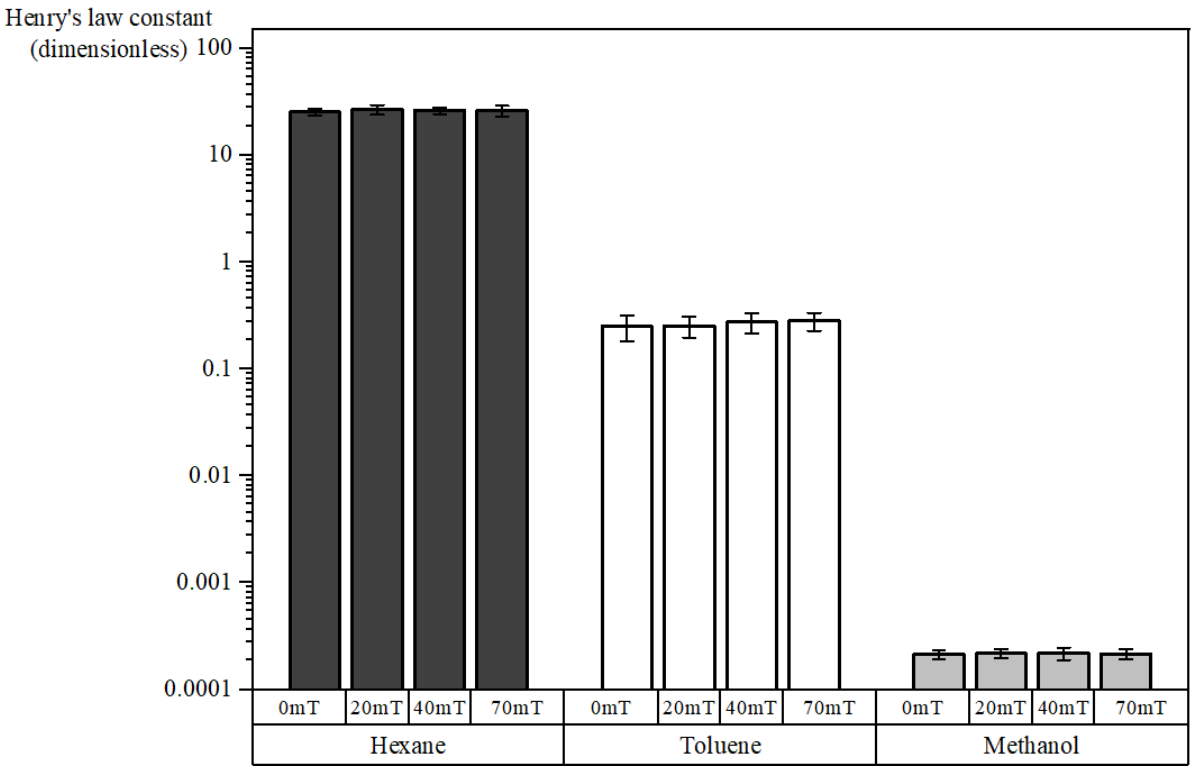

Fig. 2.1 Results of the different SMF exposure on Henry´s law for hexane, toluene and methanol.

Methanol displayed the lowest Henry's constants (≈ 0.001–0.005), confirming its high solubility in water [37]. As with the other compounds, SMF did not produce measurable differences in methanol's H values. Overall, the results demonstrate that SMF exposure tested did not affect VOC mass transfer, indicating that the physicochemical properties governing gas–liquid partitioning remained unchanged under all magnetic treatments

2.4.3 Kinetic consumption parameters for toluene, hexane and methanol

The consumption of each of the three VOCs was fitted with the Gompertz model, in absence of a SMF, and in presence of SMFs of 20, 40, and 70 mT. The kinetic essays were processed sequentially, with a new addition of VOC after its full consumption on the previous essay. In order to visualize the gradual adaptation of microorganisms to the VOC consumption and to the SMFs exposure, several

kinetics were analyzed all along the fed-batch experiments. Representative examples of the Gompertz fitting are displayed for one replica at the final day of the kinetic experiment, in presence of different SMF intensities, for toluene, hexane and methanol (Fig. 2.2).

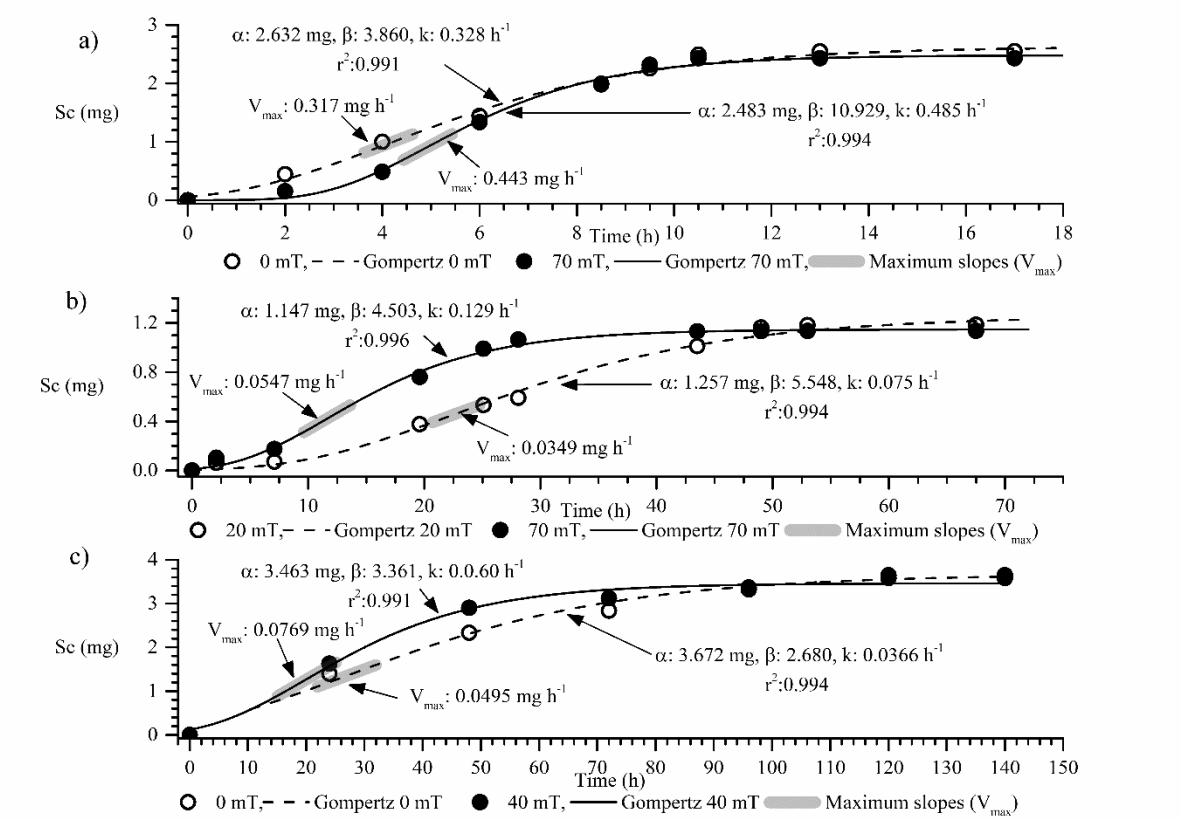

Fig. 2.2 Example of a replica of the Gompertz fitting taken in the last day of the kinetic study for a) toluene (day 17) under a SMF of 0 and 70 mT, b) hexane (day 20) under a SMF of 20 and 70 mT, and c) methanol (day 17) under a SMF of 0 and 40 mT.

As can be observed, all the introduced VOCs were consumed at the end of each kinetic, as Sc reached a final plateau of around 2.5-2.6, 1.1-1.3, and 3.5-3.7 mg for toluene, hexane and methanol, for the different SMF intensities displayed, respectively (equivalent to the α Gompertz parameter). It is worth noting that for the

toluene example (Fig 2.2a), significant substrate consumption started faster in absence of a SMF than in presence of a 70 mT SMF. Significant consumption (5% of total VOC introduced) was predicted by the Gompertz model at 0.8 and 2.6 h, for the non-exposed and 70 mT exposed experiment, respectively. This nearly 3 times longer lag phase in presence of the SMF is depicted by a corresponding 3 times higher Gompertz lag phase related parameter (β). Even if the toluene consumption started later in presence of the 70 mT SMF, a higher rate of consumption (k) and maximum slope of the Gompertz curve (represented in Fig. 2.2 by the grey shading slope associated with the V_{max} value) was noted (V_{max} of 0.443 vs. 0.317 mg h^{-1}, respectively). Finally, quicker complete toluene removal was achieved in presence of a SMF, as nearly complete consumption of toluene (=95%) was predicted by the model within 11.1 and 13.2 h, for the experiment carried out under a 70 mT SMF, and without SMF, respectively (Fig. 2.2a). Regarding hexane, a slower consumption was observed under 20 mT than under 70 mT (Fig. 2.2b), with nearly complete consumption predicted within 62.2 h, against 34.5 h, respectively. For methanol, consumption was stimulated by the SMF of 40 mT, with a predicted nearly complete removal in only 69.2 h, against 108.0 h for the non-exposed kinetic (Fig. 2.2c).

More detailed results of the Gompertz fittings, considering all the replica, and the statistical analysis of the average values, as well as initial, intermediary and final VOC additions, are displayed in Table S2.1. Satisfactory correlation coefficients (r^2) were obtained for all VOCs, with average values of 0.989 ± 0.007, 0.995 ± 0.002, and 0.982 ± 0.009 for toluene, hexane, and methanol, respectively. The total amount of VOC consumed at the end of each kinetic, fitted with the parameter α (mg), was consistent with the controlled initial dosing of each compound (≈3, 2 and 5 µL (≈2.6, 1.2, and 3.5 mg), for toluene, hexane and methanol, respectively). On average, for the three days reported on Table S2.1, the total average consumption was 2.70±0.15, and 3.62±0.36 mg for toluene and methanol, respectively. For the first kinetic day, a smaller amount of hexane was introduced (1 µL), which corresponded to an average of 0.59±0.05 mg, followed by 1.25±0.08 mg (2 µL), for the intermediate and final set of kinetics (Table S2.1). As expected, the α parameter did not vary significantly across SMF treatments for toluene, indicating a good repeatability of the

VOC injection. For the hexane consumption kinetics, only one significant difference was noted, for the experiment carried out on day 12, under a SMF of 40 mT, with a slightly higher amount of hexane introduced (+10%) compared to the control without SMF (p=0.008). Regarding methanol consumption kinetics, on day 1, a slightly higher methanol amount (+ 14%) was introduced in the control compared to the essays carried out under a SMF of 40 mT (p=0.034). Similarly, on day 10, the Gompertz fitted methanol consumption reached ≈12% higher values in the control than for the essays under 40 and 70 mT (p<0.024). However, no significant differences regarding α were computed for the last set of methanol consumption kinetics (day 17). Given the stability and very small variation of the parameter α across kinetic sets (<14 %), such parameter served as a validation point for model consistency and repeatability of VOC injection, rather than an indicator of the SMF effects.

The lag phase-related dimensionless constants (β), and the VOC consumption rates (K, h^{-1}) are displayed in Fig. 2.3, for a practical visualization of the effect of the different SMFs.

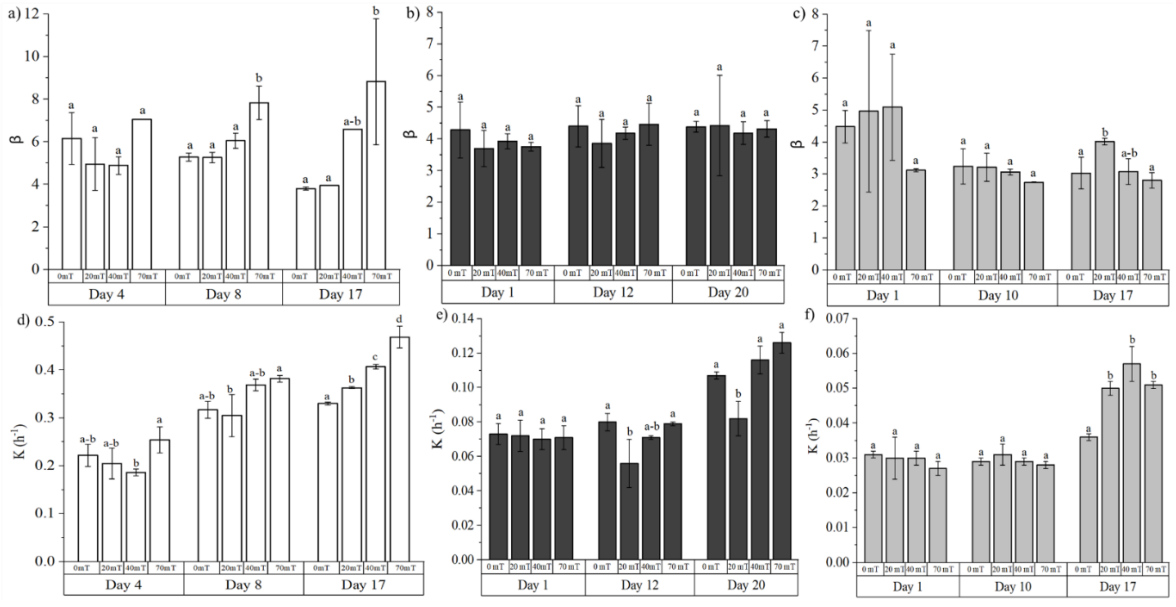

Fig. 2.3 Beta parameter (β) for a) toluene, b) hexane and c) methanol and consumption rate (K, h^{-1}) for d) toluene, e) hexane and f) methanol at the beginning,

intermediate and final days of sequential batch experiments, under different magnetic field intensities (0, 20, 40 and 70 mT). Different letters indicate statistically significant differences under different SMF intensities, for a given day and a given VOC, at a 95 % confidence interval.

The β parameter exhibited compound and treatment-specific responses. For toluene, a reduction of β was observed through time in the control without SMF (passing from 6.156±1.223 to 5.285±0.191, and to 3.804±0.079¸ on days 4, 8 and 17, Table S2.1). Such decrease in β is related to the progressive adaptation to the specific batch operating conditions, with a shorter lag-phase for toluene consumption at the start-up of each subsequent fed-batch experiment [38]. Regarding the impact of the presence of a SMF, no effect was noted on day 4 (Fig 2.3a). However, in the consecutive days, a significant difference was noted for the higher SMF intensity (70 mT), with a 48 and 132% higher β, compared to the control, for days 8 and 17 ($p=0.005$ and 0.028), respectively. The effect was not statistically significant for lower SMF intensities, and particularly, on the last day under a SMF of 20 mT (day 17), average β remained very similar to the one without SMF (β=3.949 ($p=0.927$), Table S2.1). This suggests that the higher SMF intensity of 70 mT acted as a non-lethal stressor that prolonged the time required to start toluene consumption, likely due to interference with membrane processes involved in toluene uptake or metabolism, and change microbial community [39].

In contrast, for the Gompertz fitting of hexane consumption, no significant changes in β were observed through time in absence of a SMF, with equivalent values of 4.288±0.885, 4.406±0.650, and 4.385±0.167, on days 1, 12 and 20 (Table S2.1). Thus no evolution with time was noted regarding the lag-phase needed for hexane consumption. Additionally, no difference was noted regarding the values of β under any SMF intensity (Fig 2.3b). This stability in β indicated that the lag-phase of hexane consumption was not affected by the magnetic field, contrarily to what was observed for toluene, possibly due to slow differences in microbial uptake mechanisms or compound volatility that render magnetic effects negligible [40].

In absence of a SMF, the lag-phase related parameter (β) regarding methanol consumption decreased progressively with time, reaching 4.484±0.518, 3.240±0.552, and 3.033±0.498, for days 1, 10 and 17, probably due to a progressive adaptation of the microbial utilization of methanol (Table S2.1). At early stages (days 1 and 10), no significant differences in β were observed under any SMF intensity (Fig. 2.3c). However, on day 17, a slightly significant increase in β was detected under 20 mT (+33%, p=0.046), while no changes were observed under 40 and 70 mT.

These findings suggest that specific SMF intensities can delay the consumption of some VOC, by increasing microbial degradation lag-phase. This effect was found to be dependent on the microbial process studied, particularly on the type of VOC treated, as well as the specific magnetic field intensity and exposure duration. While no additional delay of VOC consumption was noted in presence of a SMF for the more hydrophobic compound (hexane), consistent increase of lag-phase duration was noted after prolonged exposure to a 70 and 20 mT SMF during the microbial utilization of toluene and methanol, respectively. In the case of toluene degradation, the consistent increase in lag phase at higher intensities suggests that SMF acts as a metabolic stressor, likely delaying degradation through temporary energy redirection or oxidative stress responses [41]. In contrast, the lack of a measurable effect at 20 mT implies the existence of a threshold intensity below which SMF does not significantly influence microbial dynamics in this system. These variable effects are consistent with observations by [42], who reported a pronounced increase in lag phase under 80 mT SMF during cocoa fermentation (control: 1.24–2.59 h; 80 mT: 13–38 h), highlighting the inhibitory influence of high-intensity SMF on the growth rate and population dynamics of certain bacterial.

The substrate consumption rate (K) also exhibited distinct compound-specific and SMF time exposure trends. For toluene, in absence of a SMF, K progressively increased from 0.222±0.023, to 0.317±0.018, and to 0.330±0.003 h^{-1}, on days 4, 8, and 17, consecutive to the adaptation to the substrate consumption (Table S2.1). Whereas the presence of a SMF did not initially (days 4 and 8) influence the toluene

consumption rate, significant alterations were noted on day 17 (Fig. 2.3d). K increased significantly under all SMF treatments, with enhancements of 10% (p=0.047), 23% (p=0.003), and 42% (p=0.0001) at 20, 40, and 70 mT, respectively. This positive dose-response relationship suggests that once the lag phase is overcome, SMF may enhance the active degradation phase, possibly by stimulating metabolic activity [26], [43].

For hexane, in absence of a SMF, a progressive acclimation to VOC consumption was also noted, with K reaching 0.073±0.006, 0.080±0.005, and 0.107±0.002 h^{-1}, on days 1, 12 and 20, respectively (Table S2.1). No difference was noted regarding the presence of any SMF intensity for day 1. However, on subsequent days, K significantly decreased under a SMF of 20 mT by 30% (p=0.031) and 23% (p=0.022), for days 12 and 20, respectively (Fig. 2.3e). This implies that low-intensity SMF may disrupt the enzymatic pathways involved in hexane metabolism, even if the lag phase remains unaffected. The absence of effects at higher intensities may reflect microbial adaptation or inactivation of magnetic sensitivity [44].

For methanol, in absence of a SMF, the progressive adaptation to the VOC consumption was not as pronounced as for the two other VOCs, with initial and final K values of 0.031±0.001 and 0.036±0.001 h^{-1}, respectively (Table S1). On the first days (1 and 10), the presence of any SMF intensity did not affect the K values (Fig. 2.3f). However, on the last day (17), all tested SMF intensities presented a clear stimulatory effect, with a statistically significant increase of K (p=0.008, 0.002, and 0.007, under 20, 40, and 70 mT, respectively). Even if the higher K increase was noted under a SMF of 40 mT (reaching 0.057±0.005 h^{-1}), no significant difference was noted between the three SMF intensities tested (p>0.088), with an average increase of 46%, under the tested SMFs. These findings suggest that SMFs can enhance the methanol degradation efficiency, potentially through upregulation of methanol dehydrogenase activity or improving redox balance [45], [46].

Overall, the application of SMF exerted compound-specific and intensity-dependent effects on microbial biodegradation kinetics. Both the lag phase related parameter (β) and the substrate consumption rate (K) were significantly influenced by SMF in

a time- and intensity-dependent manner. These findings highlight the potential of SMF as a tool for modulating microbial activity but also underscore the importance of optimizing both intensity and exposure time to avoid unintended inhibitory effects.

For all tested VOCs, V_{max} increased along time between the first and the last tested kinetics. In the case of toluene, the average V_{max} for all SMF intensities passed from 0.22±0.03 (day 4) to 0.36±0.05 mg h^{-1} (day 17). Similarly, average V_{max} increased from 0.015±0.001 and 0.040±0.003 to 0.047±0.007 and 0.064±0.009 mg h^{-1} between the first (day 1) and the last kinetic, for hexane and methanol, respectively. Such increase in the VOC consumption is related to biomass growth and to a progressive adaptation of the microorganisms to the kinetic conditions. Interestingly, the VOC consumption rates were higher for toluene than for methanol, and for hexane, respectively.

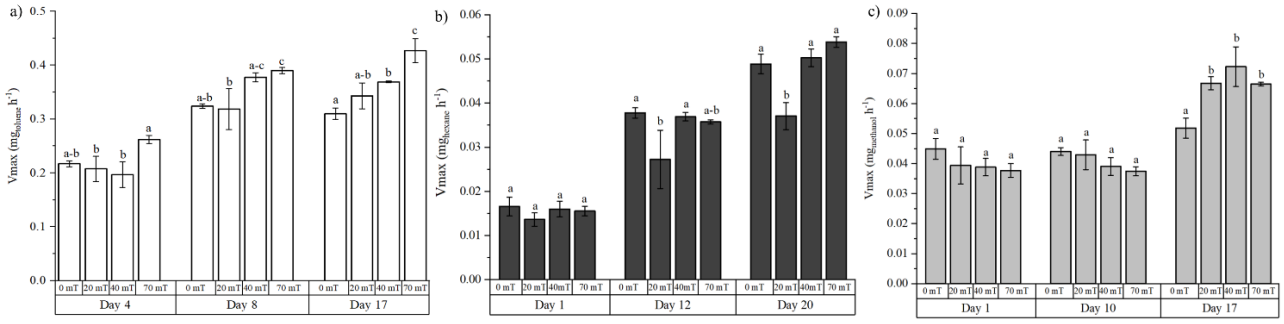

Fig. 2.4 Maximum consumption rates of a) toluene, b) hexane and c) methanol consumption at the beginning, intermediate and final days of sequential batch experiments, under different magnetic field intensities (0, 20, 40 and 70 mT). Different letters indicate statistically significant differences under different SMF intensities, for a given day and a given VOC, at a 95 % confidence interval.

Fig. 2.4 presents the maximum toluene, hexane and methanol consumption rates (V_{max}) obtained, under different SMF intensities (0, 20, 40, and 70 mT), during the first, intermediate, and final days of the batch kinetic experiments.

The lowest consumption rates observed for hexane were expected, as hydrophobic VOCs are usually harder to treat, due to limited transfer from gas to liquid phase.

However, the limited relative methanol consumption rates can be surprising, as this compound is usually easier to treat than toluene. Such low consumption rates can be linked with methanol consumption auto-inhibition at high initial concentrations.

More specifically, for the toluene kinetics carried out 4 days after starting the exposure to the magnetic fields, no statistically significant differences were noted when comparing the V_{max} values obtained at 20, 40, and 70 mT, with respect to the control ($p>0.062$) (Fig. 2.4a). However, the values obtained at 70 mT (V_{max}: 0.262 ± 0.007 mg h^{-1}) were significantly higher than those obtained at 20 and 40 mT (V_{max}: 0.207 mg h^{-1} ($p=0.035$), and V_{max}: 0.197 mg h^{-1} ($p=0.020$), respectively). Such improvement under the higher tested SMF intensity was corroborated on the following days with a longer magnetic field exposure time. Notably, the toluene consumption under 70 mT was increased by 22 and 38% compared to the non-exposed control, reaching V_{max} values of 0.390 ± 0.005 (p:0.029) and 0.427 ± 0.022 mg h^{-1} (p:0.002), for days 8 and 17, respectively. Interestingly, on the last day of the kinetic, the exposure to the SMF of 40 mT also promoted the toluene degradation, with a significant increase of V_{max} of 16% (0.369 ± 0.001 mg h^{-1} (p:0.0026). However, on day 17, the toluene consumption improvement at 40 mT remained lower than at 70 mT (p:0.028). In contrast, the lowest intensity of 20 mT never presented a significant difference in toluene consumption compared to the control system. These findings suggest a threshold effect, in which stimulation of toluene degradation occurs above a certain SMF intensity. The enhanced could be attributed to a possible effect in membrane permeability that could affect the uptake of toluene. Toluene has an aromatic and hydrophobic nature that could make it particularly responsive to changes in membrane associated with electron transfer processes.

The impact of the SMF intensity was quite different when treating hexane vapors as the SMF exposure had only null or negative effects on hexane consumption all along the kinetics (Fig. 2.4b). Interestingly, compared to the control, no effects were noted when applying SMF intensities of 40 and 70 mT, while 20 mT negatively affected the hexane consumption. The hexane consumption decrease was particularly significant on days 12 and 20, with similar decrements of 28% (V_{max}: 0.027 ± 0.007 mg h^{-1},

p:0.036) and of 24% (V_{max}: 0.037 ± 0.003 mg h^{-1}, p:0.006), respectively. This compound-dependent negative effect might be related to the lower reactivity and aliphatic structure of hexane, which is typically degraded more slowly and may be less influenced by membrane transport or enzyme induction. In some cases, sub-optimal SMF intensities can disrupt microbial homeostasis or interfere with redox processes, leading to reduced metabolic performance [24], [47].

In the case of the methanol consumption (Fig. 2.4c), during the first kinetics (days 1 and 12), the presence of a SMF did not have a significant impact, whatever the intensity. However, by day 17, the presence of a SMF significantly improved the methanol consumption in all magnetic treatments, with a V_{max} increase compared to the control of 29% (p:0.018), 39% (p:0.006), and 28% (p:0.019), under 20, 40 and 70 mT, respectively. Although no significant differences were detected regarding the three SMF intensities tested, reaching equivalent values of 0.067 ± 0.015 (p>0.23), 0.072 ± 0.007 (p>0.21) and 0.066 ± 0.001 mg h^{-1} (p>0.21), under 20, 40, and 70 mT, respectively. The late-stage increase in V_{max} suggests a delayed adaptive response, possibly involving the upregulation of methanol dehydrogenases or associated coenzyme systems [48]. Methanol has high polarity and a simple structure that may limit membrane-related effects, but enzymatic activity modulation by SMF remains a plausible mechanism. In addition, due to the high solubility of methanol, it is rapidly transferred from the gas phase to the liquid phase almost entirely, which generates stress on the micro-organisms, which could delay their adaptation process to a second external stimulus such as the SMF [49], [50].

Regarding the impact of the SMF intensities, higher differences with respect to the non-exposed control were observed during the final days of the kinetic study. Thus, in the present case, it seems that longer magnetic field exposure times accentuated the effect of the SMFs. This suggests that the SMF effect is not immediate and may be related to a progressive adaptation of the microbial community. Overall, these results indicate that exposure to different intensities of SMF can significantly influence the maximum consumption rate of VOCs. Although, the magnitude and the positive or negative nature of the effect seems to depend on the type of compound

treated. The strongest stimulation of VOC consumption was observed during the biodegradation of toluene and methanol with a 38-39% V_{max} increase at 70 and 40 mT, respectively. A lower susceptibility to the magnetic treatment was noted during hexane biodegradation, with negative effects on V_{max} at 20 mT (-28%) and no effects under higher intensities.

Similar results were reported by [18], who observed a 40% increase in H_2 production under 70 mT SMF during fed batch fermentation compared to the control. Their study also revealed that an increased abundance of specialized genera, such as *Terrisporobacter*, *Clostridium,* and *Lactobacillus* was developed under SMF exposure. Their findings highlight how SMFs can promote the enrichment of specific microbial population that favored the bioprocess of BioH_2 production. Similarly, [51] observed a 34% increase in phenol degradation and a 28% increase in biomass of *Rhodococcus erythropolis* under a 370 mT SMF, which was attributed to a 10% increase in respiration activity. These examples further support the notion that SMFs can stimulate microbial metabolism by influencing cell membrane dynamics and energy-related processes. Previous studies reporting the modulation of enzymatic activity and microbial kinetics under SMF. It has been suggested that SMF modifies membrane permeability, affects electron transport, or induces conformational changes in key enzymes [52], [53]. Such mechanisms could explain the observed increases in V_{max}, particularly for less hydrophobic compounds such as toluene and methanol. Furthermore, the differences in response among the compounds may be attributed to their distinct chemical properties and the specific metabolic pathways involved in their biodegradation [48], [54].

2.4.4 SMF effect on CO_2 production, mineralization, OD, and TOC

The results presented in Table 2.2 showed, for toluene, that the exposure to a SMF of 20–70 mT significantly increased CO_2 production and mineralization compared to the control, with the highest values obtained at 40 and 70 mT. These improvements were accompanied by higher OD and lower TOC, indicating enhanced microbial activity and greater conversion of the carbon substrate into biomass and CO_2. The absence of significant pH changes across treatments suggests that the stimulatory

effect is biological rather than driven by alterations in medium chemistry. In contrast, hexane exhibited minimal sensitivity to SMF exposure. Although CO_2 production increased slightly at 20 mT, mineralization, OD, and TOC remained statistically similar to the control across most intensities. Hexane is an extremely low water-soluble compound, which restricts its gas-liquid mass transfer, limiting its bioavailability to such an extent that the potential metabolic improvements induced by SMF cannot compensate for this limitation [6], [36]. These results indicate that SMF stimulation is insufficient to overcome hydrophobicity-driven limitations in hexane biodegradation.

Table 2.2 SMF effect on CO_2 production, mineralization, OD, TOC and pH on toluene, hexane, and methanol at the end of the kinetics

System	CO_2 (mg)	Mineralization (%)	OD	TOC (mg)	pH
			Toluene		
Control (0 mT)	2.11 ± 0.11^{a}	24.23 ± 1.21^{a}	0.66 ± 0.02^{a}	0.38 ± 0.02^{a}	6.67 ± 0.07^{a}
20 mT	2.55 ± 0.19^{b}	29.27 ± 1.81^{b}	0.72 ± 0.03^{b}	0.21 ± 0.03^{b}	6.71 ± 0.01^{a}
40 mT	$2.95\pm0.18^{b,c}$	$33.88\pm2.12^{b,c}$	0.79 ± 0.01^{c}	0.32 ± 0.01^{a}	6.69 ± 0.01^{a}
70 mT	2.99 ± 0.09^{c}	34.51 ± 1.06^{c}	0.80 ± 0.01^{c}	0.23 ± 0.03^{b}	6.72 ± 0.02^{a}
			Hexane		
Control (0 mT)	1.82 ± 0.04^{a}	22.66 ± 0.49^{a}	0.33 ± 0.04^{a}	0.28 ± 0.06^{a}	6.67 ± 0.02^{a}
20 mT	2.08 ± 0.09^{b}	25.90 ± 1.15^{b}	0.29 ± 0.01^{a}	0.21 ± 0.02^{b}	6.65 ± 0.02^{a}
40 mT	1.88 ± 0.01^{a}	23.46 ± 0.01^{a}	0.29 ± 0.05^{a}	0.10 ± 0.01^{c}	6.66 ± 0.02^{a}
70 mT	$1.89\pm0.09^{a,b}$	$23.58\pm0.66^{a,b}$	0.39 ± 0.03^{a}	0.29 ± 0.02^{a}	6.63 ± 0.06^{a}

	Methanol				
Control (0 mT)	2.33±0.18[a]	21.43±1.69[a]	0.21±0.03[a,b]	0.19±0.02[a]	6.70±0.02[a]
20 mT	2.71±0.28[a]	21.66±2.03[a]	0.23±0.01[a]	0.08±0.02[b]	6.66±0.03[a]
40 mT	3.29±0.14[b]	24.94±2.62[b]	0.18±0.01[b]	0.19±0.038[a]	6.68±0.02[a]
70 mT	3.31±0.06[b]	28.02±1.77[b]	0.19±0.01[a,b]	0.07±0.01[b]	6.68±0.05[a]

For methanol, SMF intensities of 40 and 70 mT increased the CO_2 production and mineralization (24% and 38% compared to control), while TOC decreased significantly at 20 and 70 mT. Contrary to toluene and hexane, methanol is highly soluble and rapidly transported into cells; thus, SMF effects are more directly attributable to metabolic modulation than to mass-transfer phenomena [6]. The observed improvements may reflect SMF-induced stimulation of alcohol dehydrogenases and related oxidative enzymes[48]. OD values fluctuated slightly across treatments but remained within a narrow range, suggesting that metabolic stimulation occurred without major changes in biomass concentration.

2.4.5 Bacterial diversity analysis

The bacterial community diversity was determined through diversity analysis such as, Shannon, Simpson, and Pielou (Table 2.3). Lower Shannon or higher Simpson indexes are usually related to lower α-diversity of a microbial community. Pielou index closer to 1 indicate more uniformity in the species abundance [55], [56].

The diversity indices revealed that exposure to the SMF influenced the bacterial community structure differently depending on the type of VOC degraded. For the toluene degrading consortium, the Shannon and Simpson indices slightly increased under SMF exposure (2.824 and 0.899, respectively) compared to the control without SMF (2.616 and 0.861), suggesting that the magnetic treatment favored a more balanced and diverse bacterial community. The concurrent rise in Pielou's evenness

(from 0.483 to 0.516) supports the idea that SMF exposure reduced dominance by specific taxa, promoting a more even distribution of species [19].

In contrast, for the hexane-degrading system, diversity markedly decreased after biodegradation in both treatments compared to the initial inoculum, indicating a selective enrichment of specialized degraders. However, the SMF-exposed sample showed slightly higher Shannon (2.403 vs. 2.127) and Simpson (0.807 vs. 0.791) values, suggesting that SMF may have mitigated the loss of diversity typically associated with hexane biodegradation [10].

The methanol-degrading community exhibited the lowest diversity values among all VOCs. Both the Shannon and Simpson indices decreased sharply during biodegradation, and SMF exposure did not produce noticeable differences between treatments. This outcome indicates that methanol degradation likely favored a few dominant and highly adapted species, with minimal influence from SMF [57].

These results suggest that SMF exposure can modulate microbial community structure, particularly by maintaining or slightly enhancing diversity in systems exposed to more complex or less readily biodegradable compounds, such as toluene and hexane. This response may contribute to improved system stability and biodegradation performance under magnetic stimulation.

Table 2.3 The diversity indices of different experiments in the final kinetic evaluated

Sample	Reads	ASVs observed	Shannon	Simpson	Pielou
Toluene					
Initial	179028	287	2.734	0.886	0.483
Final (0 mT)	190307	224	2.616	0.861	0.483
Final (70 mT)	186635	239	2.824	0.899	0.516
Hexane					
Initial	97939	280	3.558	0.929	0.632
Final (0 mT)	183892	221	2.127	0.791	0.394
Final (70 mT)	128009	211	2.403	0.807	0.449
Methanol					
Initial	181716	267	2.798	0.869	0.501
Final (0 mT)	176918	212	1.739	0.602	0.325

Final (70 mT)	179473	217	1.739	0.609	0.323

2.4.6 Shift in microbial community

a)

Phylum	Genus	Toluene Inicial	Final (Control)	Final (MF70 mT)
Actinobacteriota	*Rhodococcus*	31.5	33.6	29.1
Proteobacteria	*Parvibaculum*	0.4	1.0	1.4
	Brucella	0.0	1.9	2.2
	NA (f_Rhizobiaceae)	0.1	1.5	1.5
	Sphingopyxis	0.1	2.3	3.1
Chloroflexi	NA (o_SBR1031)	4.3	0.0	0.0
Bacteroidota	*Terrimonas*	0.2	1.9	0.8
	NA (f_Chitinophagaceae)	1.8	0.2	0.3
	Moheibacter	24.3	6.6	10.0
Proteobacteria	*Achromobacter*	0.0	0.6	2.5
	Castellaniella	1.4	0.0	0.1
	Pusillimonas	1.0	25.2	18.2
	Limnobacter	1.5	2.3	3.7
	Alicycliphilus	2.0	3.9	1.1
	Thauera	22.7	0.0	0.0
	Pseudomonas	0.0	2.7	10.9
	Luteimonas	1.0	3.5	5.7
	Pseudoxanthomonas	0.0	3.0	2.7
NA	NA	1.2	5.5	1.5
	Otros (<1%)	6.5	4.1	5.4

%
40
20
10
5
1

b)

Phylum	Genus	Hexane Inicial	Final (Control)	Final (MF70 mT)
Actinobacteriota	*Rhodococcus*	0.0	26.8	35.3
	Ilumatobacteraceae	22.1	0.0	0.0
	Nocardioides	5.8	0.0	0.0
	Microlunatus	7.1	0.0	0.0
	Actinomycetospora	3.2	0.0	0.0
	Pseudonocardia	14.8	0.0	0.0
Bacteroidota	*Flavobacterium*	0.0	20.0	24.6
	Terrimonas	0.2	3.6	4.3
Proteobacteria	*Sphingomonas*	0.0	31.2	8.4
	Aquicella	1.5	4.0	4.0
	Sphingopyxis	3.6	2.7	3.4
	Pseudaminobacter	0.2	1.0	2.2
	NA	6.8	0.9	0.6
	Fontimonas	4.4	0.0	0.0
Verrucomicrobiota	Verrucomicrobiaceae	4.0	0.0	0.0
NA	NA	0.2	0.3	2.1
	Otros (<1%)	26.2	9.8	17.3

%
40
20
10
5
1

c)

Phylum	Genus	Methanol Initial	Final (Control)	Final (MF70 mT)
Actinobacteriota	*Rhodococcus*	4.5	0.9	0.4
Bacteroidota	*Moheibacter*	23.3	11.9	10.7
Proteobacteria	Fodinicurvataceae	4.1	0.4	0.5
	Parvibaculum	1.8	0.6	0.6
	Hyphomicrobium	8.7	9.7	10.8
	Aminobacter	1.2	1.6	1.2
	Ciceribacter	0.0	0.8	1.2
	Castellaniella	4.6	1.2	1.5
	Parapusillimonas	1.2	0.4	0.3
	Limnobacter	3.7	2.6	1.8
	Methylobacillus	25.0	62.7	62.2
	Aquicella	1.1	0.1	0.1
	Luteimonas	9.6	2.5	4.9
NA	NA	1.4	0.6	0.2
	Otros (<1%)	9.9	3.9	3.6

%
70
35
20
10
1

Fig. 2.5 Heatmaps displaying the changes in the relative abundance of the most prevalent microbial taxa in the batch systems with and without the application of magnetic field. Panels a, b, and c, display the most abundant microbial taxa in the experiments fed with toluene, methanol, and hexane respectively.

For the toluene-degrading batch tests, some bacterial genera showed increased relative abundances under the 70 mT conditions (Fig. 2.5a). This was the case of the *Pseudomonas* and *Luteimonas* genera which presented relative abundances of ~8.2 and ~2.2 higher in the 70 mT treatment when compared to the experimental controls lacking the application of SMF. Moreover, both *Pseudomonas* and *Luteimonas* were almost negligible in the sludge used as inocula (<1%), thus their significant increase indicates a high affinity for toluene as previously reported [58].

Importantly, the increase in *Pseudomonas* could explain the increase in toluene consumption in the batch exposed to 70 mT, when compared to the control. *Pseudomonas* species are highly effective in toluene biodegradation due to their metabolic versatility and their genetic adaptations [59]. An additional genus apparently stimulated by the magnetic field was *Moheibacter* whose relative abundance increased by ~3.4% when compared to the control. A bacterial taxon consistently present in the toluene experiments was *Rhodococcus*, however, its relative abundance did not show a significant increase respect to the control or the inoculum (~30%). These results are in line with the literature in which these genera have been consistently reported as toluene degraders in several configurations of VOC-degrading systems.

In Fig. 2.5b the results of bacteria genera during hexane degradation are shown. *Rhodococcus* and *Flavobacterium* genera increased their relative abundance by ~8.5% and ~4.6%, respectively, under exposure of 70 mT compared with the control. In addition, these genera were absent at the beginning of experiments at the initial sludge (<1%). This indicates that *Rhodococcus* and *Flavobacterium* have a high affinity to consume hexane. *Pseudaminobacter* increases its relative abundance by ~1.2% in reactor exposed to SMF than in control without field. On the contrary, *Sphingomonas* significantly decreases its relative abundance by ~22.8 under 70 mT, compared with the control, which may indicate that SMF negatively affects the growth of *Sphingomonas*. *Rhodococcus* is widely described as a bioresource for removing hexane and other recalcitrant compounds, such as aromatics, alkanes, ketones, etc [40], [60].

In experiments with methanol the relative abundance of *Methylobacillus*, *Hyphomicrobium* and *Moheibacter* was modified (Fig. 2.5c). *Methylobacillus* significantly increased its relative abundance from ~25% in inoculum to ~65% in reactors control and exposed to 70 mT, which indicates the affinity of this genus to consume this compound. The genus *Hyphomicrobium* expressed constitutively in the three samples evaluated with a relative abundance of ~10%. In contrast, *Moheibacter* shows a decrease in the relative abundance in the inoculum (~23.3%)

compared to the control (~11.9) and with the exposure to 70 mT (~10.7%). The SMF did not significantly modify the genus during methanol biodegradation. There are previous reports that *Proteobacteria (Methylobacillus* and *Hyphomicrobium), Actinobacteria,* and *Bacteroidetes* (*Moheibacter*) phyla are methanol-utilizers at a neutral pH, such as the present study. *Proteobacteria* are mainly related to methanol degradation, many enzymes have the ability to oxidize methanol, such as pyrroloquinoline quinone (PQO)-dependent methanol dehydrogenase [61]. Zhu et al., 2021 [62], reported that exposure to 50 mT a sequential batch reactor increases the key enzyme activities during nitrogen removal. There has also been reported that exposure to 40, 20, and 10 mT change the Cytichrome C content as well as energy generation of microorganisms [26]. These results were evaluated in the nitritation process, however, the effect of SMF on the enzymatic activity and amount could explain the effect observed during the kinetic of methanol.

2.5 Conclusions

This study evaluated the influence of SMF on the biodegradation of VOCs with different solubility. SMF of 40 and 70 mT significantly enhanced the biodegradation of toluene, a moderately soluble VOC, whereas no improvement was observed for hexane, which has much lower aqueous solubility. The enhanced toluene removal was associated with shifts in the bacterial community, particularly a four-fold increase in Pseudomonas abundance under 70 mT, suggesting that SMF exposure may selectively stimulate taxa involved in aromatic hydrocarbon degradation.

In the case of methanol, a highly soluble VOC, the response to SMF was variable but overall positive, with 40 and 70 mT increasing mineralization by 24% and 38%, respectively. These improvements may be linked to SMF-induced stimulation of enzymatic pathways involved in alcohol oxidation. Overall, the findings demonstrate that low-intensity SMFs can modulate microbial activity and community structure in ways that enhance the biodegradation of certain VOCs. This work provides new insight into the potential application of SMFs as an energy-efficient process-intensification strategy for air pollution bioremediation technologies.

2.6 References

[1] K. Sheoran *et al.*, “Air Pollutants Removal Using Biofiltration Technique: A Challenge at the Frontiers of Sustainable Environment,” *ACS Eng. Au*, vol. 2, no. 5, pp. 378–396, 2022, doi: 10.1021/acsengineeringau.2c00020.

[2] P. A. Lamprea Pineda, K. Demeestere, M. Toledo, H. Van Langenhove, and C. Walgraeve, “Enhanced removal of hydrophobic volatile organic compounds in biofilters and biotrickling filters: A review on the use of surfactants and the addition of hydrophilic compounds,” *Chemosphere*, vol. 279, no. February, p. 130757, 2021, doi: 10.1016/j.chemosphere.2021.130757.

[3] EPA, (2025). United States Environmental Protection Agency. 2022. “TRI Explorer (2023 National Analysis Dataset (updated July 2025, released July 2025)) [Internet database]. Retrieved from https://enviro.epa.gov/triexplorer/, (September23, 2025)

[4] X. Wu, Y. Lin, Y. Wang, S. Wu, and C. Yang, “Volatile organic compound removal via biofiltration: Influences, challenges, and strategies,” *Chem. Eng. J.*, vol. 471, no. June, p. 144420, 2023, doi: 10.1016/j.cej.2023.144420.

[5] M. Ferdowsi, A. Avalos Ramirez, J. P. Jones, and M. Heitz, “Elimination of mass transfer and kinetic limited organic pollutants in biofilters: A review,” *Int. Biodeterior. Biodegrad.*, vol. 119, pp. 336–348, 2017, doi: 10.1016/j.ibiod.2016.10.015.

[6] S. Keramati, M. Ferdowsi, and S. M. Zamir, “Compounds interactions during simultaneous biodegradation of hydrophobic n-hexane and hydrophilic methanol vapors in one- and two-liquid phase conditions,” *Process Saf. Environ. Prot.*, vol. 147, pp. 283–291, 2021, doi: 10.1016/j.psep.2020.09.040.

[7] M.-F. Han *et al.*, “Comparison of separated and combined photodegradation and biofiltration technology for the treatment of volatile organic compounds: A critical review,” *Crit. Rev. Environ. Sci. Technol.*, vol. 52, no. 8, pp. 1325–1355, 2022, doi: doi.org/10.1080/10643389.2020.1854566.

[8] B. Cruz-García, A. S. Geronimo-Meza, C. Martínez-Lievana, S. Arriaga, Y. Huante-González, and A. Aizpuru, “Biofiltration of high concentrations of methanol vapors: removal performance, carbon balance and microbial and fly populations,” *J. Chem. Technol. Biotechnol.*, vol. 94, no. 6, pp. 1925–1936, 2019, doi: 10.1002/jctb.5974.

[9] M. E. Acuña, F. Pérez, R. Auria, and S. Revah, “Microbiological and kinetic aspects of a biofilter for the removal of toluene from waste gases,” *Biotechnol. Bioeng.*, vol. 63, no. 2, pp. 175–184, 1999, doi: 10.1002/(SICI)1097-0290(19990420)63:2<175::AID-BIT6>3.0.CO;2-G.

[10] A. Amouric, F. Verhé, R. Auria, and L. Casalot, “Study of a hexane-degrading consortium in a biofilter and in liquid culture: Biodiversity, kinetics and characterization of degrading strains,” *FEMS Microbiol. Ecol.*, vol. 55, no. 2, pp. 239–247, 2006, doi: 10.1111/j.1574-6941.2005.00017.x.

[11] T. Gu *et al.*, “Biodegradation of isobutyraldehyde with high removal efficiency by using

a modified biotrickling filter," *J. Environ. Chem. Eng.*, vol. 11, no. 2, p. 109630, 2023, doi: 10.1016/j.jece.2023.109630.

[12] M. Ferdowsi, B. Khabiri, G. Buelna, J. P. Jones, and M. Heitz, "Air biofilters for a mixture of organic gaseous pollutants: an approach for industrial applications," *Crit. Rev. Biotechnol.*, vol. 43, no. 7, pp. 1019–1034, 2023, doi: 10.1080/07388551.2022.2100735.

[13] D. zhi Chen *et al.*, "Enhanced chlorobenzene removal by internal magnetic field through initial cell adhesion and biofilm formation," *Appl. Microbiol. Biotechnol.*, vol. 108, no. 1, 2024, doi: 10.1007/s00253-024-13001-z.

[14] Y. Wang *et al.*, "Application of magnetic fields to wastewater treatment and its mechanisms: A review," *Sci. Total Environ.*, vol. 773, 2021, doi: 10.1016/j.scitotenv.2021.145476.

[15] N. Benyoucef, A. Pauss, N. Abdi, C. O. Sarde, H. Grib, and N. Mameri, "Enhancement of the denitrification performance of an activated sludge using an electromagnetic field in batch mode," *Chemosphere*, vol. 262, pp. 1–10, 2021, doi: 10.1016/j.chemosphere.2020.127698.

[16] Y. Liu, J. Li, W. Guo, H. H. Ngo, J. Hu, and M. tian Gao, "Use of magnetic powder to effectively improve the performance of sequencing batch reactors (SBRs) in municipal wastewater treatment," *Bioresour. Technol.*, vol. 248, pp. 135–139, 2018, doi: 10.1016/j.biortech.2017.06.069.

[17] A. Tomska and L. Wolny, "Enhancement of biological wastewater treatment by magnetic field exposure," *Desalination*, vol. 222, no. 1–3, pp. 368–373, 2008, doi: 10.1016/j.desal.2007.01.144.

[18] S. Arriaga, M. F. Carboni, and P. N. L. Lens, "Effect of static magnetic field exposure on biohydrogen production via dark fermentation of glucose," *Process Saf. Environ. Prot.*, vol. 176, no. June, pp. 375–388, 2023, doi: 10.1016/j.psep.2023.06.022.

[19] M. Zieliński, M. Zielińska, A. Cydzik-Kwiatkowska, P. Rusanowska, and M. Dębowski, "Effect of static magnetic field on microbial community during anaerobic digestion," *Bioresour. Technol.*, vol. 323, no. December 2020, pp. 600–605, 2021, doi: 10.1016/j.biortech.2020.124600.

[20] Y. Quan, H. Wu, Z. Yin, Y. Fang, and C. Yin, "Effect of static magnetic field on trichloroethylene removal in a biotrickling filter," *Bioresour. Technol.*, vol. 239, pp. 7–16, 2017, doi: 10.1016/j.biortech.2017.04.121.

[21] Y. Quan, H. Wu, C. Guo, Y. Han, and C. Yin, "Enhancement of TCE removal by a static magnetic field in a fungal biotrickling filter," *Bioresour. Technol.*, vol. 259, no. March, pp. 365–372, 2018, doi: 10.1016/j.biortech.2018.03.031.

[22] D. Chen *et al.*, "Enhanced gaseous chlorobenzene removal and its microbial mechanism through innovative modified packings coupled with magnetic field in a

biotrickling filter," *Front. Environ. Sci. Eng.*, vol. 19, no. 11, 2025, doi: 10.1007/s11783-025-2072-x.

[23] Q. Li *et al.*, "Static magnetic field enhances the purification of gaseous n-hexane in airlift two-phase partitioning bioreactor," *Process Biochem.*, vol. 156, no. June, pp. 209–216, 2025, doi: 10.1016/j.procbio.2025.06.003.

[24] G. Beretta, A. F. Mastorgio, L. Pedrali, S. Saponaro, and E. Sezenna, *The effects of electric, magnetic and electromagnetic fields on microorganisms in the perspective of bioremediation*, vol. 18, no. 1. Springer Netherlands, 2019.

[25] M. Cortés-Castillo, A. Encinas, A. Aizpuru, and S. Arriaga, "Effect of applying a magnetic field on the biofiltration of hexane over long-term operation period," *Environ. Sci. Pollut. Res.*, no. 0123456789, 2024, doi: 10.1007/s11356-024-34671-2.

[26] B. Hu *et al.*, "Impact of static magnetic field on electron transport and microbial community shifts in the nitritation sequencing batch reactor," *J. Environ. Chem. Eng. Please*, vol. 10, no. 5, pp. 2213–2221, 2022, doi: 10.1016/j.jece.2022.108774.

[27] Y. Dong *et al.*, "Weak magnetic field stimulated nitrite oxidizing bacteria and destroyed the SNAD process," *Bioresour. Technol. Reports*, vol. 13, no. October 2020, p. 100631, 2021, doi: 10.1016/j.biteb.2021.100631.

[28] S. Arriaga and S. Revah, "Improving hexane removal by enhancing fungal development in a microbial consortium biofilter," *Biotechnol. Bioeng.*, vol. 90, no. 1, pp. 107–115, 2005, doi: 10.1002/bit.20424.

[29] S. Esquivel-Gonzalez, A. Aizpuru, A. Patrón-Soberano, and S. Arriaga, "Characterization of bioaerosol emissions from two biofilters during treatment of toluene vapours using epifluorescence microscopy," *Int. Biodeterior. Biodegrad.*, vol. 123, 2017, doi: 10.1016/j.ibiod.2017.06.007.

[30] B. J. Callahan, P. J. Mcmurdie, M. J. Rosen, A. W. Han, A. J. Johnson, and S. P. Holmes, "DADA2 : High resolution sample inference from amplicon data," *Nat. Methods*, vol. 13, pp. 581–583, 2016, doi: https://doi.org/10.1038/nmeth.3869.

[31] T. R Core, "R: A Language and Environment for Statistical Computing, R Foundation for Statistical Computing," *Vienna*, 2021.

[32] C. Quast *et al.*, "The SILVA ribosomal RNA gene database project : improved data processing and web-based tools," vol. 41, no. November 2012, pp. 590–596, 2013, doi: 10.1093/nar/gks1219.

[33] I. Covarrubias-García, A. Aizpuru, and S. Arriaga, "Effect of the continuous addition of ozone on biomass clogging control in a biofilter treating ethyl acetate vapors," *Sci. Total Environ.*, vol. 584–585, pp. 469–475, 2017, doi: 10.1016/j.scitotenv.2017.01.031.

[34] Ó. J. Prado, M. C. Veiga, and C. Kennes, "Effect of key parameters on the removal of formaldehyde and methanol in gas-phase biotrickling filters," *J. Hazard. Mater.*, vol.

138, no. 3, pp. 543–548, 2006, doi: 10.1016/j.jhazmat.2006.05.093.

[35] E. Lopez-Bello, L. Vargas-Estrada, A. Aizpuru, S. Arriaga, and R. Muñoz, “Journal of Environmental Chemical Engineering Stimulation of microalgae growth and high-value compounds production by magnetic field exposure,” vol. 13, no. August, 2025, doi: 10.1016/j.jece.2025.119171.

[36] S. R. Clough, “Hexane,” in *Encyclopedia of Toxicology*, 3rd ed., 2014, pp. 900–904.

[37] J. Staudinger and P. V. Roberts, “A critical compilation of Henry’s law constant temperature dependence relations for organic compounds in dilute aqueous solutions,” *Chemosphere*, vol. 44, no. 4, pp. 561–576, 2001, doi: 10.1016/S0045-6535(00)00505-1.

[38] N. M. Chong, M. L. Luong, and C. S. Hwu, “Biogenic substrate benefits activated sludge in acclimation to a xenobiotic,” *Bioresour. Technol.*, vol. 104, pp. 181–186, 2012, doi: 10.1016/j.biortech.2011.11.004.

[39] M. Mihoub, A. El May, A. Aloui, A. Chatti, and A. Landoulsi, “Effects of static magnetic fields on growth and membrane lipid composition of Salmonella typhimurium wild-type and dam mutant strains,” *Int. J. Food Microbiol.*, vol. 157, no. 2, pp. 259–266, 2012, doi: 10.1016/j.ijfoodmicro.2012.05.017.

[40] E. H. Lee, J. Kim, K. S. Cho, Y. G. Ahn, and G. S. Hwang, “Degradation of hexane and other recalcitrant hydrocarbons by a novel isolate, Rhodococcus sp. EH831,” *Environ. Sci. Pollut. Res.*, vol. 17, no. 1, pp. 64–77, 2010, doi: 10.1007/s11356-009-0238-x.

[41] S. Ghodbane, A. Lahbib, M. Sakly, and H. Abdelmelek, “Bioeffects of static magnetic fields: Oxidative stress, genotoxic effects, and cancer studies,” *Biomed Res. Int.*, vol. 2013, 2013, doi: 10.1155/2013/602987.

[42] T. M. Guzmán-Armenteros, J. Villacís-Chiriboga, L. S. Guerra, and J. Ruales, “Electromagnetic fields effects on microbial growth in cocoa fermentation: A controlled experimental approach using established growth models,” *Heliyon*, vol. 10, no. 3, 2024, doi: 10.1016/j.heliyon.2024.e24927.

[43] A. Wasak, R. Drozd, D. Jankowiak, and R. Rakoczy, “Rotating magnetic field as tool for enhancing enzymes properties - laccase case study,” *Sci. Rep.*, vol. 9, no. 1, pp. 1–9, 2019, doi: 10.1038/s41598-019-39198-y.

[44] J. Filipič, B. Kraigher, B. Tepuš, V. Kokol, and I. Mandic-Mulec, “Effects of low-density static magnetic fields on the growth and activities of wastewater bacteria Escherichia coli and Pseudomonas putida,” *Bioresour. Technol.*, vol. 120, pp. 225–232, 2012, doi: 10.1016/j.biortech.2012.06.023.

[45] Y. L. Dorokhov, A. V. Shindyapina, E. V. Sheshukova, and T. V. Komarova, “Metabolic methanol: Molecular pathways and physiological roles,” *Physiol. Rev.*, vol. 95, no. 2, pp. 603–644, 2015, doi: 10.1152/physrev.00034.2014.

[46] M. Łebkowska, A. Rutkowska-Narozniak, E. Pajor, and Z. Pochanke, “Effect of a static magnetic field on formaldehyde biodegradation in wastewater by activated sludge,” *Bioresour. Technol.*, vol. 102, no. 19, pp. 8777–8782, 2011, doi: 10.1016/j.biortech.2011.07.040.

[47] P. E. Kovacs, R. L. Valentine, and P. J. J. Alvarez, “The effect of static magnetic fields on biological systems: Implications for enhanced biodegradation,” *Crit. Rev. Environ. Sci. Technol.*, vol. 27, no. 4, pp. 319–382, 1997, doi: 10.1080/10643389709388503.

[48] T. K. Le, Y. J. Lee, G. H. Han, and S. J. Yeom, “Methanol Dehydrogenases as a Key Biocatalysts for Synthetic Methylotrophy,” *Front. Bioeng. Biotechnol.*, vol. 9, no. December, pp. 1–11, 2021, doi: 10.3389/fbioe.2021.787791.

[49] M. Yang, T. G. Bell, B. W. Blomquist, C. W. Fairall, I. M. Brooks, and P. D. Nightingale, “Air-sea transfer of gas phase controlled compounds,” *IOP Conf. Ser. Earth Environ. Sci.*, vol. 35, no. 1, 2016, doi: 10.1088/1755-1315/35/1/012011.

[50] N. S. Zaidi, K. Muda, and M. Sillanpää, “Effects of extra-cellular polymeric substances towards physical properties of biomass under magnetic field exposure,” *Int. J. Environ. Sci. Technol.*, vol. 16, no. 7, pp. 3801–3808, 2019, doi: 10.1007/s13762-018-1897-2.

[51] L. Křiklavová, M. Truhlář, P. Škodová, T. Lederer, and V. Jirků, “Effects of a static magnetic field on phenol degradation effectiveness and Rhodococcus erythropolis growth and respiration in a fed-batch reactor,” *Bioresour. Technol.*, vol. 167, pp. 510–513, 2014, doi: 10.1016/j.biortech.2014.06.060.

[52] Hsien Chiao Teng, “A Puzzle of the Effect of Magnetic Field on Biological Cells,” *Life Sci. J.*, vol. 2, no. 1, pp. 16–21, 2005, [Online]. Available: http://www.lifesciencesite.com/lsj/life0201/life-0201-04.pdf.

[53] W. W. C. Albuquerque, R. M. P. B. Costa, T. de Salazar e Fernandes, and A. L. F. Porto, “Evidences of the static magnetic field influence on cellular systems,” *Prog. Biophys. Mol. Biol.*, vol. 121, no. 1, pp. 16–28, 2016, doi: 10.1016/j.pbiomolbio.2016.03.003.

[54] R. E. Parales, J. L. Ditty, and C. S. Harwood, “Toluene-degrading bacteria are chemotactic towards the environmental pollutants benzene, toluene, and trichloroethylene,” *Appl. Environ. Microbiol.*, vol. 66, no. 9, pp. 4098–4104, 2000, doi: 10.1128/AEM.66.9.4098-4104.2000.

[55] L. Ren, R. Chen, X. Zhang, J. Shao, and Y. He, “Bioresource Technology Phenol biodegradation and microbial community dynamics in extractive membrane bioreactor (EMBR) for phenol-laden saline wastewater,” *Bioresour. Technol.*, vol. 244, no. August, pp. 1121–1128, 2017, doi: 10.1016/j.biortech.2017.08.121.

[56] L. Jost, “The Relation between Evenness and Diversity,” pp. 207–232, 2010, doi: 10.3390/d2020207.

[57] J. László and J. Kutasi, “Static magnetic field exposure fails to affect the viability of different bacteria strains,” *Bioelectromagnetics*, vol. 31, no. 3, pp. 220–225, 2010, doi: 10.1002/bem.20551.

[58] L. Malhautier, G. Quijano, M. Avezac, J. Rocher, and J. L. Fanlo, “Kinetic characterization of toluene biodegradation by Rhodococcus erythropolis: Towards a rationale for microflora enhancement in bioreactors devoted to air treatment,” *Chem. Eng. J.*, vol. 247, pp. 199–204, 2014, doi: 10.1016/j.cej.2014.02.099.

[59] R. Muñoz, L. F. Díaz, S. Bordel, and S. Villaverde, “Response of Pseudomonas putida F1 cultures to fluctuating toluene loads and operational failures in suspended growth bioreactors,” *Biodegradation*, vol. 19, no. 6, pp. 897–908, 2008, doi: 10.1007/s10532-008-9191-5.

[60] E. H. Lee and K. S. Cho, “Characterization of cyclohexane and hexane degradation by Rhodococcus sp. EC1,” *Chemosphere*, vol. 71, no. 9, pp. 1738–1744, 2008, doi: 10.1016/j.chemosphere.2007.12.009.

[61] S. Kolb, “Aerobic methanol-oxidizing Bacteria in soil,” *FEMS Microbiol. Lett.*, vol. 300, no. 1, pp. 1–10, 2009, doi: 10.1111/j.1574-6968.2009.01681.x.

[62] Y. M. Zhu, H. Ji, H. Ren, J. Geng, and K. Xu, “Enhancement of static magnetic field on nitrogen removal at different ammonium concentrations in a sequencing batch reactor: Performance and biological mechanism,” *Chemosphere*, vol. 268, 2021, doi: 10.1016/j.chemosphere.2020.128794.

2.7 Supplementary materials

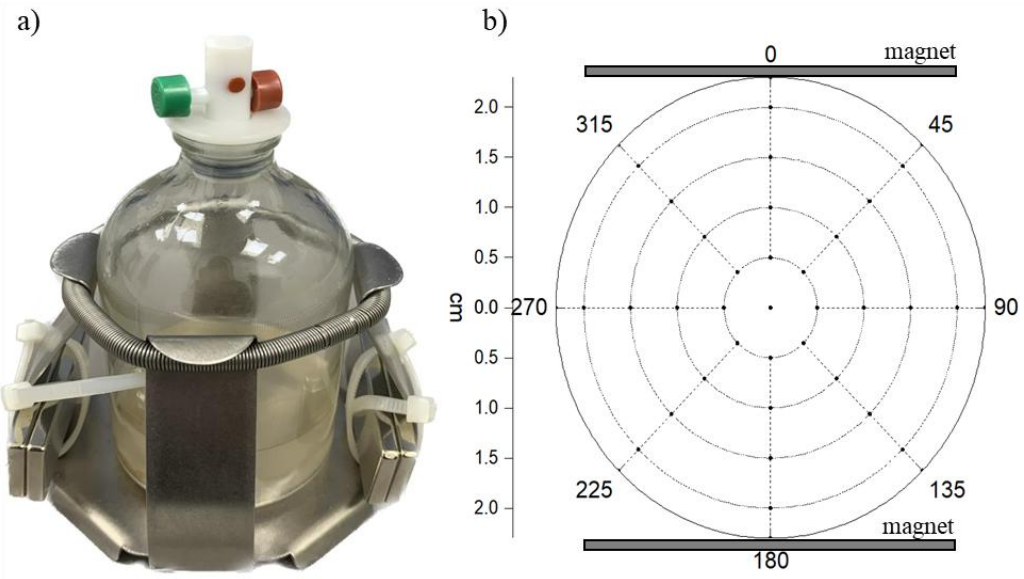

Fig. S2.1 Microcosm, case with two stacked neodymium magnetic blocks (a). Location of static magnetic field measurements inside the flasks. Magnets were placed at angles of 0 and 180^0. (b).

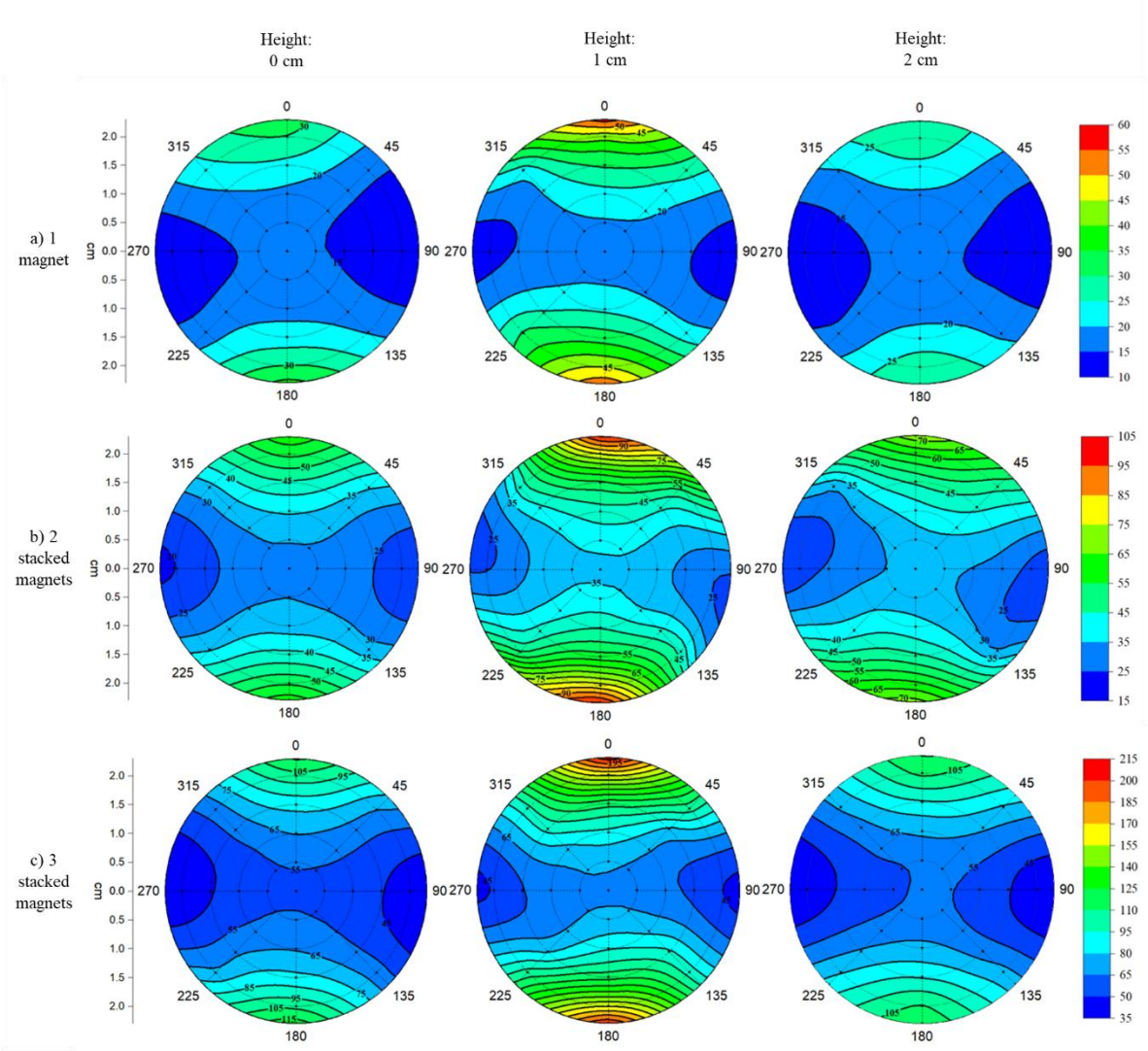

Fig. S2.2 Distribution of magnetic field inside the flask 20 mT (1 magnet on each side), 40 mT (2 magnets on each side), 70 mT (3 magnets on each side).

Table S2.1 Average of kinetic parameters of the Gompertz model for the biodegradation of toluene, hexane, and methanol with and without magnetic field

Day of kinetic	SMF (mT)	α (mg_{hex})	β	K (h^{-1})	Vmax	r^2
			Toluene			
4	0	2.663±0.205[a]	6.156±1.223[a]	0.222±0.023[a,b]	0.217±0.005[a,b]	0.998±0.001
	20	2.764±0.121[a]	4.959±1.241[a]	0.205±0.032[a,b]	0.207±0.023[b]	0.995±0.007
	40	2.875±0.247[a]	4.889±0.420[a]	0.186±0.007[b]	0.197±0.024[b]	0.993±0.003
	70	2.829±0.383[a]	7.059±0.011[a]	0.254±0.027[a]	0.262±0.008[a]	0.986±0.015
8	0	2.781±0.201[a]	5.285±0.191[a]	0.317±0.018[a,b]	0.324±0.005[a,b]	0.977±0.009
	20	2.847±0.066[a]	5.270±0.245[a]	0.305±0.044[b]	0.319±0.038[b]	0.984±0.002
	40	2.784±0.033[a]	6.057±0.355[a]	0.369±0.012[a,b]	0.378±0.008[a,c]	0.981±0.003
	70	2.777±0.010[a]	7.838±0.788[b]	0.382±0.007[a]	0.390±0.006[c]	0.984±0.003
17	0	2.553±0.112[a]	3.804±0.079[a]	0.330±0.003[a]	0.309±0.010[a]	0.987±0.006
	20	2.569±0.179[a]	3.949±0.005[a]	0.363±0.002[b]	0.343±0.024[a,b]	0.996±0.002
	40	2.463±0.041[a]	6.591±0.018[a,b]	0.407±0.005[c]	0.369±0.001[b]	0.995±0.001
	70	2.476±0.010[a]	8.833±2.965[b]	0.469±0.023[d]	0.427±0.022[c]	0.993±0.001
			Hexane			
1	0	0.618±0.026[a]	4.288±0.885[a]	0.073±0.006[a]	0.017±0.002[a]	0.988±0.006
	20	0.520±0.126[a]	3.699±0.573[a]	0.072±0.009[a]	0.014±0.001[a]	0.995±0.001
	40	0.622±0.013[a]	3.928±0.242[a]	0.070±0.006[a]	0.016±0.002[a]	0.995±0.001
	70	0.596±0.013[a]	3.762±0.135[a]	0.071±0.007[a]	0.016±0.001[a]	0.994±0.005
12	0	1.277±0.047[a,b]	4.406±0.650[a]	0.080±0.005[a]	0.038±0.001[a]	0.994±0.0002
	20	1.313±0.001[a]	3.858±0.764[a]	0.056±0.014[b]	0.027±0.007[b]	0.996±0.002
	40	1.404±0.015[c]	4.185±0.195[a]	0.071±0.001[a,b]	0.037±0.001[a]	0.994±0.0002
	70	1.223±0.017[b]	4.465±0.665[a]	0.079±0.001[a]	0.036±0.001[a,b]	0.994±0.001
20	0	1.236±0.028[a]	4.385±0.167[a]	0.107±0.002[a]	0.049±0.002[a]	0.998±0.0001
	20	1.229±0.041[a]	4.425±1.588[a]	0.082±0.010[b]	0.037±0.003[b]	0.996±0.003
	40	1.182±0.037[a]	4.185±0.358[a]	0.116±0.008[a]	0.050±0.002[a]	0.997±0.0005
	70	1.165±0.025[a]	4.321±0.257[a]	0.126±0.006[a]	0.053±0.001[a]	0.995±0.0001
			Methanol			
	0	3.939± 0.253[a]	4.484±0.518[a]	0.031±0.001[a]	0.045±0.003[a]	0.993±0.007

1	20	3.639±0.157[a,b]	4.966±2.534[a]	0.030±0.006[a]	0.039±0.006[a]	0.987±0.008
	40	3.463±0.009[b]	5.093±1.665[a]	0.030±0.002[a]	0.038±0.003[a]	0.983±0.005
	70	3.736±0.020[a,b]	3.123±0.053[a]	0.027±0.002[a]	0.038±0.002[a]	0.982±0.008
10	0	4.075±0.035[a]	3.240±0.552[a]	0.029±0.001[a]	0.044±0.001[a]	0.966±0.021
	20	3.802±0.116[a,b]	3.213±0.436[a]	0.031±0.003[a]	0.043±0.005[a]	0.977±0.013
	40	3.661±0.171[b]	3.067±0.097[a]	0.029±0.001[a]	0.039±0.003[a]	0.979±0.008
	70	3.629±0.103[b]	2.744±0.013[a]	0.028±0.001[a]	0.037±0.002[a]	0.965±0.005
17	0	3.908±0.333[a]	3.033±0.498[a]	0.036±0.001[a]	0.052±0.003[a]	0.987±0.001
	20	3.608±0.043[a]	4.021±0.105[b]	0.050±0.002[b]	0.067±0.002[b]	0.990±0.009
	40	3.457±0.009[a]	3.077±0.402[a,b]	0.057±0.005[b]	0.072±0.007[b]	0.986±0.003
	70	3.550±0.071[a]	2.807±0.240[a]	0.051±0.001[b]	0.066±0.001[b]	0.986±0.007

Different letters indicate statistically significant differences under different SMF intensities, for a given day and a given VOC, at a 95 % confidence.

CHAPTER III. Stimulation of toluene biofiltration under continuous and intermittent operation by a static magnetic field

Highlights

- 50 mT SMF exposure improved the biodegradation of toluene
- The biofilter recovery after shutdown periods was favored by the SMF
- Biofilm formation is quicker under SMF
- SMF triggered a higher microbial activity

The present chapter is a modified version of the article under submission: López-Bello E, Aizpuru, A, Arriaga S, 2025. ***Stimulation of toluene biofiltration under continuous and intermittent operation by a static magnetic field***. Journal of Process Biochemistry.

3.1 Abstract

Impact of exposure to static magnetic field (SMF) was assessed during the biological treatment of toxic toluene vapors. Two identical biofilters were operated, one in presence of a 50 mT SMF, the other without. The treatment was first carried out with a continuous toluene inlet load of 60 $gm^{-3}h^{-1}$, then with discontinuous airflow, including weekend and night shutdowns. During steady-state operation under continuous toluene load, the presence of the SMF improved the toluene removal by 23%, achieving a significantly higher elimination capacity (EC) (53 vs. 43 g $m^{-3}h^{-1}$). During the intermittent load operation, higher robustness regarding shutdowns was noted in the exposed biofilter, with a prompter recovery of removal efficiency (RE) after shutdowns (1.5 h vs. ≈2.5 h). Although impacted by the discontinuous load operation, the EC remained significantly higher in presence of the SMF (42.2 vs. 36.1 g $m^{-3}h^{-1}$). The SMF mostly boosted biofilm formation during the startup (first 15 days), generating a 30% higher biomass. This was mediated by an increase in the protein content of extracellular polymeric substances (EPS), which allowed for better microbial attachment on the packing material, and lower lixiviation of organic carbon. The better toluene removal under the SMF could be linked with higher microbial activity, confirmed by higher CO_2 production. Moreover, the observed consumption of EPS as an alternative carbon source during discontinuous toluene loads was reduced in presence of the SMF. These results demonstrated that applying SMFs can be an economically and environmentally friendly technology to enhance the performance of biofiltration.

3.2 Introduction

Volatile Organic Compounds (VOCs) are a large family of chemicals which evaporate easily in ambient conditions, causing health and environmental issues, even at low concentrations [1]. VOCs are also the main precursors of tropospheric ozone and photochemical smog [2], [3] and include a wide range of compounds such as aliphatic and aromatic hydrocarbons, halocarbons (particularly chlorinated), and oxygenated hydrocarbons (alcohols, ketones, aldehydes, etc.) [1], [4].

Anthropogenic VOCs can be released into the air by both mobile and stationary sources (transport and industrial activities). Particularly, stationary sources are associated with petrochemical refineries and various solvent-using processes in the food, chemical, printing, paint, and textile industry. Exposure to VOCs vapors can affect the respiratory and immune systems, cause irritations and damages to different organs, and even promote the development of cancers [1], [5]. Consequently, effective treatment of VOC emissions from point sources is essential.

Among the end-of-pipe treatments, biological processes have emerged as a promising technology for treating low concentrations of VOCs (<5 g m^{-3}), as they allow for minimal operation costs, and no secondary pollution [5], [6]. Among them, biofiltration is the most common technology in which the contaminated airflow circulates through a humidified packing material which supports the growth of microorganisms, and the development of the biofilm. The biological oxidation generates non-toxic products like CO_2, water and biomass [3].

However, biofilter performance can be limited by challenges in mass transfer or biodegradation kinetics, especially for hydrophobic VOCs or recalcitrant compounds like chlorinated VOCs [3], [5], [7]. In the case of hydrophobic VOCs, which are prone to mass transfer limitations, several strategies have been addressed to improve VOCs degradation such as the use of hydrophobic fungal biomass which can favor the transport of the VOCs from the air to the biofilm phase. The combination of biofiltration with physicochemical pre-treatments has also been reported to improve hydrophobic VOCs degradation as such processes help to reduce high VOCs inlet loads, and also contribute to their partial oxidation, thus, improving the subsequent

biofiltration process. Another process reported to alleviate the biodegradation of hydrophobic VOCs is the use of two phase partition bioreactors that employ a non-liquid aqueous phase to trap the hydrophobic VOCs enhancing their mass transfer, however these bioreactors are expensive to operate and there can be a loss of the non-aqueous phase as an emulsion can be formed [1], [8], [9]. For recalcitrant VOCs, like chlorinated compounds, slow biodegradation can be improved with a co-substrate that promotes microbial growth and enzyme release [1], [2], [10], [11]. Additionally, fluctuations in pollutant concentrations, often due to intermittent industrial emissions, represent a challenge in the reliability of biofilter performance. This is particularly evident during shutdown periods which are part of the routine manufacturing practice (night, weekends, or holidays) [6], [12]. Temporary disruptions in pollutant supply can adversely impact microbial activity, leading to microbial decay and cell lysis. In some cases, during the intermittent period, control strategies such as real-time monitoring and adaptive feedback systems can help maintain optimal biofilter operation by adjusting airflow or pollutant concentration thresholds in response to changes [13]. Another solution is the use of hybrid biofiltration systems, combining traditional biofiltration with activated carbon or other materials to buffer fluctuations in pollutant concentrations and to enhance system resilience during periods of disruption in pollutant supply [2], [10].

Recently, the application of magnetic fields (MFs) has been investigated to overcome biofiltration of VOCs limitations and to achieve higher removal efficiencies [2], [10], [14]. Although, most studies of biological processes using magnetic stimulation have been focused on wastewater treatment or bioenergy production [15]–[18]. In most cases, MFs have been maintained constant over time (static magnetic fields (SMFs)), within a moderate intensity (> 1 miliTesla (mT), but < 500 mT) [15], [19]. As illustrated by the wide range of SMFs intensities tested in the literature, no consensus has been reached regarding which intensities achieve positive outcomes. It is known that the effects do not progress linearly with the intensity of the SMF, as positive or negative impacts can be observed, and the best results have been observed within a specific intensity window, such as 30-90 mT [16] or 10-30 mT [14]. The impact observed under a given SMF intensity can also depend on other biotic

or abiotic factors, such as the type of microorganisms involved, the initial amount of biomass, the growth media, or even the influent concentrations and reactor configuration. For example, in wastewater treatment, SMFs have been shown to enhance nitrogen reduction, boosting nitrification and denitrification rates [17], [20], [21]. Also, the chemical oxygen demand reduction was enhanced due to the stimulation made by SMF [21]–[23]. These effects were directly related to changes in the microbial community that improved the development of denitrifying bacteria. Interestingly, in the specific case of wastewater containing volatile organic pollutants, application of a SMF of 7 mT, and 370 mT have allowed for a 30 and 34% higher biodegradation of formaldehyde [23], and phenol [24], respectively, stimulating the microbial growth.

Only three studies have been carried out regarding the impact of SMFs in biofilters. Two of them deal with the treatment of trichloroethylene (TCE) [2], [10], a low biodegradable pollutant [11]. The first study tested SMFs of 30, 60 and 130 mT, with a microbial consortium coming from activated sludge [2], the other tested SMFs of 20, 60, and 80 mT, with a fungal consortium [10]. Regarding the microbial consortium, the higher performance was achieved at 60 mT, with better efficiency than the non-exposed biofilter throughout the whole experiment, achieving a +35% higher maximum elimination capacity (EC_{max}) (2.66 vs. 1.97 g m^{-3} h^{-1}). Interestingly, the lower intensity of 30 mT allowed for some performance increase (+10% of EC_{max}), while 130 mT caused a notable inhibition of the biodegradation of TCE (-15% of EC_{max}). For the fungal consortium, different magnetic fields were successively applied in the same reactor [10]. On steady state, the EC_{max} values were consistently higher at SMF intensities of 20 mT (2548 mg m^3 h^{-1}), 60 mT (2412 mg m^3 h^{-1}), and 80 mT (2318 mg m^3 h^{-1}) compared to the control at 0 mT (2038 mg m^3 h^{-1}). Additionally, a 7-day complete shutdown (without air and TCE) was tested. Once the biofilter restarted, the recovery was evaluated under the influence of the most effective SMF intensity (20 mT). Around 6 days were needed to recover the original EC_{max} obtained before the shutdown. However, recovery after the shutdown

period was not evaluated in absence of a SMF [10]. To date, the impact of the presence of a SMF on biofiltration robustness against shutdowns has never been assessed.

In a previous study, the effect of a SMF on the biofiltration of hexane, a strongly hydrophobic VOC, was evaluated. An increase of the maximum hexane removal efficiency from 25% (without SMF) to 36 and 40% was reached for the two tested intensities of 10 and 30 mT, respectively [14]. Moreover, a memory effect was observed, as the biofilter improvement could be maintained for several days after suspending the SMFs stimulation.

While the mechanism of SMF action remains unclear, several hypotheses have been proposed to explain their impact on biological processes [11], [15]. Certain SMF intensities may alter the orientation of the membrane phospholipid bilayer, increasing permeability and exchange fluxes [10], [14], [17], [20]. SMFs have also been shown to enhance enzymatic activities, possibly by interacting with charged particles and affecting electron spin states [15], [17], [25]. These effects can explain the increased microbial growth observed in the presence of some SMFs [2], [10], [16], [22], [24], [26]–[28]. SMFs also influence the amount and composition of EPS, which enhance biofilm cohesion and properties like surface charge and hydrophobicity [15], [28]. Higher EPS levels can improve biofilm formation and biosorption of hydrophobic substrates [18], [20], [25], [29], [30].

As very little work has been done on the biological air treatment under SMFs, the present study aims to investigate the effects of SMFs on biofiltration efficiency, focusing on toluene, a moderately hydrophobic VOC (0.1<H (dimensionless Henry's law constant) <0.99) commonly used in industry [9]. Toluene is a major VOC pollutant and has been associated with liver, kidney, and central nervous system damage [31]. This research will assess the impact of a SMF on the toluene biofiltration efficiency, during continuous and intermittent periods, with a particular focus on biomass viability and biomass growth, as well as the EPS production.

3.3 Methodology

3.3.1 Experimental setup

Two identical biofiltration reactors were simultaneously operated, consisting of cylindrical towers with a diameter of 9.7 cm, and an effective volume of 1.1 L. Biofilters were packed with perlite from La Laguna, Mexico. Perlite was inoculated with activated sludge from the wastewater treatment plant of the University (Universidad del Mar, Oaxaca, Mexico), previously acclimated to toluene for 6 months. Three times a week, 20 mL of medium was added to each system to ensure bed moisture content and availability of nutrients for microorganisms' growth. The mineral medium composition has been previously described [32] and was adjusted to pH 7 with NaOH. For each biofilter, toluene vapor was generated within a stripping reactor and the resulting air stream was combined with humidified air and delivered into the bioreactor in an upward direction mode at 1.1 L/min, which resulted in 60 seconds of empty bed residence time (EBRT). During the overall operation, the inlet load (IL) was kept constant around 60 $gm^{-3}h^{-1}$ (average of 62±1 $gm^{-3}h^{-1}$, for both biofilters).

One of the reactors was exposed to an average SMF of 50 mT, while the other, the control reactor, was not exposed. The SMF was generated by neodymium magnet blocks (50 x 10 x 4 mm). The magnets were fixed radially outside of the biofilter column. Two sets of magnets were used, each consisting of 4 magnets arranged in circle, at 90º of each other, as shown in Fig. 1. The SMF intensity inside the cylindrical reactor was measured with a Tesla-Meter (HT20, Hengtong, Shanghai, China), in 6 horizontal cross sections located at biofilter heights of 6, 8, 10, 12, 14 and 16 cm (Fig. 3.1). In each cross section, magnetic field intensity measurements were taken every 1 cm from the center to the reactor wall, following diameter lines at angles of 45º from each other.

The operation of the reactors consisted of two stages. The first stage lasted 45 days under a continuous flow of toluene polluted air, the second stage lasted 20 days under intermittent load, with shutdown periods where no air flow was provided. Intermittent load conditions simulated for a 5-days working week, where the reactors

were fed for 8 hours a day, followed by a 16 h air shutdown. During the weekend, air flow was suspended for 60 h (2.5 d).

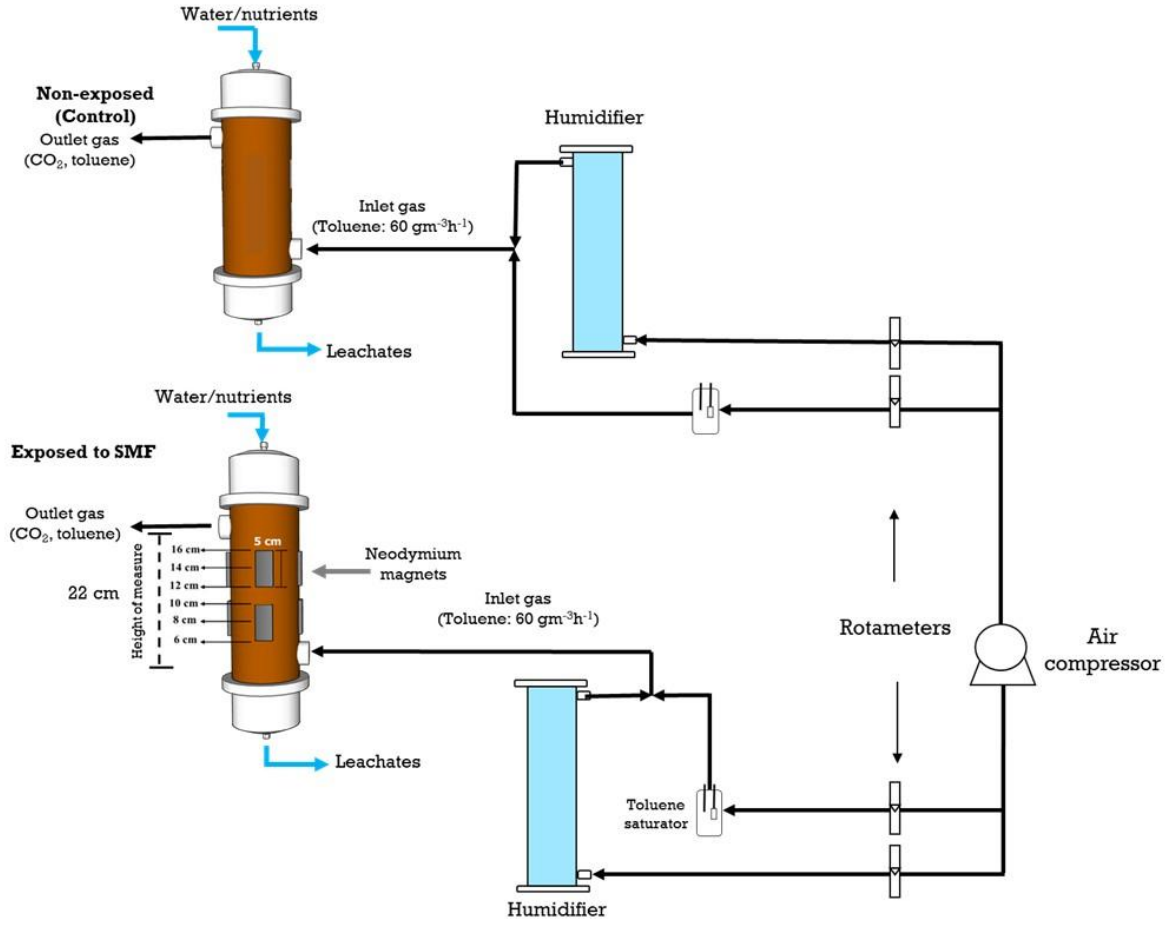

Fig. 3.1 Schematic diagram of the biofilter set-up with neodymium magnets

3.3.2 Analytical methods

3.3.2.1 Gas chromatography

Gaseous samples of 100 µL were collected with a gas-tight syringe from the inlet and outlet of the biofilters (Vici Precision Sampling, Inc.) to determine toluene and CO_2 contents. The concentration of toluene was assessed using a flame ionization detector incorporated in a gas chromatograph 6890N Network GC System (equipped with a DB-624 capillary column). Temperatures were maintained at 140, 250 and 250 °C for the oven, injector, and detector, respectively. CO_2 concentration was measured through a thermal conductivity detector within a 6850N Network GC

System (fitted with an HP Plot Q column). The oven, injector, and detector were set at temperatures of 60, 200, and 200 °C, respectively.

3.3.2.2 Total organic carbon and biomass content

Leachate samples from the bottom of the biofilters were collected once a week to quantify total organic carbon (TOC) content (TOC-VCSH SHIMADZU ASI-V). Leachates were previously centrifuged at 4500 rpm for 20 minutes and filtrated through a 0.22 µm membrane. Perlite samples were periodically collected from the biofilter. Their biomass content was determined by volatile solids [33].

3.3.2.3 Extracellular polymeric substances

EPS content was extracted from 1 g of perlite containing biomass using the NaOH-formaldehyde method [34]. Protein and carbohydrate contents of the EPS were determined following standard methodologies [35], [36].

3.3.3 Cell viability

The cell viability was determined at the beginning and at the end of the continuous and intermittent load stages. Samples were examined under a 40X magnification in an epifluorescence microscope (Axio Imager M2, Zeiss). The microorganisms were stained with propidium iodide (red) to mark dead cells, and with thiazole orange to mark live cells (green), as previously reported [37]. A digital camera was used to capture fluorescent micrographs, and ZEN 2012 acquisition software was used to process and analyze the images. Approximately 10 images per sample were processed and analyzed in duplicate. Cell viability was calculated according to previously reported methodology [37].

3.3.4 Treatment of data

The inlet load (IL, g $m^{-3}h^{-1}$) (eq. 1), removal efficiency (RE, %) (eq. 2), elimination capacity (EC, g $m^{-3}h^{-1}$) (eq. 3), and CO_2 production rate (P_{CO2}, $gm^{-3}h^{-1}$) (eq. 4) were calculated with the following equations [38]:

$$IL = \frac{Q}{V_r} C_{in} \qquad (eq. 1)$$

$$RE = \frac{100\ (C_{in} - C_{out})}{C_{in}} \qquad (eq. 2)$$

$$EC = \frac{Q\ (C_{in} - C_{out})}{V_r} \qquad (eq.3)$$

$$P_{CO2} = Q * \frac{C_{CO2,out} - C_{CO2,in}}{V_r} \qquad (eq.4)$$

where C_{in} and C_{out} are the inlet and outlet toluene concentrations (g m^{-3}), $C_{CO2,\ in}$ and $C_{CO2,\ out}$ are the inlet and outlet carbon dioxide concentrations (g m^{-3}), Q the volumetric air flow rate (m^3 h^{-1}), and V_r the effective reactor volume (m^3). It is worth noting that REs and ECs are relied with each other as [6]:

$$EC = IL * \frac{RE}{100} \qquad (eq.5)$$

3.3.5 Carbon balance

A carbon balance was calculated during the 45 days of operation under continuous toluene load. The total amount of toluene removed during this period was calculated by integration of the area under the curve of EC plotted vs. time (h), with the software *OriginPro 2024b*. The result was multiplied by the volume of the biofilter. The mass of the toluene removed from the airflow was expressed in quantity of carbon present in the treated toluene considering the respective molecular weights (MW C/MW toluene). A similar procedure was carried out to obtain the amount of carbon recovered as CO_2, integrating P_{CO2}, and adjusting to the ratio of carbon present in CO_2 (MW C/MW CO_2). Carbon in biomass was calculated based on the assumption that biomass contains 50% (w/w) of carbon. CO_2 concentrations also allowed to evaluate the degree of toluene mineralization. The reaction of complete mineralization of toluene is as follows: $C_7H_8 + 9\ O_2 \rightarrow 7\ CO_2 + 4\ H_2O$, corresponding to 3.3 g of CO_2 produced per g of toluene degraded in case of total mineralization. The ratio between the measured CO_2 and the maximum theoretical amount of CO_2 achievable allowed to estimate the percent of mineralization [39].

3.3.6 Statistical analysis

Statistical analysis was carried out with Minitab 19.1 software. As exposed in a previous study, a paired sample Student's t-test was used to assess if differences

between biofilters were significant [38]. A p-value < 0.05 allowed to confirm the impact of the SMF. All measurements for biomass content, cell viability, TOC, and EPS were performed in triplicate, allowing estimation of standard deviation.

3.4 Results and Discussion

3.4.1 SMF characterization

It is well known that magnetic fields generated by magnets are nonhomogeneous, in contrast to those generated by Helmholtz coils, which are more homogeneous [14], [40]. Thus, the SMF intensity inside the reactor was characterized. Due to the reactor symmetry across a horizontal plane at medium height (11 cm), SMF intensities were identical at cross sections located at heights of 6 and 16 cm (Fig. 3.2-a), 8 and 14 cm (Fig. 3.2-b), and 10 and 12 cm (Fig. 3.2-c), respectively. A similar behavior was noted in the different cross sections, with higher SMF intensity (>130 mT, red zone) in small regions located at proximity of the magnets. Such regions were surrounded with regions of medium intensity (70-100 mT, green zone). A lower intensity region (<50 mT, blue zone) with a diagonal cross shape covered the area of the center of the biofilter, and the biofilter walls which were not in direct contact with the magnets. Most of the biofilter was covered by a SMF intensity between 30 and 100 mT, reaching an average SMF of 50 mT.

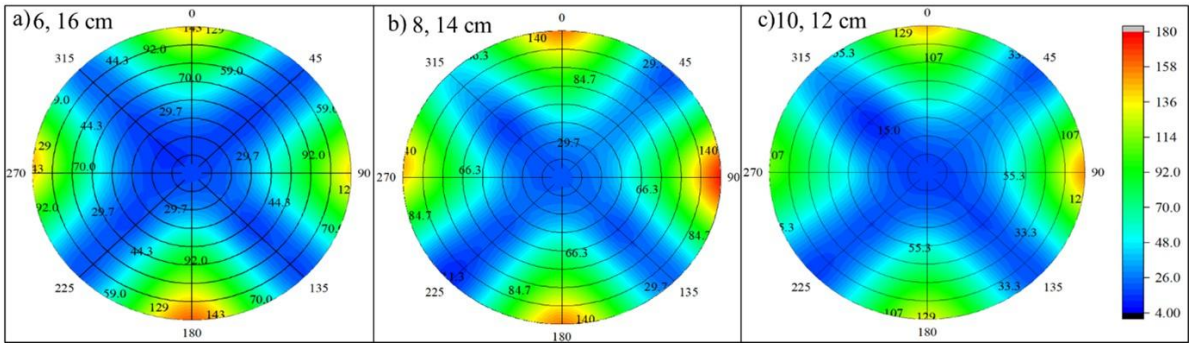

Fig. 3.2 SMF intensity inside the biofilter (mT). Horizontal cross sections at heights of a) 6 and 16 cm, b) 8 and 14 cm, and c) 10 and 12 cm.

3.4.2 Effect of the magnetic field on the toluene removal performance

RE is a useful parameter to get an overall overview of the performance of a given biofilter, as it indicates how much percent of the entering pollutant is treated. Fig. 3.3-a reports the REs obtained under continuous load and during the last 2 weeks of operation under intermittent load (days 54 to 65), measured after the stabilization of biofilter performance consecutive to the airflow restoration (minimum 5 h after air restart). A high RE was noted from the first day of biofilters' operation (48.3 and 37.5%, with and without SMF, respectively). REs progressively increased till reaching maximum values of 95 and 92%, on day 22, for the biofilters exposed and non-exposed to the SMF, respectively. During such initial RE increase, differences between biofilters were not significant ($p=0.108$). After a small decrease of REs, values reached steady states of around 83±3 and 77±6%, in presence or in absence of the SMF, respectively (days 25 to 45). It is worth noting that although such RE difference was minimal between biofilters (6%), a paired Student´s t-test indicated that the SMF allowed for a significant performance improvement ($p=0.002$). Actually, during such period, 78.5% of the time, the REs were higher in the presence of the 50 mT SMF. During the last stage of operation, the interruptions of the air supply had a negative impact, causing a nearly 15% reduction of the REs, reaching average values of 68±5 and 59±5%, with and without SMF, respectively. However, under such intermittent loads, the presence of the 50 mT SMF still allowed for a significant improvement of the toluene removal ($p=0.0001$), with a high RE observed on every measurement day.

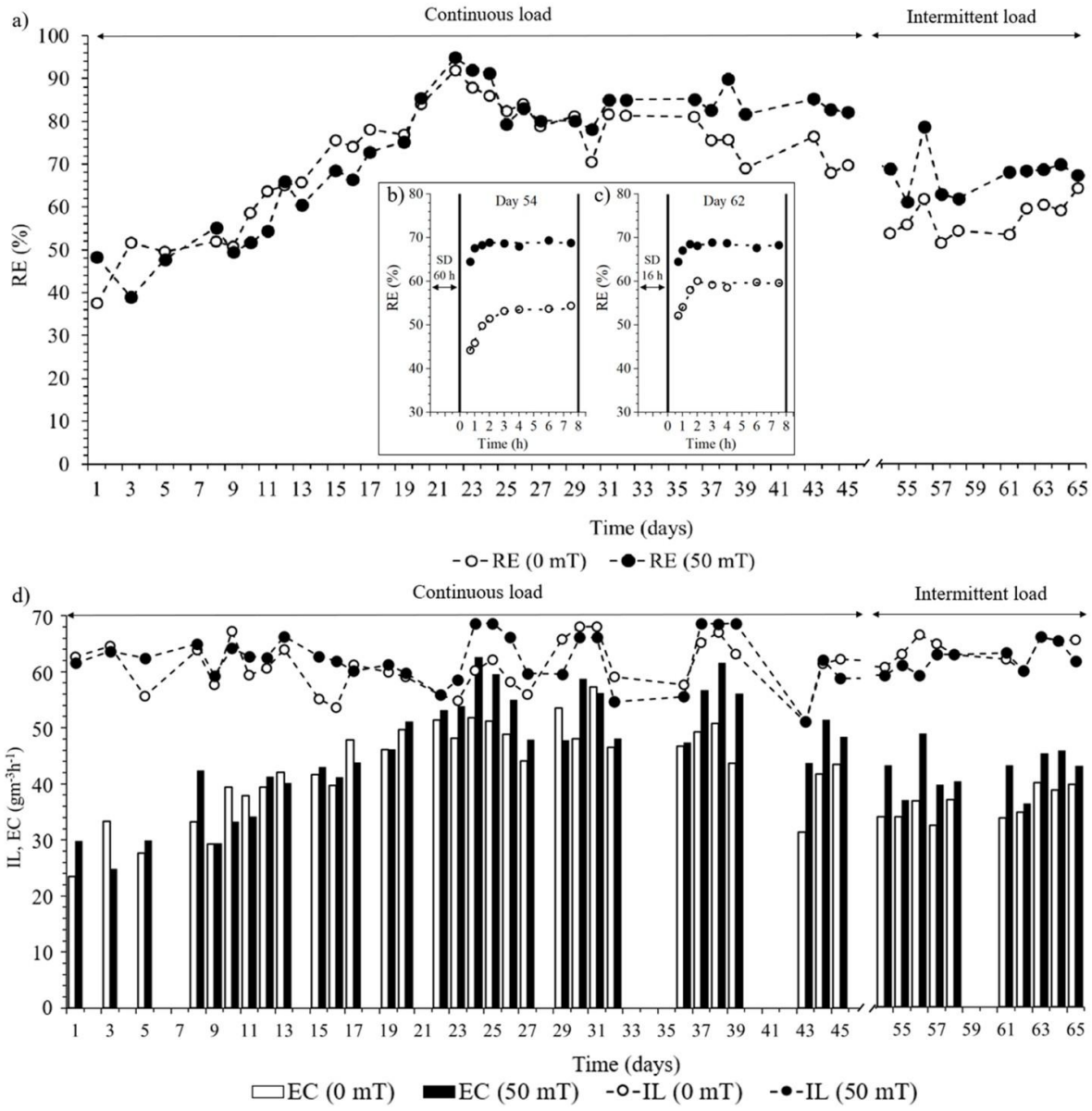

Fig. 3.3 Evolution of toluene removal efficiency (RE) (a) along biofilters' operation and after shutdown periods (SD) of (b) 60 and (c) 16 h; and (d) evolution of inlet load (IL) and elimination capacity (EC) along biofilters' operation with and without the SMF.

Fig 3.3-b and 3.3-c give the typical RE evolution after the restoration of the toluene IL, exemplified by days 54 and 62. In absence of the SMF, RE reached steady-states in around 2 and 3 h for shutdowns of 16 (Fig. 3.3-b) and 60 h (Fig. 3.3-c), respectively. The longer recovery period for the 60 h shutdown is in accordance with

previous studies, where longer toluene deprivations required a longer acclimation period to fully restore biofilter microbial activity [6], [41]. For example, for a similar toluene IL (65 g m^{-3} h^{-1}), a time lapse of 1 h and 6 h has been required to achieve stationary RE values after overnight or weekend biofilter closures [41]. The specific time needed to recover biofilter performance after a shutdown period is variable between studies, as it depends on several factors and particularly on the specific resistance to starvation of the microorganisms involved, and the presence of reservoir organic content in the biofilter packing material [6]. However, in the case of the biofilter exposed to the 50 mT SMF, after both shutdown periods, stabilization of the RE, reaching 68%, occurred in only 1.5 h, and in the biofilter without SMF the stabilization of the RE occurred in 2-3 h, reaching only 60 and 54 % for the intermittent periods of 16 and 60 h, respectively. The faster performance recovery in the presence of the SMF suggests that magnetic fields can improve biofilter robustness to discontinuous operations.

Fig. 3.3-d displays the ILs and the ECs obtained all along biofilters' operation. During the 65 days of operation, the average ILs were maintained at 62.2±4 and 61.3±4 g m^{-3} h^{-1}, for the biofilters operated with and without the SMF, respectively, with no significant difference between them (p=0.15). ILs were also equivalent between both biofilters when only considering the continuous (62.2±4 and 60.6±4 g $m^{-3}h^{-1}$) and the intermittent load stages (62.1±2 and 63.6±2 g $m^{-3}h^{-1}$) (p=0.08). Thus, as the ILs were maintained nearly constant during the overall operation, the behavior of the ECs was similar to the one of the REs (Eq. 5). However, EC is a key parameter to compare biofilters of different sizes, as it indicates the amount of pollutant treated per unit of time per unit of volume of the biofilter. As EC is normalized with respect to biofilter volume, inter-studies comparisons are typically discussed in terms of EC [38]. The first day of operation, the ECs reached 23.7 and 29.5 g $m^{-3}h^{-1}$, in presence or in absence of the SMF, respectively. Such an initial consumption of toluene can be directly related to the previous acclimation of the sludge inoculum to toluene, which was attained over several months. After a progressive increase, the ECs stabilized (days 22-45), at 53.4±4 and 47.5±4 g $m^{-3}h^{-1}$, for the biofilters exposed and non-

exposed to the SMF, respectively. Despite the strong proximity of the EC values, such differences were statistically significant (p=0.0002). During all the biofilters' operation, the highest ECs reached 62.6 (day 24) and 57.2 g $m^{-3}h^{-1}$ (day 31), in presence or absence of the SMF, respectively. Noteworthy, during the last week in continuous stage (from day 37 to 45), the effect of the presence of the SMF was more evident, with a higher EC systematically observed at each measurement made in presence of the SMF. During this period, the removal of toluene vapors in the biofilter exposed to SMF was higher than in the control by 23%, reaching average values of 53 vs. 43 g $m^{-3}h^{-1}$ (p=0.0005). Such a 23% difference in EC is higher than the intrinsic 10% variability that can be expected between identical biofilter set-ups [38], confirming the benefic impact of the SMF. Overall, the ECs were within the values typically obtained in toluene biofiltration studies, as maximum ECs of around 50 g $m^{-3}h^{-1}$ have already been reported for high toluene loads [31]. For example, very close ECs of 56 g $m^{-3}h^{-1}$ (RE of 86%) have been reported under a similar toluene continuous load of 65 g $m^{-3}h^{-1}$ [41].

The ECs were negatively affected by the operation under intermittent loads, reaching average values of 42.2±4 and 36.1±3 g $m^{-3}h^{-1}$, in presence and in absence of the SMF, respectively. It is worth noting that, in some studies, the toluene abatement is not deteriorated after a transition from continuous to intermittent load (16 h/day, 5 days/week) under analogous conditions (toluene IL around 60 g $m^{-3}h^{-1}$, and EBRT of 1 min) [6], [41]. However, as with the continuous load, the presence of the SMF allowed for a toluene removal improvement. In average, under the intermittent load, the EC was 16% higher in presence of the SMF (p=0.0003).

The enhanced ECs observed in presence of the 50 mT SMF (+23% and +16%, during continuous and intermittent toluene loads, respectively) have been observed in biofilters treating other compounds. Particularly, the ECs of TCE were increased by 35 and 25%, at SMFs of 60 and 20 mT, for bacterial and fungal biofilters, respectively [2], [10]. Similarly, the EC of a biofilter treating hexane was recently improved by 27% (from 14.2 to 18 g $m^{-3}h^{-1}$), in presence of a 30 mT SMF [14]. Thus, SMFs can enhance the biofiltration efficiency for a wide variety of compounds,

including recalcitrant (TCE), hydrophobic (hexane) and moderately hydrophobic (toluene) compounds. The exact way that SMFs can affect microbial activities has not been fully elucidated. However, biofilter removal enhancement under SMFs has been related with a higher biomass growth, higher enzymatic activities, or an improved substrate transfer from the air to the biofilm, or across microbial membranes. A deeper insight into the biofilter operation addressed in the next section, particularly considering biomass growth, CO_2 production and production of EPS, can give a better overview of the processes involved in presence of SMFs.

3.4.3 Effect of the SMF on biomass, CO_2 production and TOC content

Alterations in growth rates and in cell viability are among the most frequently analyzed parameters when evaluating the impact of magnetic fields on microorganisms [42]. Herein, the biomass content was assessed in presence or in absence of the SMF, during all the biofilters operation (Fig. 3.4-a). The cell viability, obtained at the beginning and at the end of the continuous and intermittent load stages, is presented in Fig. 3.4-b. On the first day of operation, biofilters started with the same amount of biomass (≈120 mg g^{-1} (Fig. 3.4-a)). During the first two weeks, a 30% higher biomass accumulation was noted in the biofilter exposed to the SMF (e.g. 182 vs. 136 mg g^{-1}, on day 15). For the rest of the continuous load operation, the differences between biomass concentration tend to decrease. Still, higher biomass was always recorded in the SMF exposed biofilter, with, for example, ≈10% higher contents for the last two measurements within the continuous load stage (averages of 180±8 vs. 164±4 mg g^{-1}). Regarding the intermittent load stage, the biomass contents remained almost similar to those obtained at the end of the continuous stage. Thus, the night and weekend shutdowns did not severely affect the total amount of biomass in the biofilter packing material. However, absence of a carbon source during similar or longer starvations periods can frequently lead to a significant biomass loss due to cell lysis and endogenous metabolism [6]. On average, during the intermittent load operation, the biomass growth remained marginally higher in presence of the SMF (188±9 vs. 179±10 mg g^{-1}). A pair Student's

t-test confirmed that the SMF promoted biomass growth during all the biofilter operation (continuous operation days 1-45, and intermittent period days 54 and 65) ($p=0.006$). Overall, the microbial growth mediated by the SMF mainly occurred during start-up, finally reaching very similar biomass contents after one month of operation. This suggests that the SMF merely promoted the establishment of the biofilm. In a study dealing with the biofiltration of TCE by a bacterial consortium, a similar statement was made, as a SMF of 60 mT was believed to have shortened the time of biofilm formation [2].

However, there is no global consensus regarding the impact of magnetic fields on microorganism growth, as negative, neutral or positive outcomes have been observed in the literature, without a full understanding of underlying mechanisms. Actually, the effect of magnetic fields depends on several experimental parameters, such as the chemical composition of the medium, the type and intensity of the magnetic field, the time of exposure, as well as the proper nature of the microorganisms [42], [43]. However, in several environmental applications, higher microbial growth has been observed under SMFs, allowing for a better pollutant removal. For example, SMF stimulation of bacterial growth has already been noted in batch reactors treating wastewater, with shorter lag-phases and higher growth rates in presence of moderate SMFs (5 and 20 mT), while higher SMF intensities inhibited growth (200 and 500 mT) [22]. Similarly, during the treatment of formaldehyde in wastewater, the presence of a 7 mT SMF allowed for a 30 % higher removal efficiency, which also promoted the growth of biomass from 4684 to 6391 mg L^{-1} [23]. However, in the present case, the SMF mostly started to promote the toluene EC from the last weeks under continuous load, when the increase of the biomass content under SMF was minimal, suggesting that the total amount of biomass was not the main determinant factor of the performance improvement. Still, the SMF could have induced qualitative modifications regarding microbial populations. Actually, in two studies treating VOC vapors, the presence of a SMF has already been linked with a better removal performance associated with significant changes in microbial richness and diversity. Particularly, a reduction of bacterial diversity and a higher relative abundance of microorganisms involved in the

VOC degradation has been noted during the treatment of trichloroethylene in a biofilter exposed to a 30-130 mT SMF [2]. Very recently, during the biodegradation of hexane vapors in a two phase partitioning airlift bioreactor subjected to SMF, an increase of the relative abundance of all potential hexane-degrading bacteria was noted in presence of a 20 mT SMF. Particularly, the family of *Chitinophagaceae* had been intensively enriched in presence of the SMF, reaching a four times greater relative abundance. Such modifications of microbial population induced by SMFs might contribute to the observed higher VOC removal performance [44].

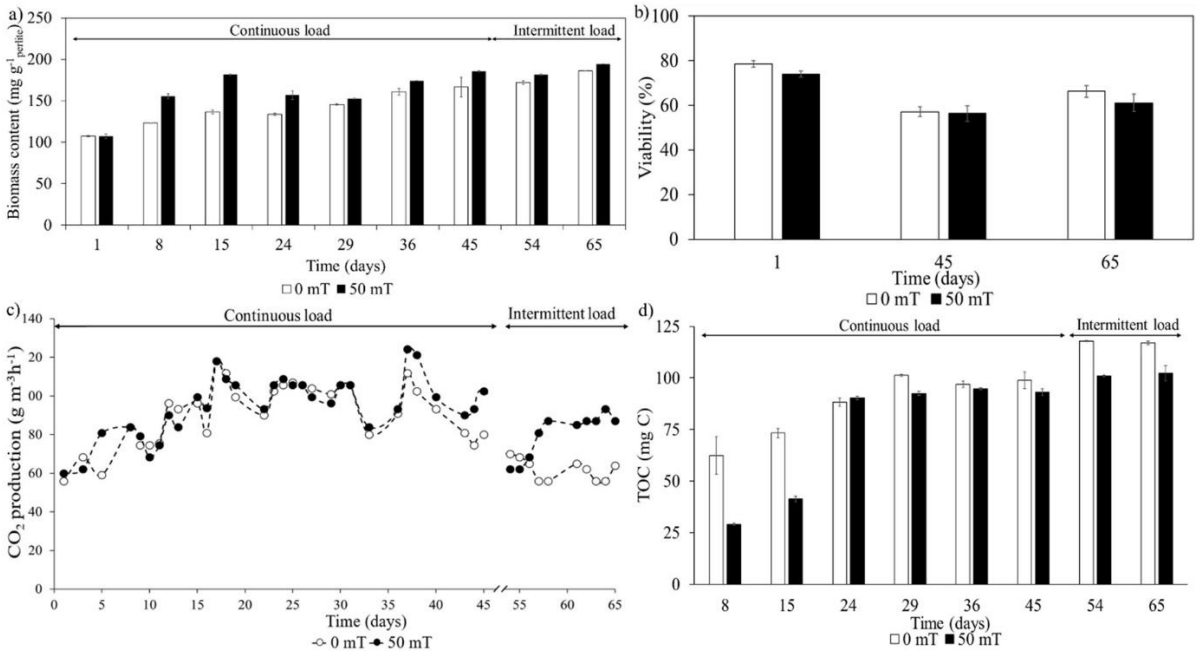

Fig. 3.4 Evolution of (a) biomass content, (b) cell viability, (c) P_{CO2}, and (d) TOC during the biofiltration of toluene with and without the SMF. Error bars represent the standard deviation between triplicates.

On the first day of operation, a bit lower cell viability was noted in presence of the SMF (74.0±1.4 vs. 78.5±1.5%) (Fig. 3.4-b). At the end of the continuous load stage, on day 45, the cell viability decreased, reaching similar values in presence or in absence of the SMF (56.4±3.4 and 57.2±2.3%, respectively). Finally, after the intermittent load stage, cell viability increased, without a significant difference between biofilters (61.2±3.8 and 66.3±2.7%, with and without SMF, respectively). An

increase in cell viability has already been observed in a biofilter after a starvation period, as living cells alternatively utilize dead cells as a carbon source [41]. In brief, the SMF did not significantly affect the cell viability. However, in some cases, under SMF, some microorganisms can present cell surface damages, with a loss of viability [45]. Such effects on cell viability widely depend on experimental parameters including the type, time and intensity of the magnetic field and the nature of the microorganisms exposed [43]. It was recently suggested that cellular damage induced by magnetic fields depends on the type of cell wall, as screening of several bacterial strains exposed to a 18 mT magnetic field only exhibited a notable viability loss for gram-negative bacteria, while promoting gram-positive growth [42]. In the biofilter, the SMF did not significantly affect the cell viability, supporting the fact that the field had no deleterious effect on microorganisms, which could be consistent with the higher microbial growth observed at biofilter start-up, and the higher toluene removal at steady-state.

In biofilters, the amount of CO_2 produced is often a good indicator of the degree of microbial activity [46]. Fig. 3.4-c displays the P_{CO2} evolution all along the operation of the biofilters. On the first day, the biofilters produced a high amount of CO_2 (60.0 and 55.9 g m^{-3} h^{-1}, with and without SMF, respectively), confirming the initial biological activity. On the following days, P_{CO2} increased progressively, until stabilizing between days 22 and 36, at an average of around 100.3±7.8 g m^{-3} h^{-1} for both biofilters. From day 1 to 36, no significant difference was observed in P_{CO2} in the presence of the SMF ($p=0.44$). However, from day 37 to the end of the continuous load stage, the P_{CO2} was always higher in the biofilter exposed to the SMF. During this period, P_{CO2} values were significantly higher with the SMF ($p=0.002$), with an average increase of 16% (105.1±14 vs. 90.5±14 g m^{-3} h^{-1}). The higher P_{CO2} observed in presence of the SMF seems to indicate a higher metabolic activity of the microorganisms. Actually, in the same period (day 37-45), the toluene EC was also higher under the SMF (53 vs. 43 g $m^{-3}h^{-1}$, see section 3.3.4). Interestingly, the P_{CO2} obtained corresponded to a very similar percentage of toluene mineralization (61 and 63%, with and without the SMF, respectively). Thus, the performance improvement under the SMF could be linked with an increase in

biological activity, while keeping a constant proportion between the amount of CO_2 released and the toluene removed. Moreover, the mineralization values obtained are congruent with normal operation of biofilters. At steady-state, a major portion of the degraded organic carbon is usually released as CO_2, as pollutants are primarily used for energy production rather than for biomass formation [46]. When toluene was delivered intermittently, the P_{CO2} decreased in both biofilters, stabilizing after day 56. From day 56 to 65, P_{CO2} was statistically higher in the presence of the SMF, reaching 84.4±7 vs. 59.9±4 g $m^{-3}h^{-1}$ (p=0.0002). Under intermittent toluene feeding, P_{CO2} values decreased by 20% in the SMF biofilter and by 34% in the control biofilter, compared to the stable state of the continuous load period (days 37-45). In the case of the SMF exposed biofilter, the reduction in P_{CO2} was related to the lower toluene EC observed under intermittent toluene feeding (42.2 g $m^{-3}h^{-1}$), as such CO_2 output corresponded to an unaltered percent of mineralization (60%). However, in the absence of the SMF, the P_{CO2} was lower than expected regarding the corresponding EC (36.1 g $m^{-3}h^{-1}$), as the percent of mineralization only reached 50%. Thus, the application of a SMF of 50 mT allowed for the preservation of the mineralization of toluene, which was negatively affected without the SMF. Overall, it is assumed that the presence of the SMF enhanced the microbial activity, which was exhibited by a higher CO_2 production and toluene removal. Several authors have already reported that the exposure to SMFs can enhance the microbial metabolism and enzymatic activity [15]. In a screening of the effect of a 15 mT magnetic field on several bacterial strains growing in a Brain Heart Infusion broth, the exposure to the field allowed some species to have a significant increase in metabolic activity, measured by 3-(4,5-dimethylthiazol-2-yl)-2,5-diphenyl-2H-tetrazolium bromide (MTT) essay. The highest increase of metabolic activity reached +20% for *Enterococcus faecalis,* after 8 h exposure to the magnetic field. Such increase in the metabolic activity was correlated with a higher biomass content in presence of the magnetic field [42]. However, the stronger microbial activity observed under magnetic fields is not always linked with a higher amount of biomass. In another study, a 17 mT SMF inhibited the growth of *Escherichia coli* in Luria Bertani medium, while increasing the specific enzymatic activities (per unit of biomass) of β-galactosidase and dehydrogenase.

The highest enzymatic enhancement was noted after 4 h of exposure at 17 mT, with a 29-times higher dehydrogenase activity [47]. Alteration of enzymatic activities under SMFs has also been studied during the biodegradation of wastewater pollutants. For example, during the treatment of tetracycline in swine wastewater by activated sludge, several enzymatic activities were significantly boosted in presence of a 25 mT SMF. Particularly, specific activities of ammonia monooxygenase, hydroxylamine oxidase, and cytochrome P450 enzyme increased from around 0.008 to 0.0095, 5.1 to 5.4, and 0.19 to 0.22 μmol min^{-1} $mg_{protein}^{-1}$, respectively. The study assumed that such enzymatic enhancement, and associated higher electron generation, promoted the tetracycline metabolic potential of the activated sludge under SMF, observing a complete removal of tetracycline in presence of the SMF, against a removal efficiency of only 83% without the SMF [25]. In another study, dealing with the effect of a 7 mT SMF on the biodegradation of formaldehyde containing wastewater, the SMF enhanced the specific dehydrogenase activity from 100 to 173 μmol s^{-1} $kg_{protein}^{-1}$, for a formaldehyde inlet concentration of 2400 mg L^{-1} [23]. Regarding the treatment of air pollutants, a recent study reported the biodegradation of chlorobenzene vapors in batch experiments, with microorganisms attached to modified polypropylene packing materials incorporating magnetized or non-magnetized powders [29]. The increase of the proportion of magnetized packing during the biodegradation (from 0 to 100%), corresponding to SMF intensities from 0 to 9 mT, allowed for a higher chlorobenzene removal, linked with a four times increase in the dehydrogenase activity (from 0.207 to 0.810 μmol mL^{-1} h^{-1}). The observed enhancement of enzymatic activities under SMFs is not yet fully understood, but can be related to a modification in the kinetic energy of unpaired electrons located in the catalytic center of enzymes, among others [15].

Figure 3.4-d presents the amount of TOC collected in the biofilters leachates. The first leachate contained a significantly lower amount of organic carbon in the case of the biofilter exposed to the SMF (29.1±1 vs. 62.4±9 mg C, day 8). Then, for both biofilters, the TOC increased on day 15, while maintaining the lixiviation of organic compounds notably lower in the SMF exposed biofilter (41.3±1 vs. 73.3±2 mg C). The TOC content in the leachates still increased on day 24, reaching similar values

for both biofilters, and stabilizing for the rest of the operation under a continuous toluene load (averages of 96.3±5.6 vs. 92.6±1.8 mg C, days 24-45, in presence or in absence of the SMF, respectively). Interestingly, since day 24, no significant difference was noted between the TOC amounts present in the leachates with and without the SMF ($p=0.211$). Thus, the SMF only reduced the organic content of the leachates during biofilter startup. As previously discussed, during the same initial operation period, the biomass content in the packing material was strongly increased in presence of the SMF (Fig 3.4-a), as the SMF prompted the establishment of the biofilm. Thus, the SMF seems to prevent the organic leachout from the biofilter, while favoring the formation and the adhesion of the biofilm to the packing material. The production of microbial EPS is the main responsible for the formation of biofilms, as EPS act as a cement between cells, generating cells cohesion and aggregation, as well as their adhesion to material surfaces. The specific EPS composition can also modify the surface charge and hydrophobicity of the bacterial cells, affecting the biofloculation, and the biofilm formation, as well as the affinity between cells and the packing surface [29]. It has already been reported in studies dealing with wastewater treatment that magnetic fields can have a significant influence on the microbial EPS secretion. Particularly, modification of EPS composition through SMF could favor biofilm adhesion tendency, accelerating the biofilm formation [29], [30]. Moreover, it could also facilitate the biosorption of organic compounds (including the treated pollutants) onto the biofilm [25]. Effects of SMFs on biofilm EPS content has been recently observed during the biofiltration of air polluted with hexane [14]. In the present study, such changes in EPS content and composition could be responsible for the differences obtained during the biofilter startup under the SMF, resulting in higher adhesion of organic carbon (lower TOC in leachates) and quicker biofilm formation. Analysis of the EPS evolution is carried out in a further section (section 3.4.5).

During the intermittent load period, the TOC of the leachates increased in both reactors compared with the previous state. However, during this period (days 54 and 65), the TOC of the SMF exposed biofilter was significantly lower, reaching 101±1.0 vs. 117±0.7 mg C ($p=0.048$). Increases in the lixiviation of organic compounds can

be observed after periods of substrate deprivation, which can affect microorganism activity, generate cell lysis and acidic byproducts [6]. However, the lower TOC levels in the leachates under the SMF can be related to the better oxidation of by-products, maintenance of the microbial activity, and the previously discussed improved fixation of the biofilm.

3.4.4 Carbon fate

The carbon balance during the continuous load operation stage is reported on Table 3.1. To have a better view of what specifically occurred on biofilters startup, a carbon balance was also realized for a shorter period, considering the first 24 days of operation (Table S1). During the overall 45 days, the total amount of toluene carbon entering the biofilters was similar (≈65 gC), although a slightly greater amount of toluene was eliminated in the SMF exposed biofilter (48.7 vs. 45.3 gC), finally achieving a ≈75 vs. 70 % removal efficiency. As exposed earlier (section 3.2), the overall toluene elimination was quite similar in both biofilters considering the first 24 operating days only, while the SMF allowed for a higher toluene elimination afterwards (26.4 vs. 23.5 gC, corresponding to 85.4 and 75.8 % of the total entering toluene carbon (Table S3.1). Of such eliminated carbon, a similar fraction (around 69-70%) was recovered as CO_2 in the gas phase, biomass onto the biofilters packing material, and TOC in the leachates (Table 3.1). Thus, there could be a non-estimated fraction of carbon present as organic by-products, or a systematic underestimation of the recovered carbon. However, such imprecision is usual in biofiltration studies, with a variable percentage of the carbon not accounted for, and commonly 10–50% of the degraded carbon missing [46]. Nevertheless, carbon balances may give a general idea on the fate of the pollutant carbon. In the present case, for the whole continuous load operation, most of the toluene carbon biodegraded was mineralized as CO_2, with similar values under the magnetic field (61 and 63 % for the biofilters with and without SMF, respectively, Table 3.1). As usually observed in biofiltration studies [46], CO_2 remained the main carbon endpoint even when considering the startup and final period of the continuous toluene load operation (Table S3.1). In brief, for all carbon balances (Table 3.1 and Table S3.1), the biomass only represented less than 10% of the eliminated toluene carbon, and the TOC less than

1.5%. Interestingly, as previously discussed, the final biomass was higher in presence of the SMF (3.6 vs. 2.6 g C, Table 1), particularly due to a stronger biomass accumulation during the first 24 days (2.1 vs. 0.9 g C, Table S3.1). Similarly, under the SMF, the lower TOC lixiviation in the biofilters leachates (0.44 vs. 0.52 g C), was mainly due to the biofilter startup (0.16 vs. 0.22 g C).

Table 3.1 Carbon recovery for the biofiltration of toluene with/without magnetic field during the continuous load stage

Biofilter		**0 mT**	**50 mT**
C-Toluene	g inlet load	65.0	65.1
C-Toluene	g eliminated	45.3	48.7
Elimination	%	69.7	74.8
Total recovery	%	70	69.3
C-CO_2	g produced	28.5	29.7
	% mineralization	63	61
C-biomass	g, perlite biomass	2.6	3.6
	% perlite biomass	5.8	7.3
C-total organic carbon	g TOC	0.52	0.44
	% TOC	1.2	1.0

3.4.5 Effect of SMF exposure on EPS content and composition

A critical step in the biofiltration process is the formation of a biofilm which helps to support the growth and activity of microorganisms [46]. Fig. 3.5-a shows the EPS content during the operation of the reactors. On the first day of operation, the total amount of EPS was quite similar in both biofilters, with a slightly higher content in the non-exposed biofilter (6.0 vs. 5.4 $mg_{EPS}\ g^{-1}_{perlite}$). During the following days (days 8 to 24), the presence of the SMF reduced the EPS content, as the values obtained

in the biofilter exposed to the SMF were significantly lower than the control ($p=0.004$), reaching averages of 4.76±0.2 vs. 6.8±0.9 $mg_{EPS}\ g^{-1}_{perlite}$), respectively. Afterwards (days 29 to 45), no significant difference was noted between biofilters ($p=0.43$), with an average of 5.9±1.1 $mg_{EPS}\ g^{-1}_{perlite}$ for the biofilter exposed to the SMF and 5.4±1.1 $mg_{EPS}\ g^{-1}_{perlite}$ for the biofilter not exposed to the SMF. These results indicate that, during the continuous load operation, the primary effect on EPS production occurred during the initial stage when the biofilm formation began. In the biofilter exposed to the SMF, the initial decrease in EPS content was concomitant with a higher biomass growth, and a lower TOC lixiviation, compared to the non-exposed control (Fig. 4). Contrastingly, it is usually reported that a higher EPS content facilitates the cohesion of microorganisms, and the stability and adhesion of the biofilm [28], [29]. Moreover, on the contrary to what is herein observed, several studies have noted a higher EPS production in presence of a SMF [28]. It is believed that microorganisms produce more EPS in presence of an adverse stimuli, as EPS can act as a protective barrier [14], [48]. Magnetic fields can be such a stress factor, thus leading to a higher EPS production [30]. For example, during the treatment of wastewater by anoxic/oxic treatment in a sequencing batch reactor, with a cyclic time of 8 or 12 h, a respective increase of the maximum EPS content of 33% (from 5.84 to 7.78 $mg_{EPS}\ g^{-1}_{biomass}$) and of 63% (from 5.64 to 9.22 $mg_{EPS}\ g^{-1}_{biomass}$) was noted in presence of a ≈40 mT SMF [49]. In another study dealing with wastewater treatment in a sequencing batch reactor, the content of EPS did not achieve a steady state condition, with fluctuations during all the experiment. However, the average EPS at the end of the experiment was slightly higher (+10%) in presence of a SMF of 88 mT (162.2 vs. 147.7 $mg\ g^{-1}_{biomass}$) [30]. Even for non-bacterial microorganisms, a similar increase in EPS secretion has also been noted under SMF. For example, in the case of the archaea *Haloferax mediterranei* a proportional increase of the EPS production with the SMF intensity was noted, with a rise from 62.9 to 106.5 $mg\ g^{-1}_{biomass}$ when passing from a SMF of 0 to 150 mT [50].

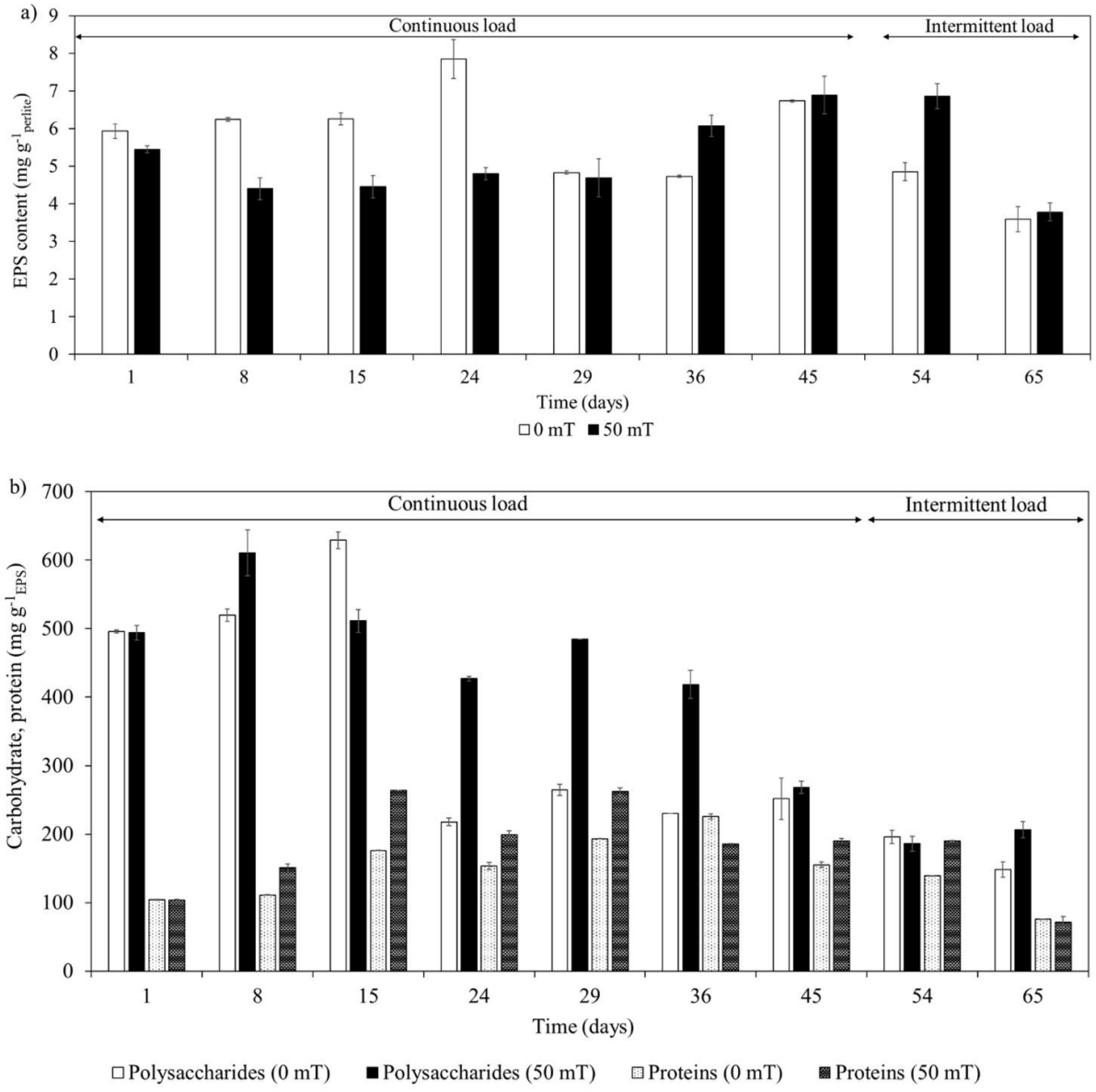

Fig. 3.5 EPS (a) content and (b) composition during the biofiltration of toluene with and without SMF. Error bars represent the standard deviation between triplicates.

However, a decrease of EPS content has also been reported in literature under SMFs. For example, in a study dealing with anaerobic ammonium oxidation for nitrogen removal during the treatment of synthetic wastewater under low and elevated loadings of NH_4^+ (180 and 780 mg L^{-1}, respectively), the presence of a higher SMF (40 and 100 mT) induced a lower EPS content (e.g. passing from 40 to 36 and 29 mg_{EPS} $g^{-1}_{biomass}$ under high loading, at 0, 40, and 100 mT, respectively)

[48]. Interestingly, regarding microalgae, in a study dealing with the EPS production of two cyanobacteria, a 25-30 mT SMF did not have a significant effect on EPS content for *Arthrospira platensis*, whereas a significant decrease was noted for the genetically closed *Spirulina* sp. LEB 18 (with a reduction of EPS from 493 to 338 $mg_{EPS}\ g^{-1}_{biomass}$). Thus, the effect of the SMF on EPS production seems to be closely dependent on the particular specie of microorganism [51]. Moreover, the effect on EPS secretion also depends on the SMF intensity and the time of exposure. For example, in the only air biofiltration study measuring biomass EPS in presence or absence of a SMF, no strong change was noted compare to the control when applying a continuous SMF intensity of 10 mT, whereas a 30% higher EPS content was noted when a continuous 30 mT SMF was applied [14]. On the whole, it appears that SMFs can have different effects on microorganisms, with positive, neutral or negative incidence on EPS secretion, depending on many still unresolved mechanisms. In the present study, the initial decrease in EPS secretion due to the SMF exposure, suggests that the effects of SMF can vary over time.

During the intermittent toluene load period, the EPS content started to decrease on day 54 for the non-exposed biofilter (4.86 $mg_{EPS}\ g^{-1}_{perlite}$), while remaining stable in presence of the 50 mT SMF (Fig. 3.5-a). On day 65, both EPS contents decreased, reaching similar values (average of 3.7 $mg_{EPS}\ g^{-1}_{perlite}$). These values were the lowest observed during the overall experiment. Such decrease in EPS during the discontinuous toluene airflow, can be linked to EPS consumption as an alternative source of carbon in absence of the usual biofilter substrate [46]. As observed on day 54, the presence of the SMF seems to temporally reduce the consumption of EPS, when biofilter was subjected to intermittent loadings.

Polysaccharides and proteins are among the major components of EPS, which can also include carbohydrates, uronic acids, as well as small amounts of nucleic acids [30], [34], [46]. A closer view of EPS composition is given in Fig. 5-b, which displays their polysaccharide and protein contents. During the continuous load operation, the sum of polysaccharides and proteins represents a range of 37-80 and 46-77 % of the total mass of EPS, for the non-exposed and SMF exposed biofilter, with averages

of 53.2±15.3 and 65.3±11.5 % respectively. Thus, a considerable amount of EPS content is present in other forms. It has been observed that uronic acids, and more particularly glucuronic acid can constitute a very considerable portion of the EPS present in biofilters [14], [52]. In comparison, during the intermittent load period (days 54-65), the sum of polysaccharides and proteins represents only 27.9±7.9 and 32.7±7.0 % of the mass of the EPS, indicating a strong consumption of polysaccharides and proteins during the temporary toluene deprivation.

In more detail, on the first day of operation, composition of EPS was similar in both biofilters, with averages of 495±1 $mg_{Polysaccharides}\ g^{-1}_{EPS}$ and 104±1 $mg_{Proteins}\ g^{-1}_{EPS}$, corresponding to a ratio of proteins to polysaccharides (PN/PS) of 0.21. Consecutively, during the first 15 days, the amount of polysaccharides in the EPS slightly increased, with no clear difference between biofilters, maintaining an average (days 8 and 15) of 561±70 and 574±77 $mg_{Polysaccharides}\ g^{-1}_{EPS}$, in presence and absence of a SMF, respectively. In the same time, the protein content of EPS increased, with a much more pronounced increase in the SMF exposed biofilter, reaching as much as 264 vs. 176 mg $_{Proteins}\ g^{-1}_{EPS}$ on day 15. On the same day, such increase of the protein content resulted in a strongly increased PN/PS ratio, which reached values of 0.52 vs. 0.28 in presence and in absence of the SMF, respectively. A greater PN/PS ratio has been linked with a higher hydrophobicity of the biomass, as proteins are among the most non-polar components of the EPS [29], [44]. Changes in composition and structure of EPS related to higher PN/PS values are particularly important at the beginning of the operation, as they promote a higher microbial adhesion on surfaces and ability to congregate and form biofilms [29], [30], [48]. Thus, such initial increment in protein content and PN/PS ratio, and consecutive enhancement of microbial fixation in the biofilter bed, can explain the observed lower TOC content in the biofilter leachates and the quicker biofilm formation in the biofilter exposed to the SMF at the beginning of the operation (Fig. 3.4).

From day 24 to the end of the continuous toluene load phase (day 45), the content of polysaccharides in the EPS was strongly reduced, and somewhat stable, in the case of the non-exposed biofilter (average of 241±21 $mg_{Polysaccharides}\ g^{-1}_{EPS}$).

Contrarily, in presence of the SMF, the polysaccharides content in the EPS remained much higher until before the day 45, at an average of 443±36 $mg_{Polysaccharides}\ g^{-1}_{EPS}$, to finally reach values close to those of the non-exposed biofilter (268 $mg_{Polysaccharides}\ g^{-1}_{EPS}$, day 45). Noteworthy, in the last weeks under continuous toluene load (day 24-45), polysaccharides were significantly higher in presence of the SMF ($p=0.045$). Thus, the decline in the polysaccharides content of the EPS was less strong and took place later in presence of the SMF, indicating a higher stability of the EPS composition for the SMF exposed biofilter. Regarding the content of proteins in the EPS, after day 15, similar averages of 182±35 and 209±36 $mg_{Proteins}\ g^{-1}_{EPS}$ were maintained until the end of the operation under continuous load, in absence or in presence of the SMF, respectively. However, it is worth noting that for the overall operation under continuous toluene load, excepting the day 36, the protein content remained 22-49% higher in presence of the SMF. In a two-phase partitioning bioreactor treating hexane vapors, the presence of a 20 mT SMF also promoted an always higher protein content of the EPS, indicating that SMF might stimulate the microorganisms to secrete more extracellular proteins [44]. Under the intermittent toluene load, in absence of the SMF, the polysaccharides content in EPS progressively decreased reaching the lowest values obtained for the overall operation, finally falling to 148 $mg_{Polysaccharides}\ g^{-1}_{EPS}$ (day 65). In presence of the SMF, the drop in the polysaccharides content was less pronounced, finally reaching 206 $mg_{Polysaccharides}\ g^{-1}_{EPS}$. Regarding the EPS protein content, a fall was also noted with and without the SMF, finally reaching similar values (71±8 and 75±1 $mg_{Proteins}\ g^{-1}_{EPS}$ in biofilters with and without SMF, day 65). However, the fall was dampened in presence of the SMF, as reduction was not yet observed on day 54, contrarily to what was noted in the non-exposed biofilter (190 vs. 139 $mg_{Proteins}\ g^{-1}_{EPS}$).

On the whole, results suggest that SMF exposure has a dynamic effect on EPS content and composition. Particularly, the presence of the SMF seemed to induce a higher EPS protein content, particularly on startup, during biofilm formation. Moreover, the observed reduction of polysaccharides EPS content during long-term operation, and on intermittent load operation, was dampened in presence of the SMF. Alterations of protein and polysaccharide contents of the EPS have already

been observed in presence of SMFs in several studies [25], [29], [30], [48]. In a batch study treating chlorobenzene vapors, different packings, containing different proportions of a magnetized material, allowed to generate inner batch SMF intensities between 0-9 mT [29]. In such study, the increase of the SMF induced higher EPS protein content, with a total amount of EPS proteins fixed in the surface of the packing material increasing from 37.9 to 180.8 mg g^{-1}. Such increase in protein content of EPS was linked with an accelerated formation and a higher adhesion of the biofilm under the SMFs. In a study dealing with the treatment of tetracycline by activated sludge, the presence of a SMF also enhanced the protein content of the EPS, which passed from 51 to 63 $mg_{Proteins}$ $g^{-1}_{biomass}$ when the SMF intensity increased from 0 to 25 mT [25].

In brief, the presence of the SMF generated an initially lower total EPS content, but with a particularly higher protein content, which can stimulate biofilm formation. Additionally, the total EPS amounts and composition seemed more stable in presence of the SMF, which could help improve the bioreactor robustness, particularly under intermittent loadings.

3.5 Conclusions

The presence of a 50 mT SMF had a significant impact on the biofiltration performance, with an increase in toluene EC of around 20%, under continuous or intermittent loads. Such boosted toluene removal could be mediated by the SMF stimulation of the microbial activity, corroborated by a higher CO_2 production, and a slight increase in biomass content. However, most SMF impact on biomass was noted during biofilter startup, with the induction of a prompter biofilm formation (30% more biomass in the first 15 days). Such initial stimulation of biofilter colonization was related to a modification of EPS composition, which contained a higher proportion of proteins, favoring the conglomeration of microorganisms and their colonization of the packing material. Moreover, the SMF allowed to maintain a significant advantage even when treating intermittent toluene loads, with a quicker removal efficiency recovery after shutdowns, a lower consumption of EPS as an

alternative carbon source, and the preservation of the percent of toluene mineralization. However, the SMF strength can be a particularly determinant factor influencing biofilter performance. Future studies should focus on testing several ranges of SMF intensities in order to optimize the benefic impact of magnetic fields during VOC biofiltration.

3.6 References

[1] D. Baskaran, D. Dhamodharan, U. S. Behera, and H. S. Byun, “A comprehensive review and perspective research in technology integration for the treatment of gaseous volatile organic compounds,” *Environ. Res.*, vol. 251, no. P1, p. 118472, 2024, doi: 10.1016/j.envres.2024.118472.

[2] Y. Quan, H. Wu, Z. Yin, Y. Fang, and C. Yin, “Effect of static magnetic field on trichloroethylene removal in a biotrickling filter,” *Bioresour. Technol.*, vol. 239, pp. 7–16, 2017, doi: 10.1016/j.biortech.2017.04.121.

[3] X. Wu, Y. Lin, Y. Wang, S. Wu, and C. Yang, “Volatile organic compound removal via biofiltration: Influences, challenges, and strategies,” *Chem. Eng. J.*, vol. 471, no. June, p. 144420, 2023, doi: 10.1016/j.cej.2023.144420.

[4] H. Wu, H. Yan, Y. Quan, H. Zhao, N. Jiang, and C. Yin, “Recent progress and perspectives in biotrickling filters for VOCs and odorous gases treatment,” *J. Environ. Manage.*, vol. 222, no. May, pp. 409–419, 2018, doi: 10.1016/j.jenvman.2018.06.001.

[5] P. A. Lamprea Pineda *et al.*, “Effect of inoculum type, packing material and operational conditions on the biofiltration of a mixture of hydrophobic volatile organic compounds in air,” *Sci. Total Environ.*, vol. 904, no. July, 2023, doi: 10.1016/j.scitotenv.2023.167326.

[6] L. Jiménez, S. Arriaga, R. Muñoz, and A. Aizpuru, “Effect of extended and daily short-term starvation/shut-down events on the performance of a biofilter treating toluene vapors,” *J. Environ. Manage.*, vol. 203, pp. 68–75, 2017, doi: 10.1016/j.jenvman.2017.07.057.

[7] M. Ferdowsi, A. Avalos Ramirez, J. P. Jones, and M. Heitz, “Elimination of mass transfer and kinetic limited organic pollutants in biofilters: A review,” *Int. Biodeterior. Biodegrad.*, vol. 119, pp. 336–348, 2017, doi: 10.1016/j.ibiod.2016.10.015.

[8] M. Marycz, Y. Rodríguez, J. Gębicki, and R. Muñoz, “Systematic comparison of a biotrickling filter and a conventional filter for the removal of a mixture of hydrophobic VOCs by Candida subhashii,” *Chemosphere*, vol. 306, no. June, 2022, doi: 10.1016/j.chemosphere.2022.135608.

[9] Y. Cheng *et al.*, “Challenges and solutions for biofiltration of hydrophobic volatile organic compounds,” *Biotechnol. Adv.*, vol. 34, no. 6, pp. 1091–1102, 2016, doi: 10.1016/j.biotechadv.2016.06.007.

[10] Y. Quan, H. Wu, C. Guo, Y. Han, and C. Yin, “Enhancement of TCE removal by a static magnetic field in a fungal biotrickling filter,” *Bioresour. Technol.*, vol. 259, no.

March, pp. 365–372, 2018, doi: 10.1016/j.biortech.2018.03.031.

[11] T. Li, H. Li, and C. Li, “A review and perspective of recent research in biological treatment applied in removal of chlorinated volatile organic compounds from waste air,” *Chemosphere*, vol. 250, p. 126338, 2020, doi: 10.1016/j.chemosphere.2020.126338.

[12] J. Liu, S. Lu, P. Li, and W. Liang, “Effect of starvation on the performance of a biotrickling filter packed with diatomaceous earth composite fillers for xylene removal,” *Process Saf. Environ. Prot.*, vol. 179, no. July, pp. 714–723, 2023, doi: 10.1016/j.psep.2023.09.051.

[13] F. Sempere, C. Gabaldón, V. Martínez-Soria, P. Marzal, J. M. Penya-roja, and F. Javier Álvarez-Hornos, “Performance evaluation of a biotrickling filter treating a mixture of oxygenated VOCs during intermittent loading,” *Chemosphere*, vol. 73, no. 9, pp. 1533–1539, 2008, doi: 10.1016/j.chemosphere.2008.08.037.

[14] M. Cortés-Castillo, A. Encinas, A. Aizpuru, and S. Arriaga, “Effect of applying a magnetic field on the biofiltration of hexane over long-term operation period,” *Environ. Sci. Pollut. Res.*, no. 0123456789, 2024, doi: 10.1007/s11356-024-34671-2.

[15] Y. Wang *et al.*, “Application of magnetic fields to wastewater treatment and its mechanisms: A review,” *Sci. Total Environ.*, vol. 773, 2021, doi: 10.1016/j.scitotenv.2021.145476.

[16] S. Arriaga, M. F. Carboni, and P. N. L. Lens, “Effect of static magnetic field exposure on biohydrogen production via dark fermentation of glucose,” *Process Saf. Environ. Prot.*, vol. 176, no. June, pp. 375–388, 2023, doi: 10.1016/j.psep.2023.06.022.

[17] Y. M. Zhu, H. Ji, H. Ren, J. Geng, and K. Xu, “Enhancement of static magnetic field on nitrogen removal at different ammonium concentrations in a sequencing batch reactor: Performance and biological mechanism,” *Chemosphere*, vol. 268, 2021, doi: 10.1016/j.chemosphere.2020.128794.

[18] M. Zieliński, M. Zielińska, A. Cydzik-Kwiatkowska, P. Rusanowska, and M. Dębowski, “Effect of static magnetic field on microbial community during anaerobic digestion,” *Bioresour. Technol.*, vol. 323, no. December 2020, pp. 600–605, 2021, doi: 10.1016/j.biortech.2020.124600.

[19] A. Tomska and L. Wolny, “Enhancement of biological wastewater treatment by magnetic field exposure,” *Desalination*, vol. 222, no. 1–3, pp. 368–373, 2008, doi: 10.1016/j.desal.2007.01.144.

[20] N. Benyoucef, A. Pauss, N. Abdi, C. O. Sarde, H. Grib, and N. Mameri, “Enhancement of the denitrification performance of an activated sludge using an electromagnetic field in batch mode,” *Chemosphere*, vol. 262, pp. 1–10, 2021, doi: 10.1016/j.chemosphere.2020.127698.

[21] J. Chen, Y. W. Cui, M. Q. Huang, H. J. Yan, and D. Li, “Static magnetic field increases aerobic nitrogen removal from hypersaline wastewater in activated sludge with coexistence of fungi and bacteria,” *Bioresour. Technol.*, vol. 382, no. May, p. 129194, 2023, doi: 10.1016/j.biortech.2023.129194.

[22] Y. Ji *et al.*, “Enhancement of biological treatment of wastewater by magnetic field,” *Bioresour. Technol.*, vol. 101, no. 22, pp. 8535–8540, 2010, doi:

10.1016/j.biortech.2010.05.094.

[23] M. Łebkowska, A. Rutkowska-Narozniak, E. Pajor, and Z. Pochanke, “Effect of a static magnetic field on formaldehyde biodegradation in wastewater by activated sludge,” *Bioresour. Technol.*, vol. 102, no. 19, pp. 8777–8782, 2011, doi: 10.1016/j.biortech.2011.07.040.

[24] L. Křiklavová, M. Truhlář, P. Škodová, T. Lederer, and V. Jirků, “Effects of a static magnetic field on phenol degradation effectiveness and Rhodococcus erythropolis growth and respiration in a fed-batch reactor,” *Bioresour. Technol.*, vol. 167, pp. 510–513, 2014, doi: 10.1016/j.biortech.2014.06.060.

[25] Y. M. Zhu *et al.*, “Simultaneous efficient removal of tetracycline and mitigation of antibiotic resistance genes enrichment by a modified activated sludge process with static magnetic field,” *Water Res.*, vol. 262, no. July, 2024, doi: 10.1016/j.watres.2024.122107.

[26] B. Hu *et al.*, “Impact of static magnetic field on electron transport and microbial community shifts in the nitritation sequencing batch reactor,” *J. Environ. Chem. Eng. Please*, vol. 10, no. 5, pp. 2213–2221, 2022, doi: 10.1016/j.jece.2022.108774.

[27] M. Lebkowska, A. Narozniak-Rutkowska, and E. Pajor, “Effect of a static magnetic field of 7mT on formaldehyde biodegradation in industrial wastewater from urea-formaldehyde resin producton by activated sludge,” *Bioresour. Technol.*, vol. 132, pp. 78–83, 2013, doi: 10.1016/j.biortech.2013.01.020.

[28] N. S. Zaidi, J. Sohaili, K. Muda, M. Sillanpää, and N. Hussein, “Effect of magnetic field on biomass properties and their role in biodegradation under condition of low dissolved oxygen,” *Appl. Water Sci.*, vol. 11, no. 7, pp. 1–12, 2021, doi: 10.1007/s13201-021-01439-9.

[29] D. zhi Chen *et al.*, “Enhanced chlorobenzene removal by internal magnetic field through initial cell adhesion and biofilm formation,” *Appl. Microbiol. Biotechnol.*, vol. 108, no. 1, 2024, doi: 10.1007/s00253-024-13001-z.

[30] N. S. Zaidi, K. Muda, and M. Sillanpää, “Effects of extra-cellular polymeric substances towards physical properties of biomass under magnetic field exposure,” *Int. J. Environ. Sci. Technol.*, vol. 16, no. 7, pp. 3801–3808, 2019, doi: 10.1007/s13762-018-1897-2.

[31] A. D. Dorado, J. A. Baeza, J. Lafuente, D. Gabriel, and X. Gamisans, “Biomass accumulation in a biofilter treating toluene at high loads - Part 1: Experimental performance from inoculation to clogging,” *Chem. Eng. J.*, vol. 209, pp. 661–669, 2012, doi: 10.1016/j.cej.2012.08.018.

[32] S. Arriaga and S. Revah, “Improving hexane removal by enhancing fungal development in a microbial consortium biofilter,” *Biotechnol. Bioeng.*, vol. 90, no. 1, pp. 107–115, 2005, doi: 10.1002/bit.20424.

[33] APHA, “Standard Methods for the Examination of Water and Wastewater, 21st ed.; APHA:Washington, DC, USA, 2005.,” *Am. Water Work. Assoc. Public Work. Assoc. Environ. Fed.*, 2005, doi: 10.2105/AJPH.51.6.940-a.

[34] H. Liu and H. H. P. Fang, “Extraction of extracellular polymeric substances (EPS) of sludges,” *J. Biotechnol.*, vol. 95, no. 3, pp. 249–256, 2002, doi: 10.1016/S0168-

1656(02)00025-1.

[35] Lowry, “Lowry Protein Assay,” *J. Biol. Chem.*, 1951.

[36] M. Dubois, K. A. Gilles, J. K. Hamilton, P. A. Rebers, and F. Smith, “Colorimetric Method for Determination of Sugars and Related Substances,” *Anal. Chem.*, vol. 28, no. 3, pp. 350–356, 1956, doi: 10.1021/ac60111a017.

[37] S. Esquivel-Gonzalez, A. Aizpuru, A. Patrón-Soberano, and S. Arriaga, “Characterization of bioaerosol emissions from two biofilters during treatment of toluene vapours using epifluorescence microscopy,” *Int. Biodeterior. Biodegrad.*, vol. 123, 2017, doi: 10.1016/j.ibiod.2017.06.007.

[38] L. Jiménez, S. Arriaga, and A. Aizpuru, “Assessing biofiltration repeatability: Statistical comparison of two identical toluene removal systems,” *Environ. Technol. (United Kingdom)*, vol. 37, no. 6, pp. 681–693, 2016, doi: 10.1080/09593330.2015.1077894.

[39] I. Covarrubias-García, A. Aizpuru, and S. Arriaga, “Effect of the continuous addition of ozone on biomass clogging control in a biofilter treating ethyl acetate vapors,” *Sci. Total Environ.*, vol. 584–585, pp. 469–475, 2017, doi: 10.1016/j.scitotenv.2017.01.031.

[40] M. Zieliński, A. Cydzik-Kwiatkowska, M. Zielińska, M. Dębowski, P. Rusanowska, and J. Kopańska, “Nitrification in Activated Sludge Exposed to Static Magnetic Field,” *Water. Air. Soil Pollut.*, vol. 228, no. 4, pp. 126–133, 2017, doi: 10.1007/s11270-017-3316-6.

[41] F. J. Álvarez-Hornos, C. Gabaldón, V. Martínez-Soria, P. Marzal, and J.-M. Penya-roja, “Biofiltration of toluene in the absence and the presence of ethyl acetate under continuous and intermittent loading,” *J. Chem. Technol. Biotechnol.*, vol. 83, no. 5, pp. 643–653, 2008.

[42] M. Konopacki and R. Rakoczy, “The analysis of rotating magnetic field as a trigger of Gram-positive and Gram-negative bacteria growth,” *Biochem. Eng. J.*, vol. 141, no. October 2018, pp. 259–267, 2019, doi: 10.1016/j.bej.2018.10.026.

[43] A. Rutkowska-Narożniak and E. Pajor, “Effect of a static magnetic field on Saccharomyces cerevisiae growth in wastewater containing phenol and p-chlorophenol,” *J. Water L. Dev.*, no. 55, pp. 178–184, 2022, doi: 10.24425/jwld.2022.142319.

[44] Q. Li *et al.*, “Static magnetic field enhances the purification of gaseous n-hexane in airlift two-phase partitioning bioreactor,” *Process Biochem.*, vol. 156, no. June, pp. 209–216, 2025, doi: 10.1016/j.procbio.2025.06.003.

[45] W. Ji, H. Huang, A. Deng, and C. Pan, “Effects of static magnetic fields on Escherichia coli,” *Micron*, vol. 40, no. 8, pp. 894–898, 2009, doi: 10.1016/j.micron.2009.05.010.

[46] A. Bordoloi and P. A. Gostomski, “Fate of degraded pollutants in waste gas biofiltration: An overview of carbon end-points,” *Biotechnol. Adv.*, vol. 37, no. 4, pp. 579–588, 2019, doi: 10.1016/j.biotechadv.2018.09.002.

[47] J. Filipič, B. Kraigher, B. Tepuš, V. Kokol, and I. Mandic-Mulec, “Effects of low-density static magnetic fields on the growth and activities of wastewater bacteria Escherichia coli and Pseudomonas putida,” *Bioresour. Technol.*, vol. 120, pp. 225–232, 2012, doi:

10.1016/j.biortech.2012.06.023.

[48] W. Fan *et al.*, “Enhancing anammox nitrogen removal by static magnetic field exposure: Performance, microbial community and symbiotic relationship analysis,” *J. Water Process Eng.*, vol. 53, no. August 2023, p. 103709, 2023.

[49] B. Hu *et al.*, “Effects of static magnetic field on the performances of anoxic/oxic sequencing batch reactor,” *Bioresour. Technol.*, vol. 309, no. April, 2020, doi: 10.1016/j.biortech.2020.123299.

[50] Z. L. Gao, Y. W. Cui, Y. Sui, and H. J. Yang, “Unveiling the mechanism of static magnetic field effects on carbon flux into polyhydroxyalkanoate synthesis by Haloferax mediterranei,” *Chem. Eng. J.*, vol. 476, no. October, p. 146647, 2023, doi: 10.1016/j.cej.2023.146647.

[51] K. M. Deamici *et al.*, “Static magnetic fields effects on polysaccharides production by different microalgae strains,” *Appl. Sci.*, vol. 11, no. 11, 2021, doi: 10.3390/app11115299.

[52] T. García-Pérez, A. Aizpuru, and S. Arriaga, “By-passing acidification limitations during the biofiltration of high formaldehyde loads via the application of ozone pulses,” *J. Hazard. Mater.*, vol. 262, pp. 732–740, 2013, doi: 10.1016/j.jhazmat.2013.09.053.

3.7 Supplementary materials

Table S3.1. Carbon recovery for the biofiltration of toluene with/without magnetic field during the first 24 days and at the end of the continuous load stage

Biofilter		Initial period (day 1-24)		Steady stage (day 24-45)	
		0 mT	50 mT	0 mT	50 mT
C-Toluene	**g inlet load**	34.0	34.2	31.0	30.9
C-Toluene	**g eliminated**	21.8	22.3	23.5	26.4
Elimination	**%**	64.1	65.2	75.8	85.4
Total recovery	**%**	69.7	75.5	70.0	64.0
C-CO_2	g produced	14.1	14.6	14.4	15.1
	% mineralization	64.6	65.5	61.3	57.2
C-biomass	g, perlite biomass	0.9	2.1	1.7	1.5
	% perlite biomass	4.1	9.3	7.4	5.7
C-total organic carbon	g TOC	0.22	0.16	0.30	0.28
	% TOC	1.0	0.7	1.3	1.1

CHAPTER IV. Stimulation of microalgae growth and high-value compounds production by magnetic field exposure

Highlights

- High magnetic field intensity (120 mT) affected microalgae growth performance
- Exposure to 60 mT for 1- 2 h d^{-1} promoted photosynthetic pigments accumulation
- *Chlorella vulgaris* presented higher tolerance to magnetic field exposure
- *Arthrospira platensis* growth was enhanced at low magnetic field intensity and exposure time
- *Coelastrella* sp. presented lower tolerance to magnetic field exposure

The present chapter is a modified version of the published article: López-Bello E, Vargas-Estrada L, Aizpuru, A, Arriaga S, Muóz R, 2025. "***Stimulation of microalgae growth and high-value compounds production by magnetic field exposure"***. Journal of Environmental Chemical Engineering.

4.1 Abstract

This study evaluated the effect of magnetic field (MF) intensities of 30, 60, and 120 militeslas (mT) applied for daily exposure times of 1, 2, or 4 h on the growth, CO_2 uptake, and pigment production of *Chlorella vulgaris*, *Coelastrella* sp., and *Arthrospira platensis*. The results support the emerging consensus that MF intensities between 30–60 mT generally enhance biological activity, while 120 mT may induce stress and inhibit growth. Specifically, 60 mT significantly enhanced CO_2 uptake and O_2 production in *C. vulgaris* and *Coelastrella* sp., suggesting an intensification of photosynthetic activity. In contrast, 120 mT inhibited growth and CO_2 uptake, particularly in *A. platensis* and *Coelastrella* sp. However, for *C. vulgaris*, exposure to 120 mT for 1 hour per day produced contrasting effects, with a reduction in biomass productivity and growth, but a 26% increase in chlorophyll content. At lower intensities, pigment production was also selectively enhanced, with carotenoids in *Coelastrella* sp. increasing by 51% at 30 mT for 2 hours per day, and phycocyanin in *A. platensis* rising by 53% at 30 mT for 4 hours per day. These findings indicated the presence of a magnetic “window” where specific field conditions optimized physiological responses in microalgae, supporting the potential use of MF in CO_2 capture technologies coupled with the production of high-value biomolecules.

4.2 Introduction

The uncontrolled release of anthropogenic CO_2 emissions into the atmosphere accounted for 36,300 million tons in 2021, which exceeded the Earth's capacity to capture and fix CO_2. This fact has triggered the need to find sustainable technologies to capture CO_2 and counteract its pernicious environmental and economic effects [1], [2]. Recently, the cultivation of photosynthetic microorganisms has demonstrated to be an effective approach to simultaneously recover CO_2 and nutrients from wastewaters or off-gases. More specifically, microalgae stand as a promising biorefinery platform since they can fix CO_2 at a 50-times-higher rate than terrestrial plants and can use inorganic sources of nitrogen and phosphorus for biomass growth [3]. Additionally, the produced algal biomass can serve as a precursor for the synthesis of biofuels or high-value added chemicals including pigments [1], [4].

Among the wide range of microalgae species, *Chlorella vulgaris*, *Coelastrella* sp. and *Arthrospira platensis* have demonstrated robustness when cultivated under extreme environments, achieving high biomass growth rates, and specific biomolecules accumulation under certain stress culture conditions. For instance, the rapid growth rate of *C. vulgaris* along with its high CO_2 tolerance has positioned this species as a workhorse for wastewater treatment and biofuel production [5], [6]. Moreover, *Coelastrella* sp. has been used in the energy sector due to its rapid growth rate (with an increase of 90-343 mg of volatile suspended solids (VSS) L^{-1} d^{-1}), high lipid accumulation (13-36% DW) and ability to accumulate carotenoids under stress conditions [7]. On the other hand, *A. platensis,* commonly known as *Spirulina,* is a filamentous cyanobacterium widely studied for CO_2 mitigation, with a growth rate of ≈ 800 mg VSS L^{-1} d^{-1} additionally, a high nutritive value and the capacity to produce bioactive substances such as phycocyanin [8], [9]. Despite the environmental and techno-economic advantages of microalgae, their large-scale cultivation still presents some drawbacks that must be overcome to make the process profitable. The main challenge of mass cultivation of microalgae is their low photosynthetic efficiency, which typically ranges between 1 and 2%.

In this context, different strategies have been implemented to improve microalgae biological performance including new photobioreactor designs [10], genetic engineering [11], and stimulation of microalgae metabolism by the addition of nanomaterials or by physical mechanisms such as exposure to ultrasound or magnetic fields (MF) [12]. Recently, the exposure to MF has emerged as a cost-effective technique to stimulate microalgae metabolism based on its negligible energy consumption and the absence of hazardous by-products. MFs can catalyze biological and physicochemical mechanisms as function of the bioprocess, MF intensity and the exposure time [13]–[16]. For instance, *Scenedesmus obliquus* was exposed to a MF of 100 milliteslas (mT) for 30 min d^{-1} for 6 days with an increase in biomass and oxygen production of 11.4 and 24.6%, respectively [15]. Similarly, [14] evaluated the effect of different MF intensities (0, 20, 40, 80 and 150 mT) on the performance of a *C. vulgaris* and *Bacillus* consortium. The exposure to 80 mT increased cellular density by 29% after 16 days of exposure. Moreover, exposures to 150 mT promoted an oxidative stress response of *C. vulgaris,* which negatively affected EPS secretion and decreased the number of aggregates by 29% [14]. On the other hand, [17] evaluated the effect of intermittent (1 h d^{-1}) MF exposure on *Chlorella fusca* to 30 and 60 mT, and observed that *C. fusca* growth was increased by 34%, regardless of the MF intensity. Additionally, CO_2 fixation was increased by 50% when *C. fusca* was exposed to 60 mT, whilst the protein content in EPS increased by 56% when exposed to 30 mT. Similarly, [18] observed that the lipid content of *Spirulina* sp. LEB 18 increased by 14 and 45% when exposed to 30 mT for 12 and 24 h d^{-1}, respectively. In brief, MF has the potential to boost microalgae growth and metabolism by modulating the synthesis of carbohydrates, proteins, and lipids. However, more research is needed to explore the potential of MF to mitigate CO_2 emissions while enhancing the production of high-value-added products.

In this context, the aim of this study was to investigate the effect of different MF intensities (30, 60, and 120 mT) and exposure times (1, 2, and 4 hours per day) on the growth and pigment production of *Chlorella vulgaris*, *Coelastrella* sp., and *Arthrospira platensis*. CO_2 fixation, biomass growth and the synthesis of

biomolecules (i.e. proteins, carbohydrates, lipids, and pigments) were systematically determined to assess the effect of the MF on microalgal metabolism.

4.3 Material and methods

4.3.1 Microalgae strains and culture conditions

C. vulgaris (SAG 211-11b) and *Arthrospira platensis* (SAG 21.99) were originally purchased from the Culture Collection of Algae of the University of Göttingen (SAG, Germany), while *Coelastrella* sp. was obtained from the culture collection MAC-CWU (WDCM 886) of V.N. Karazin Kharkiv National University (Ukraine). Prior to the batch assays, an inoculum of each strain was grown as follows: *C. vulgaris* in BG11 medium, *Coelastrella* in BBM medium, and *A. platensis* in a modified Zarrouk medium with a concentration of 7 g L^{-1} of $NaHCO_3$. The inocula were cultivated in 250 mL serum bottles with an effective mineral salt medium volume of 60 mL and containing 30% (v v^{-1}) CO_2 in the air headspace. The cultures were incubated at 25 ºC under continuous illumination (≈350 µmol m^{-2} s^{-1}) and agitation at 150 rpm.

4.3.2 Magnetic field exposure

MF intensities of 30, 60, and 120 mT, and exposure times of 1, 2, and 4 hours per day (hereafter referred to as 1, 2, and 4 h d^{-1}) were tested in the three model microalgae. MF were generated by neodymium magnet blocks (60 × 20 × 5 mm) (Superimanes, Spain), and the different intensities were achieved by modifying the number of magnets placed on each side of the glass bottles. The MF intensity was determined by measuring the MF with a Teslameter (KKnoon, Spain) at different points, varying the heights of the measurement sites inside the bottles, obtaining an average MF of 30, 60, and 120 mT for each arrangement of magnets. The results of the average MF intensity at the different measured heights are shown in the supplementary material (Table S4.1).

4.3.3 Experimental set-up

Batch experiments were carried out in triplicate in 250 mL serum bottles with an

effective liquid volume of 60 mL. The bottles were filled with the respective mineral medium for each microalgae (BG11 for *C. vulgaris*, BBM for *Coelastrella* sp. and modified Zarrouk for *A. platensis*) and sealed with butyl septa and aluminum caps. Then, the headspace of the bottles was replaced by flushing N_2 (Carburos Metalicos, Spain) for 5 min, and subsequently pure CO_2 was injected until a concentration of 30% (v v^{-1}) was reached in the headspace. Then, the bottles were inoculated with the corresponding microalgae at an initial optical density (OD_{750}) of 0.3, and incubated at 25 ºC and 150 rpm under continuous illumination of ≈375 µmol m^{-2} s^{-1} provided by visible LED lights (PHILLIPS, Spain). Gas samples of the headspace (100 µl) were collected twice daily to measure CO_2 and O_2 concentrations, while liquid samples (1 mL) were taken simultaneously to assess OD_{750}, pH, and photosynthetic activity.

The effect of the MF on microalgae growth and metabolism was evaluated by cultivating the strains under subsequently growing cycles of the cultures until a significant change in the patterns of growth, CO_2 uptake, and O_2 release was detected. Specifically, when the CO_2 present in the headspace was completely depleted and the OD_{750} reached a steady state, an aliquot of the culture was collected and used as inoculum for a new batch (fresh medium, 30% of CO_2 in the headspace, initial OD_{750} of 0.3). This procedure, referred to as “dragging process”, was repeated for a total cultivation period of 8-9 days (Fig. 4.1). The control systems were handled identically to the MF-exposed treatments, except that no MF was applied. Once the last culture cycle was completed, the microalgal biomass was harvested for macromolecular (lipids, protein, and carbohydrates) and pigment analysis.

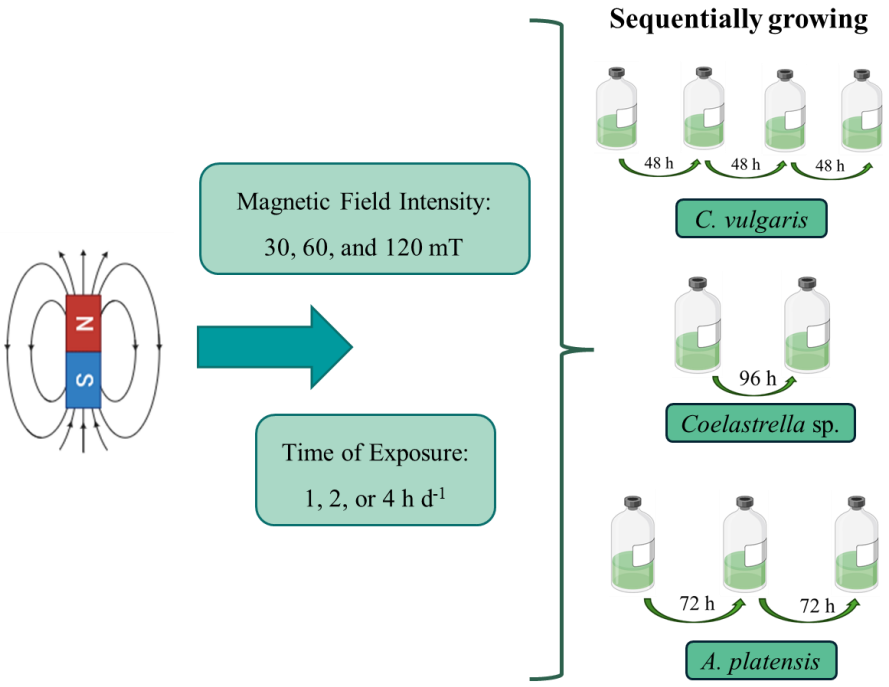

Fig. 4.1 Magnetic field intensity and time of exposure tested in *Chlorella vulgaris*, *Coelastrella* sp., and *Arthrospira platensis* cultures

4.3.4 Analytical procedures

4.3.4.1 Microalgae growth and CO_2 fixation

Microalgae growth was determined by daily measuring the OD_{750}. Biomass concentration was then estimated based on an external calibration curve relating OD_{750} to VSS (expressed as g VSS L^{-1}), which represents the organic fraction of the culture and therefore provides a quantitative measure of microalgal biomass. CO_2 and O_2 concentrations were measured twice a day by gas chromatography with thermal conductivity detection (CP-3800 GC-TCD Varian, Palo Alto, USA) according to [19]. The pH and photosynthetic activity (Quantum yield, QY) were determined twice a day with a pH meter SensION^{TM} + PH3 pHmeter (HACH, Spain) and a fluorometer AquaPen AP 110C (Photon Systems Instruments, Drasov, Czech Republic), respectively.

Microalgae biomass productivity was calculated during the exponential phase according to Eq. (1):

$$\boldsymbol{Px} = \frac{DW1-DW0}{t1-t0} \qquad \text{Eq (1)}$$

where Px is the biomass productivity (g L^{-1} d^{-1}), *DW1* and *DW0* are the biomass dry weight (g VSS L^{-1}) at time t_1 and t_0 (d) during the exponential growth phase.

The specific growth rate was calculated during the exponential phase according to Eq. (2):

$$\mu = \frac{\ln(DW1) - \ln(DW0)}{t1 - t0} \qquad \text{Eq (2)}$$

where μ represents the specific growth rate (d^{-1}).

4.3.4.2 Biomass composition and pigment quantification

To determine the protein, carbohydrate and lipid content, the microalgae biomass was centrifuged at 3500 rpm for 15 min, frozen at − 30 °C and finally freeze-dried (− 55 °C, 0.101 mbar). Protein content was determined following the procedure of BCA protein assay kit; carbohydrate content was determined by a modified phenol-sulfuric acid method [20]; and the total lipid content was determined by the phosphovanillin method [21].

Total chlorophyll and carotenoids were extracted with acetone (100%, v v^{-1}). Briefly, 1 mL of the final biomass of *C. vulgaris* and *Coelastrella* sp. was centrifuged at 10,000 rpm for 10 min, the supernatant was removed and the biomass was resuspended in 1 mL of pure acetone. Then, the samples were incubated at 4 ºC for 24 h and then centrifuged at 10,000 rpm for 10 min. The pigments were quantified by spectrophotometry (spectrophotometer UV - Vis 2550, Shimadzu, Japan) at absorbances of 644 nm (A_{644}) and 661 nm (A_{661}) for Chl, and 470 nm (A_{470}) for carotenoids. The total chlorophyll and total carotenoids concentrations were calculated using equations 3-6 [22]:

Total chlorophyll (mg L^{-1}) = $7.05A_{661} + 18.06A_{644}$ Eq (3)

Total carotenoids (mg L^{-1}) $= \frac{100*A_{470} - 1.90\,Chl_a - 63.14Chl_b}{214}$ Eq (4)

Chl_a (mg L^{-1}) = $11.24A_{661} - 2.04A_{644}$ Eq (5)

Chl_b (mg L^{-1}) = $20.13A_{644} - 4.19A_{661}$ Eq (6)

Final concentration of total chlorophyll and total carotenoids are expressed in the results section in mg $g^{-1}_{biomass}$ by dividing the calculated pigment concentrations by the final biomass content (g VSS L^{-1}).

Phycocyanin (C-PC) was extracted from *A. platensis* as follows: 1 mL sample was centrifuged at 10,000 rpm for 10 min, the supernatant was removed and the biomass was resuspended in 1 mL of phosphate buffer 20 mM, pH 8. Then, the samples were subjected to freeze-thawing periods of 24 h three times. The quantification of C-PC was conducted by spectrometry (spectrophotometer UV - Vis 2550, Shimadzu, Japan) by reading the absorbance at a wavelength of 620 nm (A620). Total C-PC was calculated as follows (Eq. 7) [23]:

$$\mathbf{C-PC\ (mg\ g^{-1})} = \frac{A620 * Ve}{3.39 * DWs} \qquad \text{Eq (7)}$$

where Ve is the total volume of the sample (1 mL) and DWs is the biomass dry weight (g VSS).

4.3.5 Statistical analysis

The results are presented as mean values ± standard deviation. To assess the impact of the MF on microalgae, a t-student test was conducted to the final kinetic for each strain (after 8 or 9 days of cultivation) by comparing the systems exposed to the MFs with their respective controls, considering *p-value* $\leq$ 0.05.

4.4 Results and discussion

4.4.1 Influence of MF intensity and exposure time on microalgae growth

The results presented below correspond to the final cultivation of each strain. The results showed the responses to MF exposure in terms of CO_2 consumption, O_2 production, and biomass. Data from previous cultivation cycles are included in the Supplementary Material (Figs. S4.1, S4.2, and S4.3), which show trends in CO_2 uptake and O_2 production across successive generations of each strain.

The response of *C. vulgaris* cultures to MF stimuli was mainly driven by the exposure time followed by the MF intensity. The exposure of *C. vulgaris* to 30 mT for 2 h d^{-1} induced a 7% increase in μ compared to the control (Table 4.1). Concomitantly, oxygen production showed an upward trend at 2 and 4 h d^{-1} of exposure time (Fig. 2d), which was correlated to an increased in biomass concentration by 7 and 5% after 30 h of cultivation (Fig. 4.2g). Similarly, Px significantly increased with the exposure time up to 2 h d^{-1} (Table 4.1). Similarly, pH and QY also increased with longer exposure time (Table S2). The observed trend of increasing QY may reflect subtle improvements in photosystem II (PSII) efficiency and photochemical performance [24]. Together with the observed rise in oxygen concentration and Px, these results point to a coordinated stimulation of carbon assimilation and photobiological processes under MF. Previous studies have suggested that such responses may be linked to improved electron transport such as an enhanced cyclic electron flow or stabilization of PSII/PSI reaction centers [18], [24], [25] .

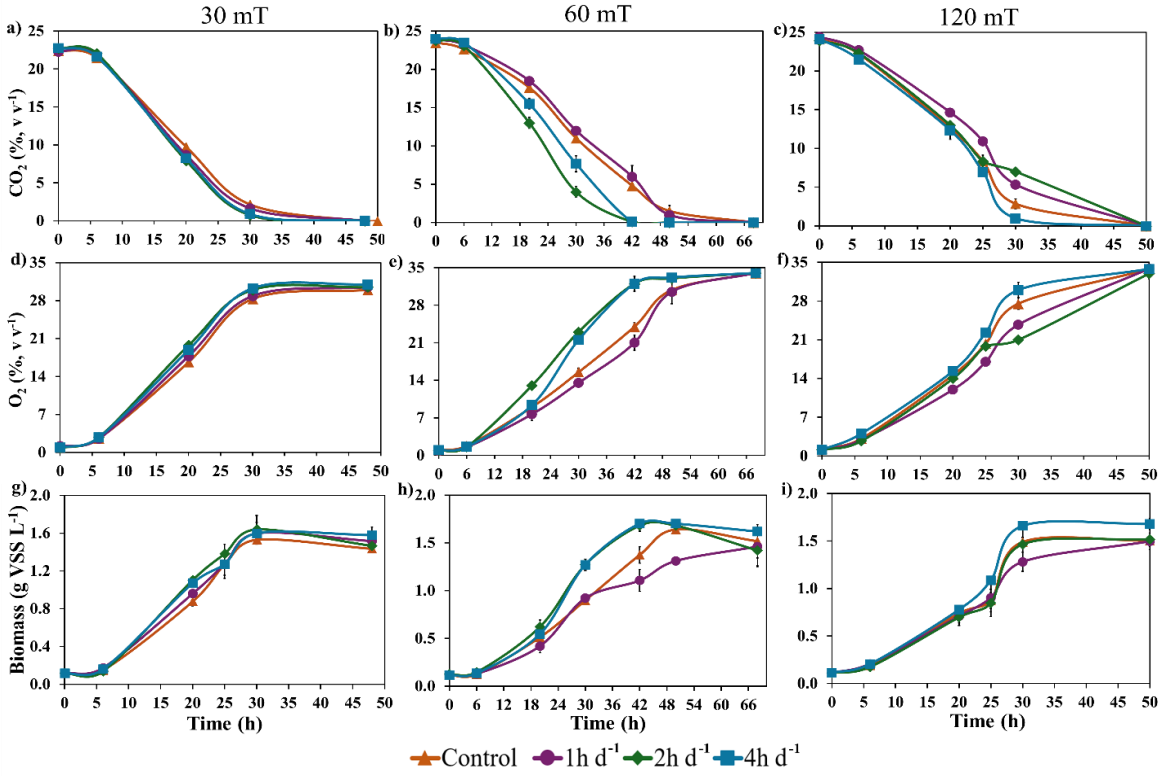

Fig. 4.2 Time course of the influence of the exposure time of *C. vulgaris* to 30, 60 and 120 mT on CO_2 consumption (a, b, c), O_2 production (d, e, f), and biomass concentration (g, h, i).

Similarly, when the MF was increased to 60 mT, CO_2 consumption in *C. vulgaris* cultures was enhanced at 2 and 4 h d^{-1} of exposure (Fig. 4.2b), resulting in a final biomass concentration of 1.68 and 1.70 g VSS L^{-1}, respectively (Fig. 4.2h). The parameters μ and Px significantly increased by 20 and 24% at 4 h d^{-1}, which represented the largest increment recorded at a MF intensity of 60 mT. Consistently, QY values rose by approximately 10–12% under exposures of 2 and 4 h d^{-1}, suggesting an upregulation in PSII efficiency (Table S4.2). Interestingly, a shorter daily exposure of 1 h d^{-1} resulted in a marked decrease in μ and Px by 31 and 21%, respectively, indicating that *C. vulgaris* requires a minimum threshold of exposure to activate beneficial responses. This contradictory effect under 60 mT could be related to acute stress that disturbs redox balance and ion homeostasis, leading to elevated reactive oxygen species (ROS) generation and impaired photosystem performance [26], [27]. However, when exposure is extended 2-4 h d^{-1}, cells may initiate compensatory mechanisms such as enhanced antioxidant activity, remodeling of thylakoid membranes, and acceleration of the repair of the D1 protein in PSII, which collectively stabilize photosynthetic function and promote carbon fixation. Thus, the contrasting outcomes observed at 1 h d^{-1} versus 2 and 4 h d^{-1} of exposure may reflect a time-dependent balance between stress induction and adaptive acclimation. These findings are consistent with previous reports showing enhanced growth of *Chlorella* species under intermediate intensities of MF exposure (20-200 mT), provided that exposure-specific times are needed to trigger adaptive acclimation [14], [28], [29].

Table 4.1. Effects of magnetic field (MF) intensity (30, 60, 120 mT) and exposure time (1, 2, 4 h d^{-1}) on biomass productivity (Px) and specific growth rate (μ) after 8 days of cultivation for *C. vulgaris* and *Coelastrella* sp., and after 9 days of cultivation for *A. platensis*.

C. vulgaris						
	Px (g L^{-1} d^{-1})			**μ (d^{-1})**		
	30 mT	**60 mT**	**120 mT**	**30 mT**	**60 mT**	**120 mT**
Control	1.37±0.001	0.93±0.057	1.29±0.048	2.32±0.031	1.41±0.001	2.07±0.015
1h d^{-1}	1.42±0.012*	0.75±0.077*	1.04±0.091*	2.22±0.073	0.97±0.001*	1.79±0.081*
2h d^{-1}	1.58±0.057*	1.12±0.039*	1.28±0.081	2.48±0.058*	1.63±0.028*	2.09±0.069
4h d^{-1}	1.52±0.003*	1.15±0.021*	1.45±0.023*	2.32±0.082	1.69±0.029*	2.07±0.007
***Coelastrella* sp.**						
	Px (g L^{-1} d^{-1})			**μ (d^{-1})**		
	30 mT	**60 mT**	**120 mT**	**30 mT**	**60 mT**	**120 mT**
Control	0.55±0.043	1.19±0.055	0.63±0.014	0.84±0.021	1.26±0.046	0.93±0.020
1h d^{-1}	0.57±0.009	0.78±0.009*	0.72±0.040*	0.88±0.003	0.75±0.012*	0.90±0.031
2h d^{-1}	0.92±0.010*	0.73±0.001*	0.74±0.061*	1.20±0.006*	0.71±0.049*	0.98±0.049
4h d^{-1}	0.58±0.054	0.71±0.018*	0.63±0.008	0.72±0.022*	0.79±0.016*	0.84±0.029*
A. platensis						
	Px (g L^{-1} d^{-1})			**μ (d^{-1})**		
	30 mT	**60 mT**	**120 mT**	**30 mT**	**60 mT**	**120 mT**
Control	0.78±0.050	0.63±0.039	0.68±0.065	0.97±0.035	0.94±0.002	0.92±0.067
1h d^{-1}	0.64±0.025*	0.81±0.065*	0.61±0.051	0.93±0.009	1.07±0.049*	0.95±0.044
2h d^{-1}	0.56±0.003*	0.86±0.039*	0.45±0.045*	0.82±0.010*	1.05±0.035*	0.77±0.042*
4h d^{-1}	0.52±0.030*	0.83±0.068*	0.39±0.064*	0.88±0.005	1.02±0.053	0.58±0.035*

* Significant differences compared to the control ($p \leq 0.05$)

Finally, when the MF was increased to 120 mT, Px in *C. vulgaris* cultures exposed for 4 h d^{-1} increased by 13%, whilst shorter exposure times (1 and 2 h d^{-1}) resulted

in a delayed CO_2 uptake and lower growth (Fig. 4.2c). Interestingly, exposures of 1 h d^{-1} significantly reduced Px and μ by 20 and 15%, respectively. This may reflect a threshold adaptation response, where 120 mT MF intensity requires longer exposure time to trigger *C. vulgaris* metabolic adjustments or cellular compensation mechanisms. While *C. vulgaris* benefited from exposures at 30 and 60 mT for both 2 and 4 h d^{-1}, only the longest time of exposure (4 h d^{-1}) at 120 mT mediated positive effects, suggesting that both intensity and duration of MF exposure influence *C. vulgaris* metabolism, but not in a linear or dose-dependent manner. This behavior is consistent with the known resilience of *C. vulgaris* to abiotic stressors, including oxidative, thermal, and salinity fluctuations, suggesting that high-intensity MF may initially act as a stressor, requiring sufficient exposure time to activate protective or acclimatory responses [30].

On the other hand, even if *Coelastrella* sp. is recognized as a robust high-value producer under extreme environmental conditions, its growth was significantly affected by the MF intensity. Similar to *C. vulgaris* cultures, a low exposure time (1 h d^{-1}) induced growth inhibition on *Coelastrella* sp. Nonetheless, exposure to 30 mT for 2 h d^{-1} resulted in the highest Px and μ, which increased significantly by 67% and 42%, respectively. QY presented the same tendency, suggesting that the exposure to 30 mT for 2 h d^{-1} enhanced the energy conversion efficiency and improved the PSII performance (Table S4.3). This improvement may be attributed to an accelerated electron transport or an increased CO_2 permeability across the cell membrane [24], [31]. Additionally, MFs influence the solubility and diffusion of CO_2, which is a diamagnetic molecule, by altering its spatial orientation and mobility in the medium. These effects potentially increase the bioavailability of inorganic carbon, thereby supporting photosynthetic activity under magnetic stimulation [32]. However, increasing the exposure time to 4 h d^{-1} caused a 15% decline in Px likely due to an induced oxidative stress mediated by an excessive ROS production, which impaired metabolic enzymes, membrane integrity, or DNA stability [28], [33]–[37].

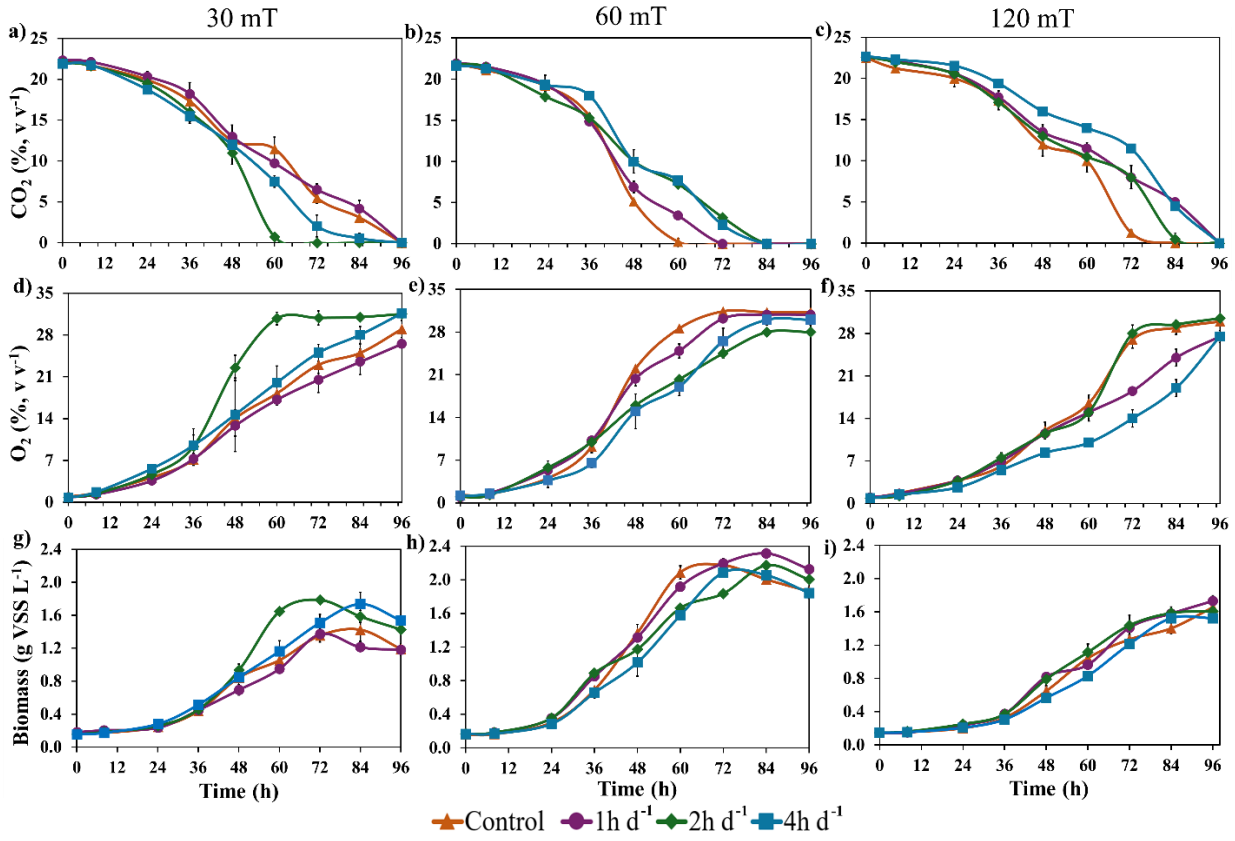

Fig. 4.3 Time course of the influence of the exposure time of *Coelastrella* sp. to 30, 60 and 120 mT on CO_2 consumption (a, b, c), O_2 production (d, e, f), and biomass concentration (g, h, i).

The exposure of *Coelastrella* sp. cultures to 60 mT resulted in a significant decrease in the Px by 34, 38, and 40% at 1, 2, and 4 h d^{-1}, respectively (Table 4.1). Additionally, QY values dropped alongside pH, with a marked lower final pH with increasing exposure time, indicating both a reduced photosynthetic activity and a potential disruption of bicarbonate uptake mechanisms (Table S4.3). This was supported by the retarded CO_2 uptake in the cultures exposed to the MF, particularly for 2 and 4 h d^{-1} (Fig. 4.3b). These results suggest that 60 mT exceeds the physiological tolerance of *Coelastrella* sp., leading to metabolic stress likely mediated by oxidative damage, impaired electron transport, or ionic imbalances [35]. Interestingly, the biomass concentration in the cultures exposed for 2 h d^{-1}, after 84 h of experimentation, was 10% higher compared to the control (2.23 vs 2.01 g VSS L^{-1}). This uncoupling of

carbon assimilation from biomass production suggests that *Coelastrella* sp. may be redistributing internal carbon pools to the production of biomolecules as a protective response to the MF exposure [38]. Finally, increasing the MF to 120 mT resulted in a retarded CO_2 uptake regardless of the exposure time (Fig. 4.3c). Particularly, at 1 and 4 h d^{-1} of exposure, the oxygen concentration in the headspace significantly decreased, nonetheless the Px increased by 12% at 2 h d^{-1}, which suggested changes in the intramolecular composition of *Coelastrella* sp.

A. platensis cultures exhibited a different response to MF exposure compared to *C. vulgaris* and *Coelastrella sp*., since this cyanobacterium was significantly sensitive to the exposure time at MF intensities of 30 and 60 mT. In this sense, the exposure to 30 mT for 1 and 2 h d^{-1} promoted biomass accumulation, reaching 1.55 and 1.42 g VSS L^{-1}, respectively, which was supported by an increased oxygen production (Fig. 4.4d). These findings suggest a transient enhancement of photosynthetic activity under short-term MF exposure. QY remained statistically similar to the control at 1 h d^{-1} of exposure, but a decrease in QY was observed at 2 h d^{-1} (Table S4.4), suggesting the onset of inhibition mediated by ROS accumulation, which could impair PSII reaction center efficiency [24]. In this way, the increased biomass concentration, particularly at 2 h d^{-1} of exposure, suggests an accumulation of specific macromolecules as a protective oxidative response rather than to cell production. Moreover, increasing the exposure time to 4 h d^{-1} resulted in a decline in biomass concentration and oxygen production, along with a sustained 13% reduction in QY. Hence, the inhibitory effects of the MF on *A. platensis* were extended to carbon assimilation and to the overall metabolic function.

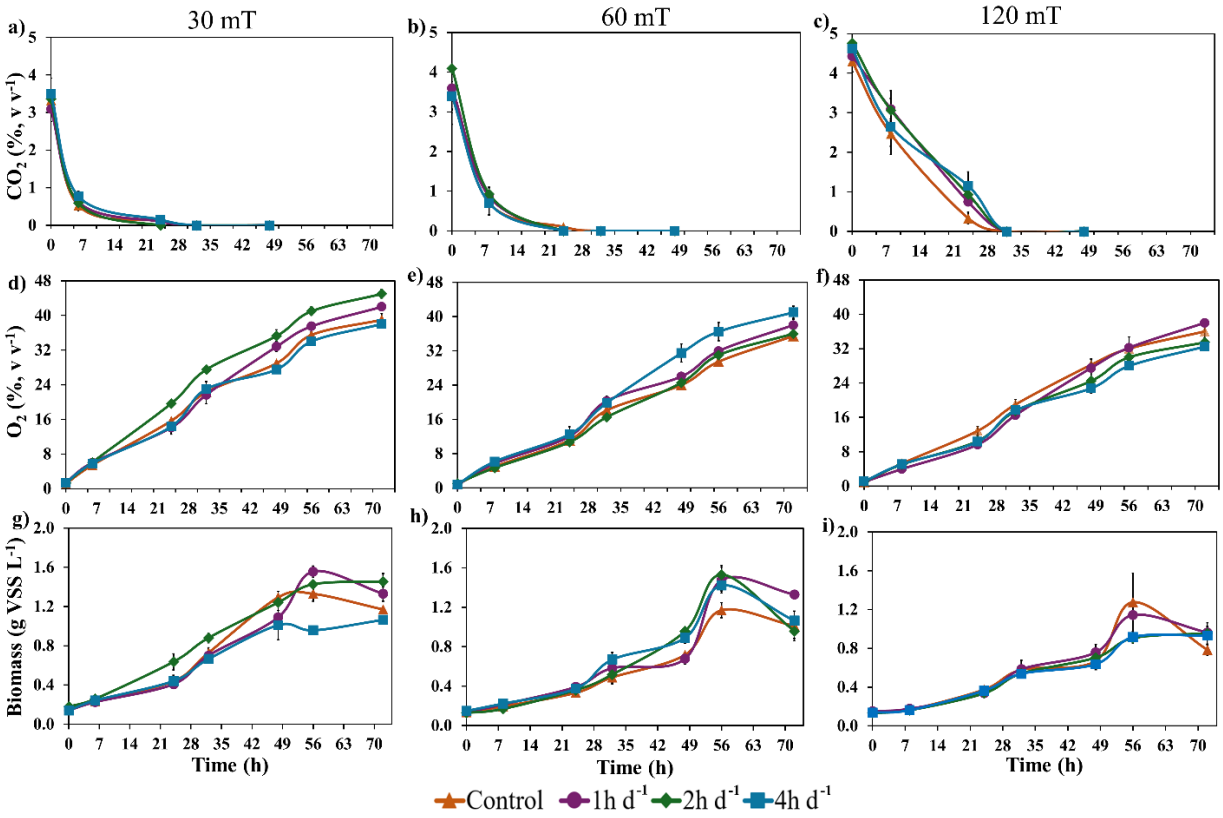

Fig. 4.4 Time course of the influence of the exposure time of *A. platensis* to 30, 60 and 120 mT on CO_2 consumption (a, b, c), O_2 production (d, e, f), and biomass concentration (g, h, i).

Interestingly, the exposure to 60 mT enhanced *A. platensis* growth, regardless of the time of exposure. The highest biomass concentration was reached after 54 h in the cultures exposed for 2 h d^{-1} (1.53 g VSS L^{-1}), followed by 1 h d^{-1} (1.47 g VSS L^{-1}) and 4 h d^{-1} (1.42 g VSS L^{-1}), and the control (1.17 g VSS L^{-1}). Similarly, Px increased by 29, 38 and 32% at 1, 2, and 4 h d^{-1} of exposure, respectively. This finding revealed *A. platensis* tolerance to MF, potentially due to its simpler thylakoid organization or robust stress adaptation mechanisms [39], [40]. Additionally, the QY values increased in the cultures exposed to MF (Tables S4.3), with a significant increment at 1 h d^{-1} compared to the control, which indicated an enhanced PSII efficiency [24], [41].

Contrary, *A. platensis* cultures exposed to 120 mT experienced an inhibitory effect regardless of the daily exposure time (Fig. 4.4c). The MF reduced *A. platensis* μ and

Px with increasing the time of exposure by 5, 30, and 42% for 1, 2 and 4 h d^{-1}, respectively. This was supported by the decrease in QY values (Table S4.4), suggesting a progressive impairment of PSII efficiency [24]. The different effects of MF intensity on cyanobacteria metabolism have been extensively reported. For instance, a high-intensity MF may exacerbate the formation of ROS, disrupt membrane integrity, or impair photosynthetic protein complexes, ultimately leading to growth inhibition [42], [43]. Previous studies have shown that *Spirulina platensis* experiences reduced μ (up to 11%) under MF intensities above 100 mT [44], while moderate intensities (5–30 mT) enhance both growth and pigment accumulation [45].

In this context, *A. platensis* exhibited a limited tolerance for low MF intensities and time of exposure, whilst an extended exposure time triggered inhibitory effects. These findings are in agreement with previous studies in cyanobacteria showing that prolonged MF exposure can boost ROS production, leading to oxidative damage in photosynthetic membranes [46]. This heightened sensitivity may stem from the unique physiology of cyanobacteria, particularly due to their vulnerability to redox imbalances. Their cultivation in high-pH media increases CO_2 solubility, which may also induce fluctuations in redox potential, which could compromise CO_2 uptake efficiency. These factors likely contribute to ionic or oxidative imbalances, limiting the potential benefits of MF exposure in *A. platensis* cultures [31], [47].

The differential responses observed among *C. vulgaris*, *Coelastrella* sp., and *A. platensis* under MF exposure can be attributed to their inherent physiological and structural differences, which determine how each strain perceives and adapts to electromagnetic stimuli. In *C. vulgaris*, the relatively flexible thylakoid organization and robust redox homeostasis allow cells to tolerate moderate intensities and to engage compensatory mechanisms such as enhanced antioxidant activity and PSII repair when stress thresholds are exceeded. By contrast, *Coelastrella* sp., despite being a robust extremophile, appears highly sensitive to MF intensities above 60 mT, suggesting that its thickened cell wall and distinct carbon assimilation pathways may impose diffusional or ionic constraints that exacerbate ROS accumulation under

stronger fields. In cyanobacteria such as *A. platensis*, the simpler thylakoid structure and alkaline growth medium confer short-term tolerance at moderate intensities but also increase vulnerability to oxidative imbalances during prolonged or high-intensity exposures. Together, these species-specific traits—ranging from differences in thylakoid architecture and membrane composition to antioxidant capacity and carbon assimilation strategies—likely underlie the divergent physiological outcomes reported here. This highlights the importance of strain-dependent variability in the response to MF, consistent with previous reports demonstrating that microalgal taxa do not exhibit uniform magnetic sensitivity but instead reflect their unique evolutionary adaptations to environmental stressors [16], [17], [33].

4.4.2 Influence of MF intensity and exposure time on biomolecules accumulation

In *C. vulgaris,* MF exposure elicited distinct metabolic reallocations that depended on both intensity and exposure time. At 30 mT exposure, the protein content showed a significant increase with increasing time of exposure (Fig. 4.5g), with enhancements of 86, 93, and 106% at 1, 2, and 4 h d^{-1} exposure, respectively. This suggests that the response of *C. vulgaris* to the MF is based on the modulation of the metabolic profile, particularly enhancing protein synthesis for biomass production, which was supported by the increased Px achieved under these conditions. On the other hand, *C. vulgaris* cultures exposed to 60 mT showed a metabolic response shifted toward lipid accumulation, which increased by 75, 125, and 130% at 1, 2, and 4 h d^{-1} of exposure, respectively, whilst carbohydrate concentration was significantly reduced. These results indicate a diversion of carbon flux from carbohydrates to lipid pathways under oxidative stress conditions that promotes lipid biosynthesis as an adaptive response. Interestingly, these metabolic shifts did not compromise biomass productivity, contrasting with traditional lipid induction strategies based on nitrogen deprivation, which often suppress microalgal growth [48]. Similar enhancements in lipid content under MF exposure have been reported in *Chlorella kessleri* with lipid increments ranging between 22 and 77% at MF intensities of 30 and 60 mT for 1 h d^{-1} of exposure, respectively [49]. Moreover,

the exposure of *Chlorella homosphaera* to 60 and 30 mT for 1 h d^{-1} increased the lipid content by 108 and 135%, respectively, reinforcing the potential of MF as a non-invasive lipid induction strategy [50]. Similarly, the exposure of *C. vulgaris* cultures to 120 mT increased the lipid content by 100 and 50% at 1 and 4 h d^{-1} of exposure, respectively. Notably, protein content substantially increased under all exposure times, which suggests a greater regulation of biosynthetic activity, possibly due to an enhanced enzyme expression or membrane repair and protein turnover under elevated oxidative pressure. Such responses align with reports of increased expression of stress-protective proteins under strong MF exposure [51]. Together, these findings suggest that *C. vulgaris* can reconfigures its metabolism according to MF intensity and time of exposure: the lower intensity (30 mT) stimulates protein accumulation, the intermediate intensity tested (60 mT) promotes lipid synthesis, and the higher intensity probed (120 mT) activates broader stress responses.

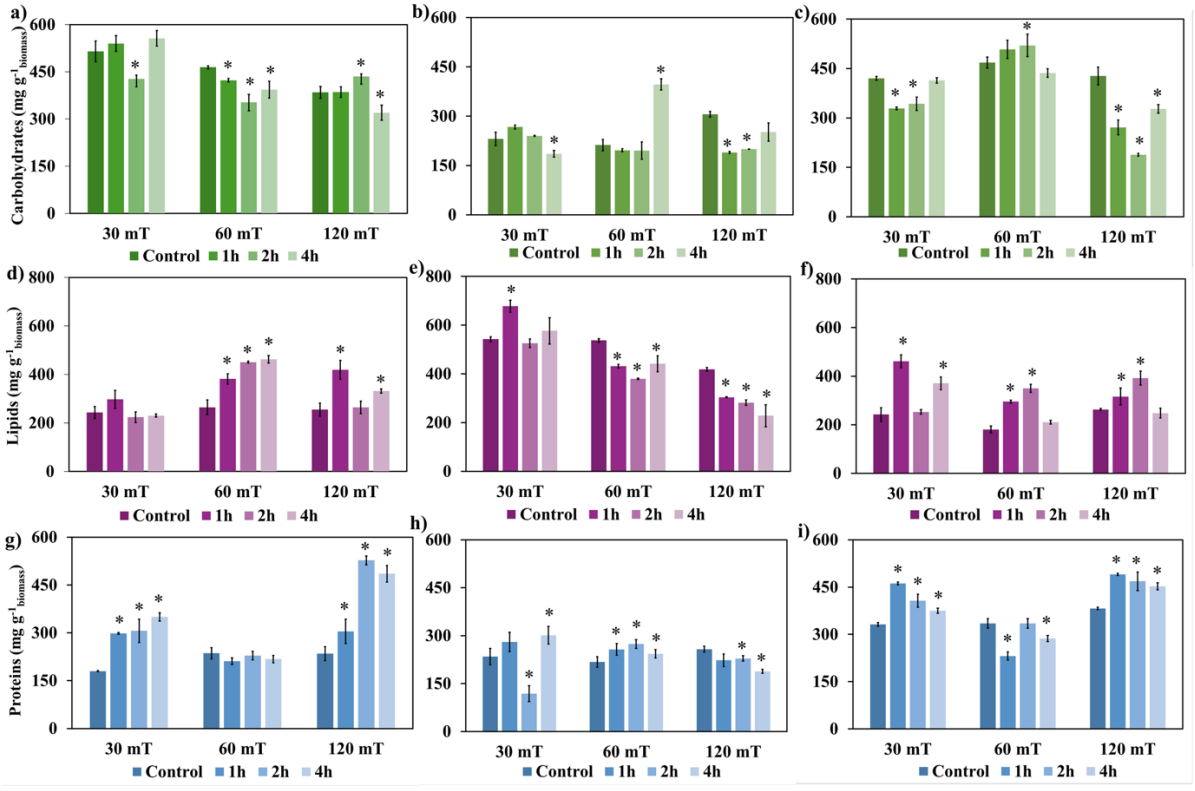

Fig. 4.5 Influence of MF intensity and exposure time on the final concentrations of carbohydrates (a, b, c), lipids (d, e, f) and proteins (g, h and i) of *C. vulgaris, Coelastrella* sp., *A. platensis*. *Significant difference compared to the control with $p \leq 0.05$.

The exposure of *Coelastrella* sp. exhibited more variable and stress-prone responses, reflecting a narrower tolerance window to MF stimulation. At 30 mT for 1 h d^{-1}, the lipid content significantly increased by 18%. However, this lipid increase compromised biomass growth, suggesting that the exposure to MF resulted in oxidative stress for *Coelastrella* sp. Interestingly, the protein content decreased by 50% after 2 h d^{-1} of exposure, while 4 h d^{-1} of exposure increased protein concentrations by 28%. Such contrasting responses suggest a temporal adaptation mechanism, potentially linked to the induction of antioxidative enzymes such as superoxide dismutase (SOD) and peroxidase, as described by [52] in *C. vulgaris* under similar MF conditions. The decrease in protein content may reflect an initial oxidative damage and metabolic reallocation, while the recovery may indicate stress adaptation and reactivation of protein biosynthesis. The variable effects related to the time of exposure to MF could be related to the synthesis of antioxidative enzymes, which could be improved at longer periods of exposure. In this context, Wang and co-workers [52] observed that the exposure to 10-35 mT for 12 h d^{-1} promoted the growth of *C. vulgaris* and regulated the antioxidant defense system to protect the cells, increasing the activity of the SOD and peroxidase. In contrast, a two-fold increase in carbohydrate content, compared to the control, was recorded when *Coelastrella* sp. cultures were exposed to 60 mT for 4 h d^{-1}. Additionally, the protein content increased at 1 and 2 h d^{-1} of exposure by 18 and 25%, respectively, indicating that moderate MF exposure triggered metabolic reallocation rather than a complete suppression. These findings suggest that MF exposure acted as a strong abiotic stressor for *Coelastrella* sp., as reflected by the reduced Px and QY values (Tables 4.1 and S4.2). The preferential accumulation of carbohydrates under stress may serve as a protective mechanism, possibly involving the synthesis of extracellular polysaccharides or cell wall remodeling [25], [53]. Finally, *Coelastrella* sp. cultures exposed to 120 mT consistently experienced a decrease in the carbohydrates, lipids, and proteins content, regardless of exposure time. These results suggest that the high-intensity MF exposure (120 mT) exceeded the physiological tolerance of this particular strain, leading to a widespread metabolic

suppression and cellular damage. Thus, while *Coelastrella sp.* shows some adaptive capacity at moderate exposures, it is more sensitive than *C. vulgaris* to MF stress.

The exposure of *A. platensis* cultures also presented a response dependent on the MF intensity but differed from green microalgae. At 30 mT the carbohydrate concentration significantly decreased by 22 and 19% under 1 and 2 h d^{-1} respectively (Fig. 4.5c), whereas protein content increased by 39, 22 and 13% at 1, 2 and 4 h d^{-1} of exposure, respectively (Fig. 4.5i). This suggests a metabolic shift favoring protein synthesis for biomass production, which is supported by the increase in biomass content, by 14%, observed at this particular MF intensity (Fig. 4.4g). When *A. platensis* cultures were exposed to 60 mT for 2 h d^{-1}, the carbohydrate content increased by 11%, whilst the lipid content significantly increased under 1 and 2 h d^{-1} of exposure. Thereby, the increased biomass concentration under this MF was likely due to *A. platensis* increase cell size rather than enhance protein content (Fig. 4.5i). Interestingly, when the MF was increased to 120 mT, the protein content was significantly increased by 28, 22 and 18% at 1, 2 and 4 h d^{-1} respectively, similarly to the lipid content. On the contrary, the carbohydrate content was significantly decreased regardless of the exposure time. This suggests that exposure to 120 mT in *A. platensis* relocates resources toward stress-related protein and lipid synthesis, potentially through transcriptional upregulation of biosynthetic or repair pathways [45].

The reallocations observed across the three strains can be mechanistically related to the interplay between MF exposure and cellular redox homeostasis. Several studies have suggested that MF can modulate the spin state of radical pairs, thereby altering ROS formation rate and leading to transient oxidative signals within the cell [54]. These ROS bursts serve as secondary messengers, activating the antioxidant defense system and influencing downstream transcriptional regulators and metabolic enzymes [55]. In *C. vulgaris*, the balance between moderate ROS signaling and antioxidant activation appears to favor anabolic processes such as protein or lipid synthesis, depending on the intensity, while *Coelastrella* sp. exhibits a narrower tolerance window in which ROS accumulation exceeds its antioxidant

buffering capacity, leading to metabolic suppression. The response of *A. platensis* suggests a cyanobacteria-specific regulation, possibly involving redox-sensitive transcriptional regulators (e.g., RecA and transcriptional repressor LexA, where the former activates auto-cleavage of the latter to induce SOS response) that redistribute carbon fluxes toward protein and lipid biosynthesis under oxidative pressure [56], [57]. Additionally, MF-induced changes in membrane potential and ion modulation biosynthetic pathways [35].

Overall, these findings demonstrate that MF exposure may act as a powerful modulator of microalgal growth and metabolic activity, with its effects determined by the interplay between intensity, exposure time, and species-specific tolerance. Rather than functioning solely as a growth enhancer, MF application promotes targeted metabolic reallocations-stimulating protein synthesis, enhancing lipid accumulation, or triggering carbohydrate storage depending on the conditions. Thus, this approach could be applied to a larger-scale cultivation system. For example, photobioreactors with permanent magnets or electromagnetic coils could be integrated into the reactor walls to ensure a homogeneous and adjustable field, while in open raceway ponds, magnetic devices could be positioned along channels or combined with recirculation through magnetically active zones. These strategies highpoint the potential of magnetic field application as a viable technology to enhance biomass productivity in biofuel generation, WWT, and other scale-up biotechnological applications.

4.4.3 Influence of MF intensity and exposure time on pigment production

The exposure of *C. vulgaris* cultures to MF tends to increase the chlorophyll content regardless of the MF intensity. However, this increment was modulated by both intensity and exposure time (Fig. 4.6a). Thus, the highest enhancement was recorded at 60 mT for 4 h d^{-1} of exposure, where chlorophyll content was 40% higher than the control. Interestingly, this increment in chlorophyll content was correlated to an increased biomass concentration. Similar behavior was also observed at 30 mT for 4 h d^{-1}, with 15% higher chlorophyll content compared to the control, reinforcing

the relation between pigment content and photosynthetic efficiency.

The enhancement in chlorophyll content under moderate MF stimulation has been mechanistically associated with an increase in Fe uptake across the plasma membrane, supporting chlorophyll biosynthesis and photosystem assembly [58]. Fe and Mg are essential cofactors for chlorophyll synthesis and photosynthetic protein complexes, indicating that MF induced modulation of ion transport through the cellular membrane transporters, enhancing the photosynthetic capacity [28], [59], [60].

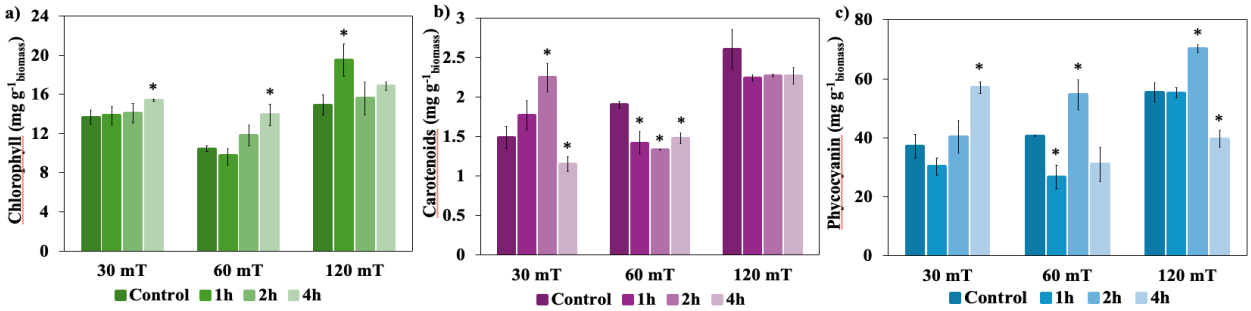

Fig. 4.6 Influence of MF intensity and exposure time on the chlorophyll content of *C. vulgaris* (a), carotenoid content of *Coelastrella sp*. (b) and phycocyanin content of *A. platensis* (c). * Significant difference compared with control $p \leq 0.05$.

However, the exposure of *C. vulgaris* cultures to the highest MF intensity (120 mT for 1 h d^{-1}) resulted in a 26% increase in chlorophyll concentration, despite this condition resulting in significant reductions in Px and μ (Table 4.1). This decoupling between pigment accumulation and physiological performance suggests that, beyond a certain threshold, increased chlorophyll content does not necessarily translate into enhanced photosynthetic efficiency. In this case, elevated chlorophyll content may impair energy transfer within the photosystems or contribute to photoinhibition. Similar outcomes have been reported by [61], who observed that excessive pigment levels disrupt light harvesting efficiency or increase ROS production.

Overall, these findings suggest that MF stimulation acts at multiple molecular levels: (i) enhancing ion fluxes (Fe^{2+}, Mg^{2+}) that support chlorophyll biosynthesis, (ii)

modulating redox-sensitive signaling pathways that regulate photosynthetic protein expression, and (iii) influencing thylakoid membrane organization and electron transport. While moderate stimulation promotes coordinated chlorophyll accumulation and biomass growth, excessive MF disrupts this balance, leading to pigment overaccumulation, impaired energy transfer, and potential ROS-mediated photoinhibition. This dual role highlights MF as a fine-tunable regulator of photosynthetic efficiency rather than a simple stimulant of pigment biosynthesis [58], [61].

Carotenoid accumulation in *Coelastrella* sp. was selectively stimulated at 30 mT for 1 and 2 h d^{-1}. However, longer exposure times and higher MF intensities led to significant reductions in carotenoid content (Fig. 4.6b). Carotenoids are known to function as non-enzymatic antioxidants involved in the scavenging of ROS, generated under stress conditions. Hence, the observed decrease under strong or prolonged MF exposure may reflect a stress response that exceeds the microalgae antioxidant capacity. Alternatively, energy and carbon fluxes may have been redirected from carotenoid biosynthesis to stress mitigation pathways. Nonetheless, the reduced biomass productivity recorded for *Coelastrella* sp. supports the inhibitory effect of the MF.

Carotenoid metabolism may be modulated by MF stimulation through a redox-sensitive pathway. MF promotes controlled ROS generation that activates transcription factors regulating antioxidant and carotenoid biosynthetic enzymes, thereby enhancing pigment accumulation [61]–[63]. In contrast, strong or prolonged exposure may disrupt redox homeostasis, leading to excessive ROS, oxidation of carotenoids, and diversion of precursors (e.g., isoprenoids) toward stress-related metabolites rather than pigment biosynthesis [25], [64]. This dual response highlights that MF acts not only as a physical stimulus but also as a regulator of redox signaling and metabolic flux partitioning, determining whether carotenoid accumulation supports photoprotection or is compromised under stress overload.

Finally, C-PC concentration in *A. platensis* cultures was more sensitive to the exposure time rather than to MF intensity (Fig. 4.6c). For instance, the C-PC content

under 30 mT for 4 h d^{-1} was 54% higher compared to the control. When the MF intensity increased to 60 and 120 mT, the C-PC content was increased by 35 and 27%, respectively at exposure times of 2 h d^{-1}. The C-PC increase recorded at 60 mT was positively correlated with an enhancement in Px, μ and CO_2 fixation rates, suggesting that under optimized conditions, MF may enhance pigment production while maintaining metabolic balance. In contrast, the increase in C-PC at 120 mT for 2 h d^{-1} was not related to an improved biomass growth or CO_2 fixation, indicating a decoupling of pigment accumulation from photosynthetic efficiency at high pigment concentrations.

C-PC accumulation under optimized MF conditions may be driven by upregulated transcription of phycobiliprotein genes and coordinated assembly of phycobilisomes, enhancing light-harvesting efficiency [65]. Excessive MF, however, can decouple C-PC synthesis from photosynthetic performance, possibly due to ROS-induced damage to photosynthetic membranes or regulatory feedback limiting functional pigment incorporation [66].

Taken together, these highlight that MF exposure can selectively modulate pigment biosynthesis in microalgae, with responses strongly dependent on species, intensity, and exposure time. Moderate MF stimulation favored chlorophyll, carotenoid, and C-PC accumulation in a manner that was often coupled with enhanced photosynthetic efficiency and biomass production, whereas excessive stimulation promoted pigment accumulation without functional benefits. This underscores the potential of MF as a controllable, non-invasive, and energy-efficient strategy tool for optimizing microalgal cultivation for future applications in biofuels, nutraceuticals, and high-value bioproducts. Outside the laboratory scale, the potential of the magnetic field to enhance biomass productivity and influence metabolic activity opens perspectives for industrial applications. Hereafter, microalgal biorefineries could couple electromagnetic coils with cultivation systems to control pigment, lipid, or any other byproduct production according to demand. Also, the combination of magnetic field with magnetic (nano)particles or magnetic support offers a dual benefit: stimulates the microalgae metabolism and at the same time facilitates the downstream

harvesting processes for biomolecules recovery. Thus, magnetic field technology is not limited to lab-scale experiments but could be integrated into pilot operations for the sustainable production of high-value biomolecules.

4.5 Conclusions

The effects found in this study are dependent on the microalgal strain, magnetic field intensity, and exposure time. *C. vulgaris* cultures exhibited a superior tolerance to MF, particularly at exposures of 2 and 4 h d^{-1}. Indeed, the exposure of *C. vulgaris* cultures to 30 and 60 mT resulted in a significant enhancement of CO_2 biofixation and Px. Additionally, protein accumulation was stimulated by ~ 50% under MF of 30 and 120 mT, while an increase in lipid accumulation by ~ 50% was recorded at a MF of 60 mT. Interestingly, the exposure to the different MF for 4 h d^{-1} positively affected *C. vulgaris* growth regardless of the intensity of the MF. On the other hand, *A. platensis* exhibited a better tolerance to low MF intensities. The exposure to 30 mT for 4 h d^{-1} significantly increased the C-PC content, although biomass growth was only significantly enhanced when exposed to 60 mT for 1 h d^{-1}. Prolonged exposures of 4 h d^{-1} decreased *A. platensis* growth regardless of the MF intensity, while an exposure to 120 mT decreased *A. platensis* growth regardless of the exposure time. Finally, *Coelastrella* sp. was the most sensitive strain to MF, and the cultures were only stimulated when exposed to 30 mT for 2 h d^{-1}. Interestingly, the response of photosynthetic pigments to MF exposure was highly species-specific and governed by a complex interplay between MF intensity, exposure time, and cellular metabolic capacity. The study reinforces the emerging consensus that 30 and 60 mT can favor biological activity, whereas 120 mT may induce stress and inhibit the growth of some microalgae species. Hence, low intensity MFs represent a scalable and sustainable strategy to enhance biomass and pigment production during CO_2 mitigation process under a photobiorefinery approach. Overall, the study highlights the potential of MF as a scalable and sustainable strategy to enhance biomass and pigment production in microalgae cultivation, contributing to CO_2 mitigation under a photobiorefinery approach. However, successful scale-up will require overcoming significant engineering challenges, particularly ensuring field uniformity in large bioreactors,

optimizing electric energy demand, and integrating magnetic field systems without compromising reactor design. In addition, long-term stability of MF effects, potential interactions with light and mixing regimes, and strain-specific variability remain critical issues. Further research is therefore needed to elucidate the molecular mechanisms underlying the observed responses and to establish practical implementation guidelines for industrial application.

4.6 References

[1] S. Z. Ayatollahi, F. Esmaeilzadeh, and D. Mowla, “Integrated CO2capture, nutrients removal and biodiesel production using Chlorella vulgaris,” *J. Environ. Chem. Eng.*, vol. 9, no. 2, p. 104763, 2021, doi: 10.1016/j.jece.2020.104763.

[2] P. Xu *et al.*, “Chemosphere Recent advances in CO 2 fixation by microalgae and its potential contribution to carbon neutrality,” *Chemosphere*, vol. 319, no. January, p. 137987, 2023, doi: 10.1016/j.chemosphere.2023.137987.

[3] M. Ashour, A. T. Mansour, Y. A. Alkhamis, and M. Elshobary, “Usage of Chlorella and diverse microalgae for CO2 capture - towards a bioenergy revolution,” *Front. Bioeng. Biotechnol.*, vol. 12, no. August, pp. 1–20, 2024, doi: 10.3389/fbioe.2024.1387519.

[4] K. S. Khoo, I. Ahmad, K. W. Chew, K. Iwamoto, A. Bhatnagar, and P. L. Show, “Enhanced microalgal lipid production for biofuel using different strategies including genetic modification of microalgae: A review,” *Prog. Energy Combust. Sci.*, vol. 96, no. December 2022, p. 101071, 2023, doi: 10.1016/j.pecs.2023.101071.

[5] H. Znad, A. M. D. Al Ketife, S. Judd, F. AlMomani, and H. B. Vuthaluru, “Bioremediation and nutrient removal from wastewater by Chlorella vulgaris,” *Ecol. Eng.*, vol. 110, no. September 2016, pp. 1–7, 2018, doi: 10.1016/j.ecoleng.2017.10.008.

[6] X. Luo, H. Zhang, Q. Li, and J. Zhang, “Effects of static magnetic field on Chlorella vulgaris: growth and extracellular polysaccharide (EPS) production,” *J. Appl. Phycol.*, vol. 32, no. 5, pp. 2819–2828, 2020, doi: 10.1007/s10811-020-02164-7.

[7] K. Nayana, M. P. Sudhakar, and K. Arunkumar, “Biorefinery potential of Coelastrella biomass for fuel and bioproducts—a review,” *Biomass Convers. Biorefinery*, no. 0123456789, 2022, doi: 10.1007/s13399-022-02519-9.

[8] B. Zhu *et al.*, “Effects of CO2 concentration on carbon fixation capability and production of valuable substances by Spirulina in a columnar photobioreactor,” *Algal Res.*, vol. 56, no. 5, p. 102310, 2021, doi: 10.1016/j.algal.2021.102310.

[9] M. C. Matsudo, R. P. Bezerra, S. Sato, A. Converti, and J. C. M. De Carvalho, “Photosynthetic efficiency and rate of CO2 assimilation by Arthrospira (Spirulina) platensis continuously cultivated in a tubular photobioreactor,” *Biotechnol. J.*, vol. 7, no. 11, pp. 1412–1417, 2012, doi: 10.1002/biot.201200177.

[10] S. Abdur Razzak *et al.*, “Microalgae cultivation in photobioreactors: sustainable

solutions for a greener future," *Green Chem. Eng.*, vol. 5, no. 4, pp. 418–439, 2024, doi: 10.1016/j.gce.2023.10.004.

[11] M. I. S. Naduthodi, N. J. Claassens, S. D'Adamo, J. van der Oost, and M. J. Barbosa, "Synthetic Biology Approaches To Enhance Microalgal Productivity," *Trends Biotechnol.*, vol. 39, no. 10, pp. 1019–1036, 2021, doi: 10.1016/j.tibtech.2020.12.010.

[12] J. Hu, W. Meng, Y. Su, C. Qian, and W. Fu, "Emerging technologies for advancing microalgal photosynthesis and metabolism toward sustainable production," *Front. Mar. Sci.*, vol. 10, no. October, pp. 1–20, 2023, doi: 10.3389/fmars.2023.1260709.

[13] E. Katz, O. Lioubashevski, and I. Willner, "Magnetic field effects on bioelectrocatalytic reactions of surface-confined enzyme systems: Enhanced performance of biofuel cells," *J. Am. Chem. Soc.*, vol. 127, no. 11, pp. 3979–3988, 2005, doi: 10.1021/ja044157t.

[14] X. Luo, H. Zhang, and J. Zhang, "The influence of a static magnetic field on a Chlorella vulgaris - Bacillus licheniformis consortium and its sewage treatment effect," *J. Environ. Manage.*, vol. 295, no. May, 2021, doi: 10.1016/j.jenvman.2021.112969.

[15] R. Tu, W. Jin, T. Xi, Q. Yang, S. F. Han, and A. E. F. Abomohra, "Effect of static magnetic field on the oxygen production of Scenedesmus obliquus cultivated in municipal wastewater," *Water Res.*, vol. 86, pp. 132–138, 2015, doi: 10.1016/j.watres.2015.07.039.

[16] S. Xu, Y. Jiang, Y. Liu, S. Esakkimuthu, H. Chen, and S. Wang, "Impact of constant magnetic field on enhancing the microalgal biomass and biomolecules accumulations and life cycle assessment of the approach," *Algal Res.*, vol. 80, no. May, p. 103563, 2024, doi: 10.1016/j.algal.2024.103563.

[17] K. M. Deamici, L. O. Santos, and J. A. V. Costa, "Use of static magnetic fields to increase CO2 biofixation by the microalga Chlorella fusca," *Bioresour. Technol.*, vol. 276, no. December 2018, pp. 103–109, 2019, doi: 10.1016/j.biortech.2018.12.080.

[18] B. da Costa Menestrino, L. Sala, J. A. V. Costa, J. G. Buffon, and L. O. Santos, "Magnetic fields exhibit a positive impact on lipid and biomass yield during phototrophic cultivation of Spirulina sp.," *Bioprocess Biosyst. Eng.*, vol. 44, no. 10, pp. 2087–2097, 2021, doi: 10.1007/s00449-021-02585-9.

[19] E. Posadas, M. L. Serejo, S. Blanco, R. Pérez, P. A. García-Encina, and R. Muñoz, "Minimization of biomethane oxygen concentration during biogas upgrading in algal-bacterial photobioreactors," *Algal Res.*, vol. 12, pp. 221–229, 2015, doi: 10.1016/j.algal.2015.09.002.

[20] M. Dubois, K. Gilles, J. K. Hamilton, P. A. Rebers, and F. Smith, "A colorimetric method for the determination of sugars," *Nature*, vol. 168, no. 4265, p. 167, 1951, doi: 10.1038/168167a0.

[21] S. K. Mishra *et al.*, "Rapid quantification of microalgal lipids in aqueous medium by a simple colorimetric method," *Bioresour. Technol.*, vol. 155, pp. 330–333, 2014, doi: 10.1016/j.biortech.2013.12.077.

[22] H. K. Lichtenthaler, "Chlorophylls Carotenoids," *Chlorophylls Carotenoids Pigment. Photosynth. Biomembr.*, vol. 148, pp. 350–382, 1987.

[23] R. Chaiklahan, N. Chirasuwan, T. Srinorasing, S. Attasat, A. Nopharatana, and B. Bunnag, "Enhanced biomass and phycocyanin production of Arthrospira (Spirulina)

platensis by a cultivation management strategy: Light intensity and cell concentration," *Bioresour. Technol.*, vol. 343, no. September 2021, p. 126077, 2022, doi: 10.1016/j.biortech.2021.126077.

[24] M. V. Rohit and S. Venkata Mohan, "Quantum yield and fatty acid profile variations with nutritional mode during microalgae cultivation," *Front. Bioeng. Biotechnol.*, vol. 6, no. SEP, pp. 1–12, 2018, doi: 10.3389/fbioe.2018.00111.

[25] K. M. Deamici, S. P. Cuellar-Bermudez, K. Muylaert, L. O. Santos, and J. A. V. Costa, "Quantum yield alterations due to the static magnetic fields action on Arthrospira platensis SAG 21.99: Evaluation of photosystem activity," *Bioresour. Technol.*, vol. 292, no. July, p. 121945, 2019, doi: 10.1016/j.biortech.2019.121945.

[26] M. Hasanuzzaman *et al.*, "Regulation of ros metabolism in plants under environmental stress: A review of recent experimental evidence," *Int. J. Mol. Sci.*, vol. 21, no. 22, pp. 1–44, 2020, doi: 10.3390/ijms21228695.

[27] V. Savchenko, O. Synyavskiy, A. Dudnyk, A. Nesvidomin, V. Ramsh, and V. Bunko, "The Impact of a Direct Magnetic Field on the Cells," *2020 IEEE KhPI Week Adv. Technol. (KhPIWeek), Kharkiv, Ukr.*, pp. 193–198, 2020, [Online]. Available: 10.1109/KhPIWeek51551.2020.9250104.

[28] B. da Costa, T. H. Chaves, L. Sala, J. A. Viera, and L. Oliveira, "Application of Static Magnetic Fields on the Mixotrophic Culture of Chlorella minutissima for Carbohydrate Production," *Appl Biochem Biotechno*, vol. 192, pp. 822–830, 2020, doi: https://doi.org/10.1007/s12010-020-03364-0.

[29] K. M. Deamici *et al.*, "Static magnetic fields effects on polysaccharides production by different microalgae strains," *Appl. Sci.*, vol. 11, no. 11, 2021, doi: 10.3390/app11115299.

[30] S. Aigner *et al.*, "Adaptation to Aquatic and Terrestrial Environments in Chlorella vulgaris (Chlorophyta)," *Front. Microbiol.*, vol. 11, no. October, pp. 1–14, 2020, doi: 10.3389/fmicb.2020.585836.

[31] S. Ghodbane, A. Lahbib, M. Sakly, and H. Abdelmelek, "Bioeffects of static magnetic fields: Oxidative stress, genotoxic effects, and cancer studies," *Biomed Res. Int.*, vol. 2013, 2013, doi: 10.1155/2013/602987.

[32] A. Pazur and M. Winklhofer, "Magnetic effect on CO2 solubility in seawater: A possible link between geomagnetic field variations and climate," *Geophys. Res. Lett.*, vol. 35, no. 16, pp. 1–5, 2008, doi: 10.1029/2008GL034288.

[33] W. W. C. Albuquerque, R. M. P. B. Costa, T. de Salazar e Fernandes, and A. L. F. Porto, "Evidences of the static magnetic field influence on cellular systems," *Prog. Biophys. Mol. Biol.*, vol. 121, no. 1, pp. 16–28, 2016, doi: 10.1016/j.pbiomolbio.2016.03.003.

[34] A. L. Buchachenko, A. P. Orlov, D. A. Kuznetsov, and N. N. Breslavskaya, "Magnetic isotope and magnetic field effects on the DNA synthesis," *Nucleic Acids Res.*, vol. 41, no. 17, pp. 8300–8307, 2013, doi: 10.1093/nar/gkt537.

[35] K. M. Deamici *et al.*, "Microalgae Cultivated under Magnetic Field Action: Insights of an Environmentally Sustainable Approach," *Sustain.*, vol. 14, no. 20, 2022, doi: 10.3390/su142013291.

[36] D. P. Small, N. P. Hüner, and W. Wan, "Effect of static magnetic fields on the growth,

photosynthesis and ultrastructure of Chlorella kessleri microalgae," *Bioelectromagnetics*, vol. 33, no. 4, pp. 298–308, 2012, [Online]. Available: https://doi.org/10.1002/bem.20706.

[37] Z. Wang, F. Hao, C. Ding, Z. Yang, and P. Shang, "Effects of static magnetic field on cell biomechanical property and membrane ultrastructure," *Bioelectromagnetics*, vol. 35, no. 4, pp. 251–261, 2014, doi: 10.1002/bem.21847.

[38] O. Spain and C. Funk, "Detailed Characterization of the Cell Wall Structure and Composition of Nordic Green Microalgae," *J. Agric. Food Chem.*, vol. 70, no. 31, pp. 9711–9721, 2022, doi: 10.1021/acs.jafc.2c02783.

[39] J. Mareš, O. Strunecký, L. Bučinská, and J. Wiedermannová, "Evolutionary patterns of thylakoid architecture in Cyanobacteria," *Front. Microbiol.*, vol. 10, no. FEB, pp. 1–22, 2019, doi: 10.3389/fmicb.2019.00277.

[40] S. Kumar *et al.*, "Unveiling the Green Gold : A Comprehensive Review of Arthrospira Platensis ' s Botanical , Pharmacological and Biotechnological Aspects with Emphasis on Anti-Oxidant Activity," vol. 2, no. 5, pp. 338–354, 2025.

[41] Y. Sun, H. Lv, H. Yao, Y. Gao, and C. Zhang, "Magnetic field-assisted electrocatalysis: Mechanisms and design strategies," *Carbon Energy*, no. January, 2024, doi: 10.1002/cey2.575.

[42] W. Shao, R. Ebaid, A. E. F. Abomohra, and M. Shahen, "Enhancement of Spirulina biomass production and cadmium biosorption using combined static magnetic field," *Bioresour. Technol.*, vol. 265, no. May, pp. 163–169, 2018, doi: 10.1016/j.biortech.2018.06.009.

[43] M. C. Veiga, M. M. Fontoura, M. G. de Oliveira, J. A. Viera Costa, and L. O. Santos, "Magnetic fields: Biomass potential of Spirulina sp. for food supplement," *Bioprocess Biosyst. Eng.*, vol. 43, no. July 2020, pp. 1231–1240, 2020, [Online]. Available: https://doi.org/10.1007/s00449-020-02318-4.

[44] Z. Y. Li, S. Y. Guo, L. Li, and M. Y. Cai, "Effects of electromagnetic field on the batch cultivation and nutritional composition of Spirulina platensis in an air-lift photobioreactor," *Bioresour. Technol.*, vol. 98, no. 3, pp. 700–705, 2007, doi: 10.1016/j.biortech.2006.01.024.

[45] K. M. Deamici, J. A. V. Costa, and L. O. Santos, "Magnetic fields as triggers of microalga growth: evaluation of its effect on Spirulina sp.," *Bioresour. Technol.*, vol. 220, pp. 62–67, 2016, doi: 10.1016/j.biortech.2016.08.038.

[46] Y. Liu, J. Li, W. Guo, H. H. Ngo, J. Hu, and M. tian Gao, "Use of magnetic powder to effectively improve the performance of sequencing batch reactors (SBRs) in municipal wastewater treatment," *Bioresour. Technol.*, vol. 248, pp. 135–139, 2018, doi: 10.1016/j.biortech.2017.06.069.

[47] A. Latifi, M. Ruiz, and C. C. Zhang, "Oxidative stress in cyanobacteria," *FEMS Microbiol. Rev.*, vol. 33, no. 2, pp. 258–278, 2009, doi: 10.1111/j.1574-6976.2008.00134.x.

[48] A. Y. Maizatul, M. S. R. Radin, A. A. Mohamed, R. A. Ambati, and R. Ranga, "Influence of nitrogen and phosphorus on microalgal growth, biomass, lipid, and fatty acid production: An overview," *Cells*, vol. 10, no. 393, pp. 10–20, 2021, doi: https://doi.org/10.3390/ cells10020393.

[49] L. M. Bauer, J. A. V. Costa, A. P. C. da Rosa, and L. O. Santos, “Growth stimulation and synthesis of lipids, pigments and antioxidants with magnetic fields in Chlorella kessleri cultivations,” *Bioresour. Technol.*, vol. 244, pp. 1425–1432, 2017, doi: 10.1016/j.biortech.2017.06.036.

[50] S. S. Costa, B. P. Peres, B. R. Machado, J. A. V. Costa, and L. O. Santos, “Increased lipid synthesis in the culture of Chlorella homosphaera with magnetic fields application,” *Bioresour. Technol.*, vol. 315, no. June, p. 123880, 2020, doi: 10.1016/j.biortech.2020.123880.

[51] K. Zienkiewicz, Z. Y. Du, W. Ma, K. Vollheyde, and C. Benning, “Stress-induced neutral lipid biosynthesis in microalgae — Molecular, cellular and physiological insights,” *Biochim. Biophys. Acta - Mol. Cell Biol. Lipids*, vol. 1861, no. 9, pp. 1269–1281, 2016, doi: 10.1016/j.bbalip.2016.02.008.

[52] H. Wang, X. Zeng, G. SY, and Z. Li, “Effects of magnetic field on the antioxidant defense system of recirculation-cultured Chlorella vulgaris,” *Bioelectromagnetics*, vol. 29, no. 1, pp. 39–46, 2008, [Online]. Available: doi: 10.1002/bem.20360.

[53] J. W. Rijstenbil *et al.*, “Oxidative stress induced by copper: defense and damage in the marine planktonic diatom Ditylum brightwellii, grown in continuous cultures with high and low zinc levels,” *Mar. Biol.*, vol. 119, no. 4, pp. 583–590, 1994, [Online]. Available: https://doi.org/10.1007/BF00354321.

[54] B. Saletnik *et al.*, “The Static Magnetic Field Regulates the Structure, Biochemical Activity, and Gene Expression of Plants,” *Molecules*, vol. 27, no. 18, 2022, doi: 10.3390/molecules27185823.

[55] D. Singh, “Juggling with reactive oxygen species and antioxidant defense system – A coping mechanism under salt stress,” *Plant Stress*, vol. 5, no. 109, p. 100093, 2022, doi: 10.1016/j.stress.2022.100093.

[56] A. Srivastava *et al.*, “Gamma (γ)-radiation stress response of the cyanobacterium Anabaena sp. PCC7120: Regulatory role of LexA and photophysiological changes,” *Plant Sci.*, vol. 326, no. July 2022, p. 111529, 2023, doi: 10.1016/j.plantsci.2022.111529.

[57] H. Badri, P. Monsieurs, I. Coninx, R. Nauts, R. Wattiez, and N. Leys, “Temporal gene expression of the cyanobacterium arthrospira in response to gamma rays,” *PLoS One*, vol. 10, no. 8, pp. 1–29, 2015, doi: 10.1371/journal.pone.0135565.

[58] A. A. H. A. Latef, M. F. A. Dawood, H. Hassanpour, M. Rezayian, and N. A. Younes, “Impact of the static magnetic field on growth, pigments, osmolytes, nitric oxide, hydrogen sulfide phenylalanine ammonia-lyase activity, antioxidant defense system, and yield in lettuce,” *Biology (Basel).*, vol. 9, no. 7, pp. 1–19, 2020, doi: 10.3390/biology9070172.

[59] L. O. Santos, K. M. Deamici, B. C. Menestrino, J. Garda-Buffon, and J. A. V. Costa, “Magnetic treatment of microalgae for enhanced product formation,” *World J. Microbiol. Biotechnol.*, vol. 33, no. 9, pp. 1–6, 2017, doi: 10.1007/s11274-017-2332-4.

[60] X.-G. Zhu, S. P. Long, and D. R. Ort, “What is the maximum efficiency with which photosynthesis can convert solar energy into biomass?,” *Curr. Opin. Biotechnol.*, vol. 19, no. 2, pp. 153–159, 2008, doi: 10.1016/j.copbio.2008.02.004.

[61] F. Didaran *et al.*, “The mechanisms of photoinhibition and repair in plants under high light conditions and interplay with abiotic stressors,” *J. Photochem. Photobiol. B Biol.*, vol. 259, no. July, p. 113004, 2024, doi: 10.1016/j.jphotobiol.2024.113004.

[62] M. Zuluaga, V. Gueguen, G. Pavon-Djavid, and D. Letourneur, “Carotenoids from microalgae to block oxidative stress,” *BioImpacts*, vol. 7, no. 1, pp. 1–3, 2017, doi: 10.15171/bi.2017.01.

[63] I. A. Shaev, V. V. Novikov, E. V. Yablokova, and E. E. Fesenko, “A Brief Review of the Current State of Research on the Biological Effects of Weak Magnetic Fields,” *Biophys. (Russian Fed.*, vol. 67, no. 2, pp. 245–251, 2022, doi: 10.1134/S0006350922020191.

[64] K. Dziergowska, S. Lewandowska, R. Mech, M. Pol, J. Detyna, and I. Michalak, “Soybean germination response to algae extract and a static magnetic field treatment,” *Appl. Sci.*, vol. 11, no. 18, 2021, doi: 10.3390/app11188597.

[65] R. R. C. Nascimento, M. R. Moreno, R. S. Azevedo, J. A. V. Costa, L. F. Marins, and L. O. Santos, “Magnetic Fields as Inducers of Phycobiliprotein Production by Synechococcus elongatus PCC 7942,” *Curr. Microbiol.*, vol. 80, no. 8, pp. 1–11, 2023, doi: 10.1007/s00284-023-03348-3.

[66] S. Khorobrykh, V. Havurinne, H. Mattila, and E. Tyystjärvi, “Oxygen and ROS in photosynthesis,” *Plants*, vol. 9, no. 1, 2020, doi: 10.3390/plants9010091.

4.7 Supplementary materials

Table S4.1 Average Magnetic Field intensities inside all three systems

Magnets on each side	Height 0 mm	Height 10 mm	Height 20 mm	Magnetic Field average
1	28.92 mT	33.90 mT	29.51 mT	30.76 mT
2	53.55 mT	74.56 mT	55.95 mT	61.35 mT
3	115.7 mT	135.6 mT	110.7 mT	120.66 mT

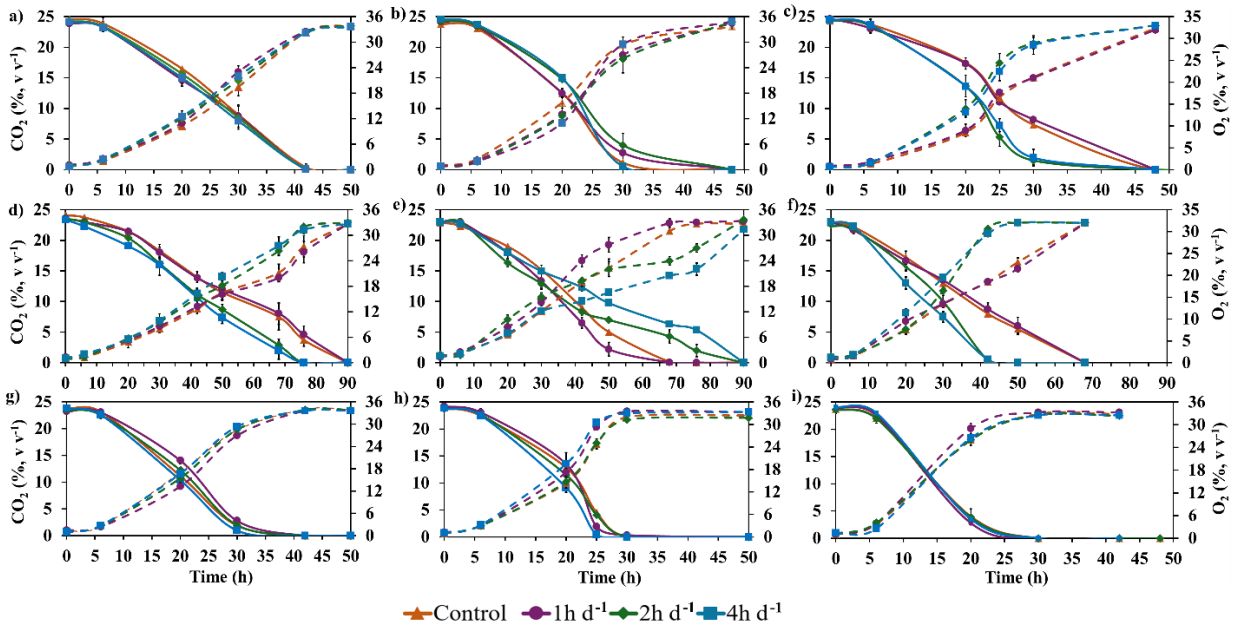

Fig. S4.1 Time course of CO_2 consumption (main axis) and O_2 production (secondary axis) by *C. vulgaris* cultures exposed to 30 mT, a) first cultivation; b) second cultivation; c) third cultivation; to 60 mT, d) first cultivation; e) second cultivation; f) third cultivation; and to 120 mT, g) first cultivation; h) second cultivation; i) third cultivation.

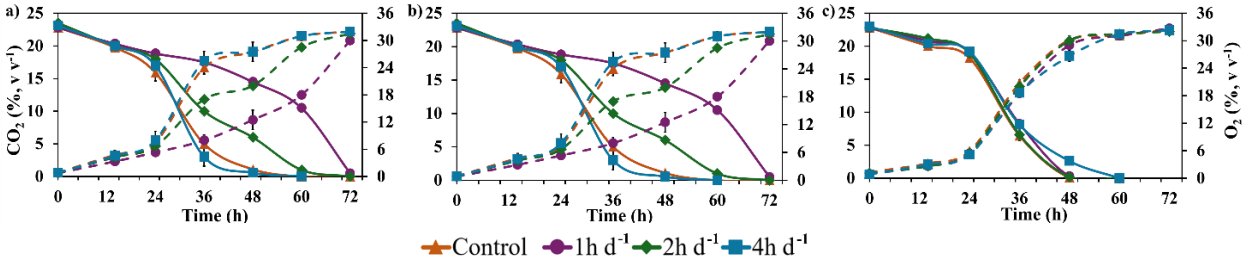

Fig. S4.2 Time course of CO_2 consumption (main axis) and O_2 production (secondary axis) by *Coelastrella* sp. cultures exposed to 30 mT, a) first cultivation; exposed to 60 mT, b) first cultivation; and exposed to 120 mT, c) first cultivation.

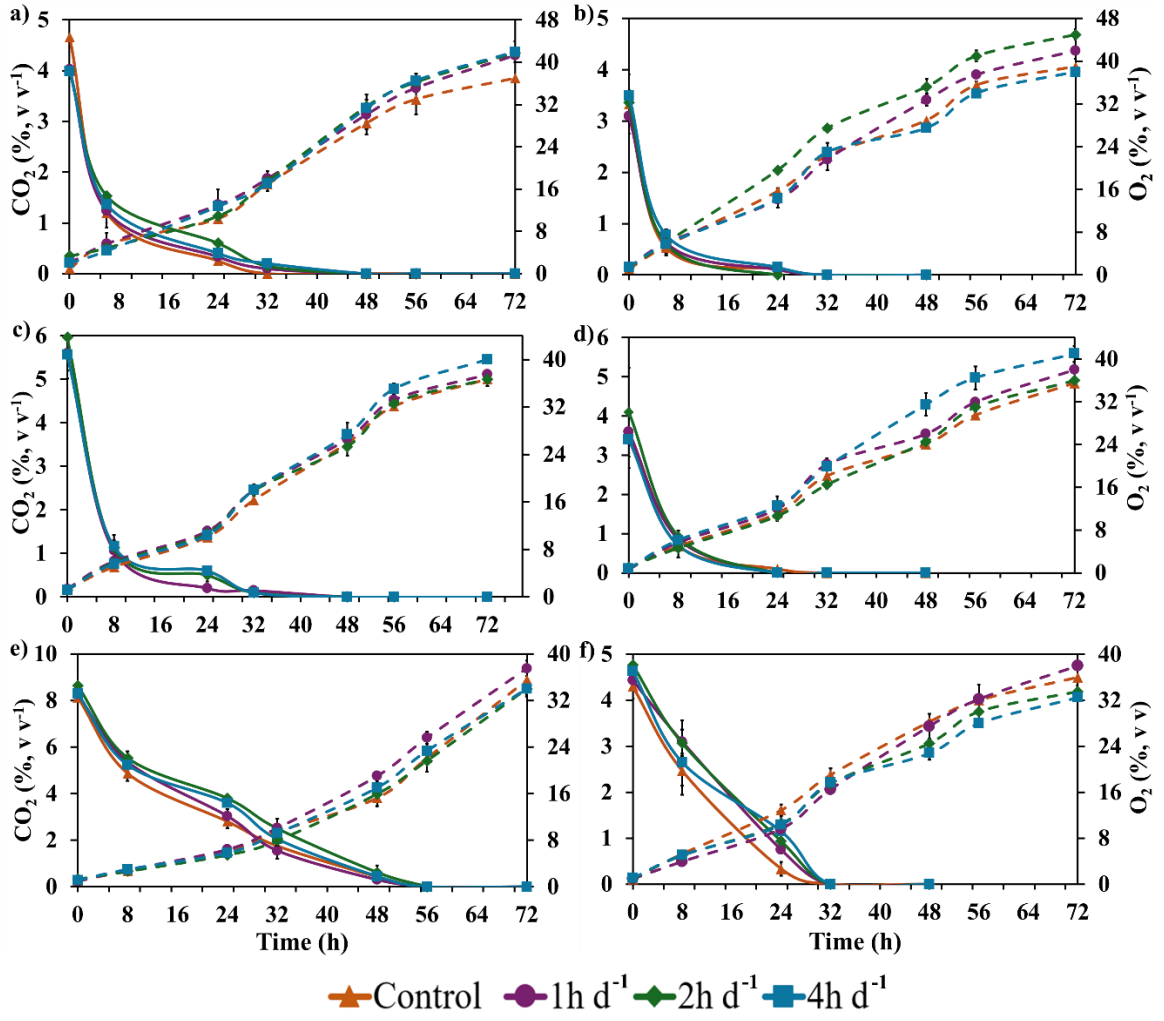

Fig. S4.3 Time course of CO_2 consumption (main axis) and O_2 production (secondary axis) by *A. platensis* cultures exposed to 30 mT, a) first cultivation, b) second cultivation; 60 mT, c) first cultivation, d) second cultivation; and to 120 mT, e) first cultivation, f) second cultivation.

Table S4.2 Evolution of pH and QY in the kinetic assays of the last cultivation of *C. vulgaris*.

C. vulgaris		**pH**		**QY**	
MF intensity	**Time of exposure ($h\ d^{-1}$)**	**Initial**	**Final**	**Initial**	**Final**
30 mT	Control (0h)	5.58±0.27	11.43±0.23	0.66±0.02	0.69±0.01
	1	5.45±0.02	11.46±0.31	0.65±0.03	0.69±0.01
	2	5.42±0.02	11.75±0.10	0.67±0.05	0.71±0.001
	4	5.39±0.01	11.70±0.10	0.66±0.01	0.70±0.01
60 mT	Control (0h)	5.56±0.14	11.27±0.14	0.59±0.02	0.64±0.02
	1	5.75±0.06	10.93±0.81	0.55±0.02	0.64±0.01
	2	5.42±0.01	10.43±0.75	0.53±0.02	0.70±0.01*
	4	5.42±0.2	10.33±0.58	0.62±0.01	0.72±0.02*
120 mT	Control (0h)	5.46±0.01	11.50±0.10	0.72±0.02	0.73±0.001
	1	5.54±0.06	11.56±0.001	0.70±0.05	0.73±0.001
	2	5.46±0.05	11.58±0.03	0.68±0.05	0.73±0.001
	4	5.45±0.01	11.64±0.10	0.66±0.02*	0.72±0.02

*Significant differences compared to the control ($p < 0.05$).

Table S4.3 Evolution of pH and QY in the kinetic assays of the last cultivation of *Coelastrella* sp.

***Coelastrella* sp.**		**pH**		**QY**	
MF intensity	**Time of exposure (h d^{-1})**	**Initial**	**Final**	**Initial**	**Final**
30 mT	Control (0h)	6.09±0.01	9.37±0.23	0.63±0.02	0.51±0.01
	1	6.07±0.04	8.70±0.36	0.62±0.01	0.53±0.02
	2	6.06±0.04	8.80±0.61	0.62±0.01	0.57±0.02*
	4	6.04±0.01	8.72±0.30	0.62±0.01	0.52±0.03
60 mT	Control (0h)	6.16±0.01	10.86±0.41	0.51±0.02	0.50±0.01
	1	6.14±0.03	10.53±0.40	0.51±0.01	0.45±0.03
	2	6.12±0.03	10.05±0.21	0.50±0.01	0.45±0.001*
	4	6.10±0.02	9.01±0.44*	0.50±0.01	0.47±0.03
120 mT	Control (0h)	6.03±0.06	9.83±0.12	0.60±0.01	0.52±0.04
	1	6.07±0.06	9.73±0.16	0.60±0.01	0.51±0.01
	2	6.13±0.06	9.73±0.25	0.59±0.01	0.53±0.06
	4	6.00±0.10	9.43±0.06*	0.59±0.01	0.54±0.05

*Significant differences compared to the control ($p < 0.05$).

Table S4.4 Evolution of pH and QY in the kinetic assays of the last cultivation of *A. platensis*.

A. platensis		**pH**		**QY**	
MF intensity	**Time of exposure (h d^{-1})**	**Initial**	**Final**	**Initial**	**Final**
30 mT	Control (0h)	8.93±0.05	11.27±0.55	0.39±0.02	0.35±0.01
	1	8.84±0.10	10.97±0.95	0.40±0.001	0.32±0.02
	2	8.94±0.05	11.20±0.26	0.40±0.002	0.31±0.02*
	4	8.89±0.02	11.33±0.58	0.43±0.001	0.31±0.02*
60 mT	Control (0h)	8.85±0.05	10.73±0.25	0.44±0.01	0.36±0.01
	1	8.83±0.06	11.20±0.69	0.45±0.02	0.38±0.01*
	2	8.87±0.02	10.98±0.63	0.43±0.01	0.37±0.01
	4	8.87±0.01	11.09±0.37	0.44±0.01	0.37±0.04
120 mT	Control (0h)	8.85±0.05	10.22±0.10	0.44±0.01	0.34±0.01
	1	8.83±0.06	10.24±0.25	0.45±0.02	0.30±0.02
	2	8.87±0.02	10.16±0.01	0.43±0.01	0.31±0.02
	4	8.87±0.01	10.02±0.43	0.44±0.01	0.30±0.02

*Significant differences compared to the control ($p \leq 0.05$).

CHAPTER V. General discussion and conclusions

5.1 General discussion

This work demonstrated the potential to use static magnetic forces to stimulate diverse biological processes to mitigate several gas effluent challenges, such as hazardous air pollutants (VOCs) and greenhouse gases (GHG).

Regarding VOC treatments, according to the literature reviewed, biological processes present difficulties related to the efficiency of biodegrading compounds with low solubility or recalcitrant [1], [2]. Employing different biological experimental setups, we found that coupling them to a physical stimulus, such as SMF, increased the rate of organic pollutant consumption.

In Chapter II, the results obtained demonstrated that the VOCs with medium- and low-solubility evaluated (toluene and methanol) had an increase in biodegradation process under SMF exposure, as presents Fig. 5.1.

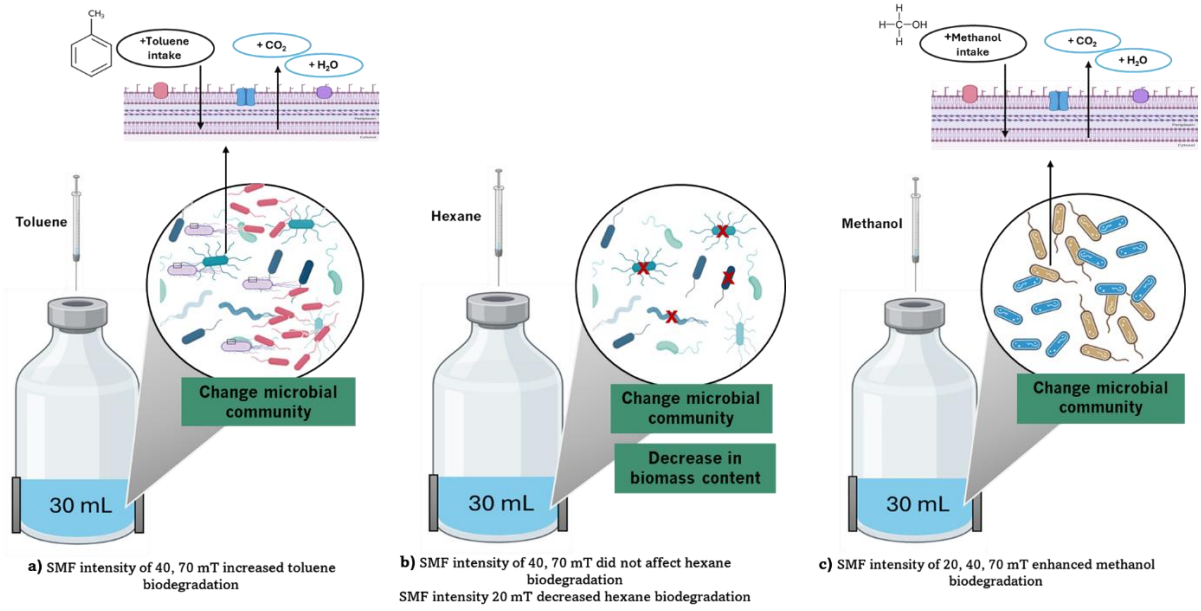

Fig. 5.1 Effects observed on the biodegradation of (a) toluene, (b) hexane, and (c) methanol, under different SMF intensities.

The application of SMF markedly influenced the microbial degradation kinetics of VOCs, although the magnitude and direction of the effects were compound-specific and dependent on SMF intensity. Overall, SMF exposure altered both the lag phase (β) and substrate consumption rate (K) (Chapter II, Fig. 2.2), revealing a dual behavior of transient inhibition followed by metabolic stimulation as microorganisms adapted to the magnetic environment.

For toluene and methanol, the exposure to higher SMF intensities (70 mT) initially extended the lag phase, suggesting a transient stress response possibly linked to membrane perturbation or altered electron transport. However, once adaptation occurred, toluene degradation was markedly enhanced, as reflected by increased K and V_{max} values (Chapter II, Fig. 2.3). This pattern aligns with previous reports describing SMF-induced activation of oxidative metabolism after an initial inhibitory phase [3], [4]. The stimulation of *Pseudomonas* and *Luteimonas* populations under 70 mT further supports the notion that SMF can act as a selective pressure, enriching metabolically efficient degraders with high tolerance to hydrophobic substrates. These results are also consistent with previous reports of improved degradation of TCE and other pollutants within similar ranges of SMF intensity [5], [6].

In contrast, hexane—a highly hydrophobic aliphatic compound—showed limited or negative responses to SMF exposure. The lack of variation in β and the reduced K under 20 mT suggest that low-intensity SMF may interfere with cellular energy transduction or membrane integrity without conferring adaptive benefit. The persistence of *Rhodococcus* and *Flavobacterium* as dominant degraders under SMF exposure suggests that microbial community composition was less sensitive to magnetic modulation for this compound, possibly because hexane biodegradation is constrained by mass transfer rather than metabolic activation.

Methanol biodegradation exhibited a delayed but clear stimulatory response to SMF exposure, particularly after prolonged contact (day 17), with all intensities enhancing both K and V_{max}. This indicates that SMFs may upregulate enzymatic systems such as methanol dehydrogenase or improve redox balance, consistent with prior findings on enhanced enzymatic activity and electron transfer under moderate SMF

intensities [7]–[9]. The predominance of *Methylobacillus* and *Hyphomicrobium* across treatments highlights the stability of methylotrophic communities, with only minor shifts in secondary taxa, suggesting that SMF acts mainly at a physiological rather than a community-selection level in this case. The observed compound-specific trends suggest that SMF effects are mediated by the interplay between substrate physicochemical properties, cell membrane permeability, and redox metabolism. The existence of a threshold intensity (20–70 mT) above which positive stimulation outweighs inhibitory stress also points to a non-linear dose–response relationship.

During toluene biofiltration (Chapter III), the application of a SMT of 50 notably enhanced the performance and resilience of the biofiltration process treating toluene vapors. Although the overall improvement in RE and EC may appear moderate (6–23%), such increases are statistically significant and exceed the intrinsic variability expected between identical biofilter systems. This confirms that SMF exposure can beneficially modulate biofilter performance both under continuous and intermittent operating conditions (Fig. 5.2).

In the initial operation phase, both biofilters reached high RE values within the first weeks, indicating that microbial communities rapidly acclimated to the biofiltration process. However, the biofilter exposed to the SMF consistently achieved higher steady-state RE and EC values and displayed a faster recovery after shutdowns, suggesting that the MF improved biofilm robustness and microbial tolerance to transient starvation (Chapter III, Fig. 3.3). This agrees with previous studies reporting. The shortened recovery time after 16 and 60 h shutdowns observed here (1.5 h vs. 2–3 h without SMF) reinforces the idea that magnetic stimulation favors a quicker reestablishment of enzymatic activity and mass transfer processes upon reloading.

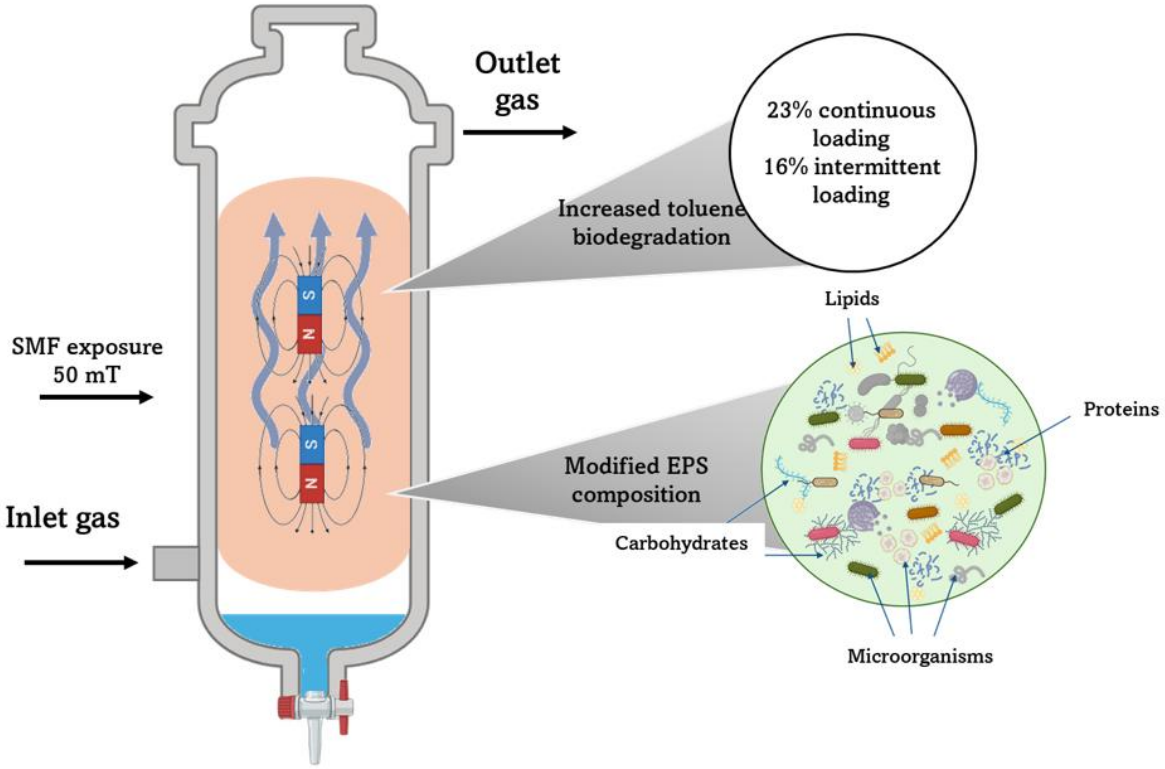

Fig. 5.2 Effect of SMF exposure on toluene biofiltration

The enhanced EC under SMF exposure (up to +23% during continuous loading and +16% under intermittent feeding) is consistent with the beneficial effects previously reported for various compounds, including TCE, hexane, and chlorobenzene, across different biofiltration and bioreactor configurations [5], [10]–[12]. This cross-compound consistency supports the hypothesis that SMF stimulation operates through general mechanisms rather than substrate-specific pathways—likely involving improved substrate diffusion across cell membranes, modulation of enzyme kinetics, and enhanced electron transport processes within microbial respiratory chains [12],[13].

Biomass evolution revealed that SMF mainly influenced the early stages of biofilm formation. During start-up, biomass accumulation was about 30% higher under the MF, suggesting accelerated microbial adhesion and colonization of the packing material. Later, biomass levels stabilized and converged between reactors,

indicating that the SMF primarily facilitated biofilm establishment rather than sustained growth. This aligns with previous reports showing that moderate magnetic intensities (10–60 mT) promote microbial attachment and biofilm maturation [13], [14]. The lower TOC observed in leachates under SMF supports this interpretation, reflecting improved biofilm fixation and reduced release of soluble microbial products.

Cell viability remained unaffected throughout operation, demonstrating that exposure to 50 mT did not induce harmful effects on the microbial consortium. Instead, the SMF enhanced metabolic activity, as evidenced by higher CO_2 production and increased mineralization efficiency under both continuous and intermittent conditions. The ratio of CO_2 produced to toluene removed remained stable, suggesting that magnetic stimulation enhanced overall respiration without altering carbon utilization pathways. Under intermittent operation, the SMF mitigated performance declines, maintaining a mineralization rate of about 60% compared with 50% in the control. The carbon balance confirmed that most removed toluene was mineralized to CO_2 (~60%), with minor incorporation into biomass (<10%). The SMF slightly favored anabolic processes during the early stages of biofilm development.

Overall, the results demonstrate that moderate SMF exposure (50 mT) exerts a multifactorial positive influence on biofiltration performance, acting simultaneously on (i) microbial adhesion and biofilm establishment, (ii) enzymatic and metabolic activities, (iii) substrate transfer and diffusion processes, and (iv) system robustness under discontinuous operation. These findings not only confirm the feasibility of applying SMF to enhance biofiltration of VOC but also contribute to elucidating the mechanistic basis of such enhancement. Future work should integrate metagenomic and metatranscriptomic analyses to identify microbial community shifts and gene expression patterns underlying the observed functional improvements, as well as assess the scalability and energy implications of SMF-assisted biofiltration systems.

Chapter IV presented the effect of SMF on CO_2 fixation by different microalgal strains. These results provide a comparative overview of how SMF modulate growth, photosynthetic activity, and metabolic allocation in three microalgal species—

Chlorella vulgaris, *Coelastrella* sp., and *Arthrospira platensis*—under varying intensities and exposure times. Overall, the responses followed a non-linear pattern characterized by an optimal stimulation window at moderate intensities (30–60 mT) and intermediate exposure times (2–4 h d^{-1}), beyond which inhibitory effects emerged. These findings reinforce the concept that magnetic stimulation acts as a biophysical modulator rather than a simple enhancer, eliciting species-specific adaptive or stress responses depending on the balance between oxidative signaling and redox homeostasis.

In *C. vulgaris*, the MF promoted a coordinated enhancement of CO_2 assimilation, O_2 evolution, and biomass accumulation, particularly at 60 mT and 2–4 h d^{-1}. The concurrent rise in quantum yield and photosynthetic performance suggests that moderate MF exposure optimizes the activity of photosystem II (PSII) and electron transport, possibly through improved cyclic electron flow and stabilization of reaction centers (Fig. 5.3). These effects were accompanied by distinct metabolic reallocations: protein accumulation predominated under 30 mT, while lipid biosynthesis was favored at 60 mT, indicating that MF intensity dictates the primary anabolic route [15]–[17].

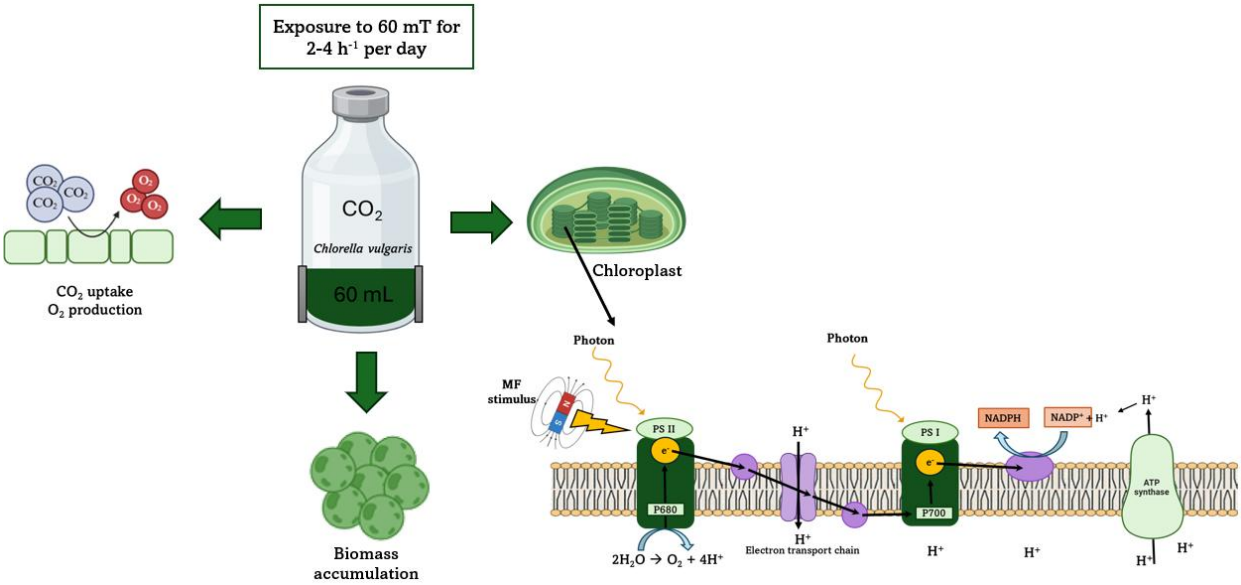

Fig. 5.3 Principal effects of 60 mT SMF exposure for 2 and 4 h^{-1} per day on *C. vulgaris*

By contrast, *Coelastrella* sp. displayed a narrower tolerance range, with pronounced growth inhibition beyond 30 mT. The decrease in photosynthetic yield and total organic carbon consumption under higher intensities indicates that MF-induced oxidative stress exceeded its physiological buffering capacity (Fig. 5.4). Nevertheless, the observed transient increases in carbohydrate or lipid content under moderate exposure times suggest a shift toward protective or storage pathways, consistent with stress-induced polysaccharide synthesis or energy redistribution. This pattern reveals that, for *Coelastrella* sp., the MF acts primarily as a metabolic stressor rather than a growth stimulant.

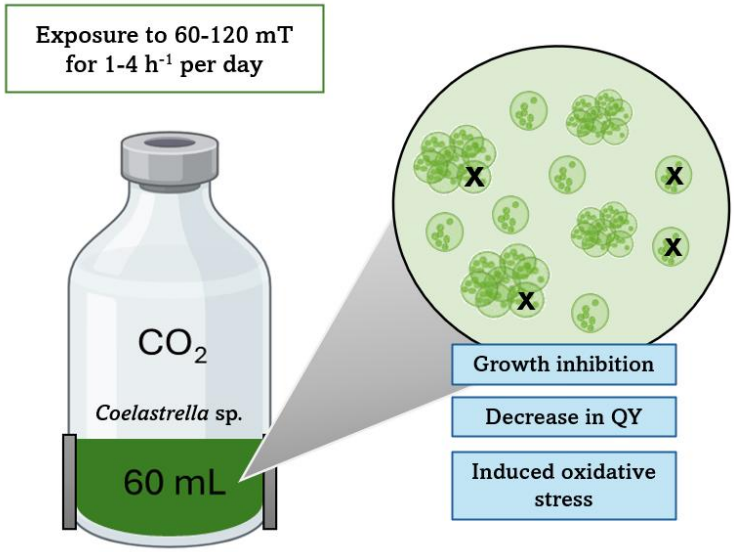

Fig. 5.4 Effects of SMF exposure on *Coelastrella* sp. under 60-120 mT exposure for 1, 2, and 4 h^{-1} per day.

In *A. platensis*, MF exposure elicited a biphasic response characterized by initial stimulation at 30–60 mT, followed by inhibition at 120 mT. Moderate intensities enhanced CO_2 fixation, pigment accumulation (notably C-phycocyanin), and biomass productivity, suggesting an activation of redox-regulated transcriptional pathways supporting protein and pigment synthesis. However, prolonged or intense exposure disrupted PSII efficiency, consistent with ROS overaccumulation and impaired photosynthetic membranes (Fig. 5.5). The distinctive sensitivity of

cyanobacteria likely arises from their simpler thylakoid organization and high-pH cultivation medium, both of which influence ion fluxes and redox balance [15]–[19].

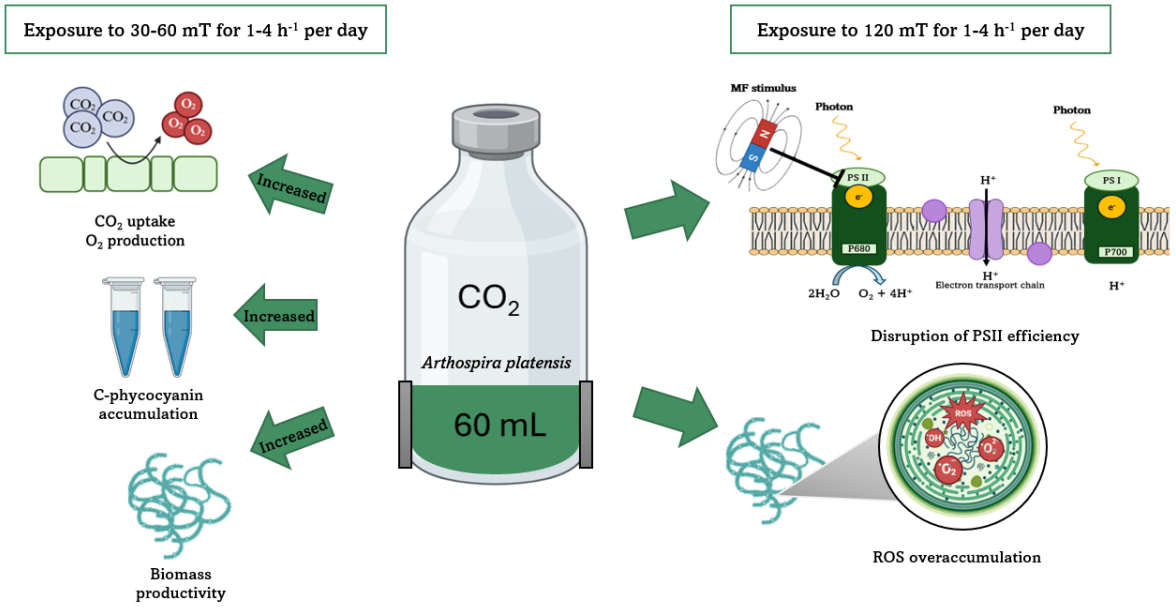

Fig. 5.5 Effects of SMF on *Arthospira platensis* under 30-120 mT exposure for 1, 2, and 4 h^{-1} per day.

Across all strains, pigment modulation emerged as a sensitive indicator of MF effects. Moderate exposure enhanced chlorophyll, carotenoid, or C-phycocyanin synthesis in correlation with photosynthetic efficiency, while excessive MF caused pigment overaccumulation decoupled from functional performance—signifying photochemical stress. Mechanistically, MF may enhance Fe^{2+} and Mg^{2+} uptake, modulate redox-sensitive transcriptional regulators, and alter radical pair recombination dynamics, thereby influencing both primary and secondary metabolism.

Collectively, these findings demonstrate that MF exposure operates through a redox-mediated control of metabolic and photosynthetic processes, leading to either adaptive enhancement or stress inhibition depending on field strength, duration, and cellular architecture. This understanding provides a foundation for applying magnetic stimulation as a tunable tool for targeted bioprocess optimization—enhancing lipid induction, pigment biosynthesis, or carbon fixation efficiency in large-scale

microalgal systems. Future work should integrate in situ magnetic control with photobioreactor design to harness these mechanistic advantages for sustainable bioresource production.

5.2 Conclusions

This thesis demonstrates that SMF can selectively enhance biological processes relevant to environmental biotechnology, including the biodegradation of VOCs and the cultivation of microalgae for CO_2 mitigation. In bacterial fed-batch experiments, SMF improved the degradation of toluene and methanol through microbial community shifts and possible enzymatic stimulation, while no effect was observed for hexane. In biofiltration, a 50 mT SMF accelerated biofilm formation, increased toluene removal capacity, and improved resilience under intermittent loading, highlighting its potential to strengthen biofilter performance.

In microalgal cultures, SMF effects were highly strain-dependent. *Chlorella vulgaris* showed the strongest positive responses, with enhanced CO_2 biofixation, biomass productivity, and macromolecule accumulation, while *Arthrospira platensis* and *Coelastrella* sp. displayed narrower tolerance ranges. Moderate intensities (30–60 mT) consistently promoted growth and pigment production, whereas higher intensities (120 mT) induced stress responses.

Overall, this work highlights SMF as a promising, scalable, and sustainable strategy to enhance microbial pollutant removal and microalgal CO_2 biofixation. However, its large-scale application will require optimization of field intensity and distribution, energy integration, and a deeper understanding of the molecular mechanisms underlying magnetic stimulation.

5.3 Perspectives

The discovery of SMF effects on VOCs biodegradation and CO_2 fixation in this thesis opens up several knowledge gaps regarding biological adaptability to physical stimulus, which improves the capability of several microorganisms to employ different waste gases.

Mechanistic understanding

While this work highlighted shifts in microbial communities, EPS production, and strain-specific responses, the underlying molecular mechanisms of SMF stimulation remain poorly understood. Future research should employ omics approaches (metagenomics, transcriptomics, proteomics, metabolomics) to identify genes, enzymes, and regulatory pathways influenced by SMF. Such knowledge would enable predictive models of SMF–biological interactions.

Optimization of SMF application

The intensity, exposure time, and application mode (continuous vs. intermittent) strongly determined the outcomes. Systematic optimization studies, including dynamic modulation of magnetic fields, could help maximize benefits while minimizing stress effects. Moreover, understanding threshold effects will be key to balancing stimulation with biological stability.

Integration into bioreactor and biofilter design

Translation of laboratory findings to large-scale applications requires addressing engineering challenges such as ensuring field homogeneity in large reactors, integrating magnetic systems without compromising hydrodynamics, and minimizing energy demand. Designing magnetic-responsive bioreactors and biofilters could pave the way toward industrial-scale applications.

Potential industrial and environmental applications

The dual applicability of SMF—enhancing VOC biodegradation and CO_2 biofixation—positions it as a promising tool for integrated environmental management strategies. Scaling these findings could support the development of sustainable air treatment technologies and bio-based carbon capture systems within a circular bioeconomy framework.

5.4 References

[1] E. H. Lee, J. Kim, K. S. Cho, Y. G. Ahn, and G. S. Hwang, “Degradation of hexane and other recalcitrant hydrocarbons by a novel isolate, Rhodococcus sp. EH831,” *Environ. Sci. Pollut. Res.*, vol. 17, no. 1, pp. 64–77, 2010, doi: 10.1007/s11356-009-0238-x.

[2] J. Hu, L. Zhang, J. Chen, Y. Luo, B. Sun, and G. Chu, “Performance and microbial analysis of a biotrickling filter inoculated by a specific bacteria consortium for removal of a simulated mixture of pharmaceutical volatile organic compounds,” *Chem. Eng. J.*, vol. 304, pp. 757–765, 2016, doi: 10.1016/j.cej.2016.06.078.

[3] S. Ghodbane, A. Lahbib, M. Sakly, and H. Abdelmelek, “Bioeffects of static magnetic fields: Oxidative stress, genotoxic effects, and cancer studies,” *Biomed Res. Int.*, vol. 2013, 2013, doi: 10.1155/2013/602987.

[4] A. Wasak, R. Drozd, D. Jankowiak, and R. Rakoczy, “Rotating magnetic field as tool for enhancing enzymes properties - laccase case study,” *Sci. Rep.*, vol. 9, no. 1, pp. 1–9, 2019, doi: 10.1038/s41598-019-39198-y.

[5] Y. Quan, H. Wu, Z. Yin, Y. Fang, and C. Yin, “Effect of static magnetic field on trichloroethylene removal in a biotrickling filter,” *Bioresour. Technol.*, vol. 239, pp. 7–16, 2017, doi: 10.1016/j.biortech.2017.04.121.

[6] Y. Quan, H. Wu, C. Guo, Y. Han, and C. Yin, “Enhancement of TCE removal by a static magnetic field in a fungal biotrickling filter,” *Bioresour. Technol.*, vol. 259, no. March, pp. 365–372, 2018, doi: 10.1016/j.biortech.2018.03.031.

[7] Y. L. Dorokhov, A. V. Shindyapina, E. V. Sheshukova, and T. V. Komarova, “Metabolic methanol: Molecular pathways and physiological roles,” *Physiol. Rev.*, vol. 95, no. 2, pp. 603–644, 2015, doi: 10.1152/physrev.00034.2014.

[8] B. Hu *et al.*, “Impact of static magnetic field on electron transport and microbial community shifts in the nitritation sequencing batch reactor,” *J. Environ. Chem. Eng. Please*, vol. 10, no. 5, pp. 2213–2221, 2022, doi: 10.1016/j.jece.2022.108774.

[9] Y. M. Zhu, H. Ji, H. Ren, J. Geng, and K. Xu, “Enhancement of static magnetic field on nitrogen removal at different ammonium concentrations in a sequencing batch reactor: Performance and biological mechanism,” *Chemosphere*, vol. 268, 2021, doi: 10.1016/j.chemosphere.2020.128794.

[10] D. Chen *et al.*, “Enhanced gaseous chlorobenzene removal and its microbial mechanism through innovative modified packings coupled with magnetic field in a biotrickling filter,” *Front. Environ. Sci. Eng.*, vol. 19, no. 11, 2025, doi: 10.1007/s11783-025-2072-x.

[11] M. Cortés-Castillo, A. Encinas, A. Aizpuru, and S. Arriaga, “Effect of applying a magnetic field on the biofiltration of hexane over long-term operation period,” *Environ. Sci. Pollut. Res.*, no. 0123456789, 2024, doi: 10.1007/s11356-024-34671-2.

[12] Q. Li *et al.*, “Static magnetic field enhances the purification of gaseous n-hexane in airlift two-phase partitioning bioreactor,” *Process Biochem.*, vol. 156, no. June, pp. 209–216, 2025, doi: 10.1016/j.procbio.2025.06.003.

[13] J. Li *et al.*, “Static magnetic fields enhance microbial aggregation and adhesion to promote aerobic granulation,” *Chem. Eng. J.*, vol. 489, no. April, p. 151392, 2024, doi: 10.1016/j.cej.2024.151392.

[14] S. Arriaga, M. F. Carboni, and P. N. L. Lens, “Effect of static magnetic field exposure on biohydrogen production via dark fermentation of glucose,” *Process Saf. Environ. Prot.*, vol. 176, no. June, pp. 375–388, 2023, doi: 10.1016/j.psep.2023.06.022.

[15] S. Xu, Y. Jiang, Y. Liu, S. Esakkimuthu, H. Chen, and S. Wang, “Impact of constant magnetic field on enhancing the microalgal biomass and biomolecules accumulations and life cycle assessment of the approach,” *Algal Res.*, vol. 80, no. May, p. 103563, 2024, doi: 10.1016/j.algal.2024.103563.

[16] K. M. Deamici, L. O. Santos, and J. A. V. Costa, “Use of static magnetic fields to increase CO2 biofixation by the microalga Chlorella fusca,” *Bioresour. Technol.*, vol. 276, no. December 2018, pp. 103–109, 2019, doi: 10.1016/j.biortech.2018.12.080.

[17] W. W. C. Albuquerque, R. M. P. B. Costa, T. de Salazar e Fernandes, and A. L. F. Porto, “Evidences of the static magnetic field influence on cellular systems,” *Prog. Biophys. Mol. Biol.*, vol. 121, no. 1, pp. 16–28, 2016, doi: 10.1016/j.pbiomolbio.2016.03.003.

[18] S. Khorobrykh, V. Havurinne, H. Mattila, and E. Tyystjärvi, “Oxygen and ROS in photosynthesis,” *Plants*, vol. 9, no. 1, 2020, doi: 10.3390/plants9010091.

[19] R. R. C. Nascimento, M. R. Moreno, R. S. Azevedo, J. A. V. Costa, L. F. Marins, and L. O. Santos, “Magnetic Fields as Inducers of Phycobiliprotein Production by Synechococcus elongatus PCC 7942,” *Curr. Microbiol.*, vol. 80, no. 8, pp. 1–11, 2023, doi: 10.1007/s00284-023-03348-3.

CHAPTER VI. Products derived from this thesis

Research paper

- López-Bello E., Vargas-Estrada L., Aizpuru A., Arriaga S., Muñoz R. (2025). Stimulation of microalgae growth and high-value compounds production by magnetic field exposure. Journal of Environmental Chemical Engineering, https://doi.org/10.1016/j.jece.2025.119171.
- López-Bello E., Aizpuru A., Arriaga S. (2025). Stimulation of toluene biofiltration under continuous and intermittent operation by a static magnetic field. Journal of Process Biochemistry. **Submitted**
- Effects of static magnetic field exposure on the biodegradation of volatile organic compounds with different hydrophilicities. **In preparation**

Co-author research paper

- Performance of Fusarium solani in degrading methanol vapors in a batch system stimulated by magnetic fields. **In preparation**

Popular science article:

- Sonia Arriaga, Yoali Camila, Estheisy López Bello (2023). “Limpiando el Aire con Magia Magnética: Explorando la Biorremediación Potenciada por Campos Magnéticos para un Futuro Sostenible”. Opinión Pública SLP, (Limpiando el Aire con Magia Magnética: Explorando la Biorremediación Potenciada por Campos Magnéticos para un Futuro Sostenible - OPINION PUBLICA S.L.P.).
- Aizpuru A., López Bello E., Torres L., Ramírez C., Arriaga S. (2024). Cleaning the Air With Microbes and Magnetic Fields. Frontiers for Young Minds, (Cleaning the Air With Microbes and Magnetic Fields · Frontiers for Young Minds).
- Sonia Arriaga, Aitor Aizpuru, Yoali Camila, Estheisy López Bello (2025). “Limpiando el Aire con Magia Magnética: Explorando la Biorremediación Potenciada por Campos Magnéticos para un Futuro Sostenible”. Boletín Scire, Facultad de Química, UASLP.

Oral presentation at conference

- ABIAER 2022 – Simposio Ambiente y Bioenergía, Asociación de Biotecnología, Ingeniería Ambiental y Energías Renovables, A.C., México.
    - Mechanisms involved in the biodegradation of volatile organic compounds stimulated with magnetic fields

- Biotechniques 2024 – 9th International Conference on Biotechniques for Air Pollution Control and Biorefinery, La Coruña, España.
    - Enhancement of CO_2 capture and microalgal biomass production in an AirLift photoreactor under static magnetic field exposure
    - Stimulation of toluene biofiltration by a static magnetic field

Research internship

National:

- Under the direction of Dr. Aitor Aizpuru at Universidad del Mar, Puerto Angel, Oaxaca, Mexico (July-December 2021).

International:

- Under the direction of Dr. Raul Muñoz at the Institute of Sustainable Processes (ISP). University of Valladolid (UVa), Valladolid, España (January-August 2024).